

**Impact of aldehyde dehydrogenase
isotypes on xenograft and
syngeneic mouse models of human
primary glioblastoma multiforme**

von Friederike Constanze Lämmer

Inaugural-Dissertation zur Erlangung der Doktorwürde
der Tierärztlichen Fakultät der Ludwig-Maximilians-Universität
München

**Impact of aldehyde dehydrogenase
isotypes on xenograft and
syngeneic mouse models of human
primary glioblastoma multiforme**

von Friederike Constanze Lämmer
aus Leipzig
München 2016

Aus dem Zentrum für Klinische Tiermedizin der Tierärztlichen Fakultät
der Ludwig-Maximilians-Universität München

Institut für Tierpathologie

Arbeit angefertigt unter der Leitung von: Univ.-Prof. Dr. Kaspar Matiasek

Angefertigt am Institut für Allgemeine Pathologie und Pathologische Anatomie der
Technischen Universität München

Mentor: Univ.-Prof. Dr. Jürgen Schlegel

**Gedruckt mit Genehmigung der Tierärztlichen Fakultät
der Ludwig-Maximilians Universität München**

Dekan: Univ.-Prof. Dr. Joachim Braun

Berichterstatter: Univ.-Prof. Dr. Kaspar Matiasek

Korreferenten: Priv.-Doz. Dr. Ivica Medugorac
Univ.-Prof. Dr. Johannes Hirschberger

Tag der Promotion: 6. Februar 2016

Contents

Abbreviations	vii
1 Introduction	1
1.1 Human Glioblastoma multiforme	1
1.2 Models in GBM reasearch	4
1.2.1 Mouse models in GBM research	6
1.2.2 Canine Glioblastoma multiforme	6
1.3 Theory of cancer growth	7
1.4 Aldehyde dehydrogenase superfamily	10
1.4.1 ALDH1A1	10
1.4.2 ALDH1A3	11
2 Objective	12
3 Materials and Methods	13
3.1 Material	13
3.2 Methods	16
3.2.1 Collection of GBM patients data	16
3.2.2 Canine GBM samples	17
3.2.3 Immunohistochemistry analysis	17
3.2.4 Analysis of ALDH isoforms on the mRNA level	19
3.2.5 Mouse experiments	23
3.2.6 Culture of cell line LN18, U87-MG, G1261, C6, and F98	29
3.2.7 Cell pellet	29
3.3 Summary of samples	29
4 Results	30
4.1 Human PGBM cohort analysis	30
4.1.1 Immunohistochemistry	30
4.1.2 Double immunoflorescence for ALDH1A1 and ALDH1A3 with Ki67	41
4.1.3 MGMT methylation status and expression of different ALDH1 isoforms	41
4.1.4 ALDH expression by RT-PCR	44
4.2 Comparative analysis of ALDH in a xenograft and a syngeneic model for GBM	47
4.2.1 U87-MG xenograft model	48
4.2.2 G1261 syngeneic model	48
4.3 Evaluation of ALDH isoforms in rat GBM cells	50

Contents

4.4	Immunohistochemistry analysis of ALDH expression in canine GBM	53
5	Discussion	55
5.1	Analysis of the distribution of ALDH in human PGBM	55
5.1.1	Primary PGBM	55
5.1.2	Secondary PGBM	59
5.1.3	Conclusion of human PGBM analysis	59
5.2	Evaluation of the syngeneic and the xenograft PGBM mouse model	59
5.2.1	ALDH expression in mouse models	60
5.3	Evaluation of rat GBM cells	61
5.4	Evaluation of the canine GBM model	61
5.5	Conclusion of animal model analysis	62
6	Outlook	64
7	Summary	65
8	Zusammenfassung	66
9	Supplemental Data	68
10	Danksagung	92

Abbreviations

AB	antibody
ALDH	aldehyde dehydrogenase
cDNA	complementary deoxyribonucleic acid
CSC	cancer stem cell
DEAB	<i>N,N</i> -diethylaminobenzaldehyde
DNA	deoxyribonucleic acid
dNTPS	deoxynucleotide
DSF	disulfiram
EDTA	ethylenediaminetetraacetic acid disodium salt solution
FFPE	formalin fixed paraffin embedded
GAPDH	glyceraldehyde 3-phosphate dehydrogenase
GBM	glioblastoma multiforme
GFAP	glial fibrillary acidic protein
H&E	hematoxylin and eosin stain
IDH	isocitrate dehydrogenase
IFC	immunofluorescence
IgG	immunoglobulin G
IHC	immunohistochemistry
MES	mesenchymal
MGMT	<i>O</i> ⁶ -methylguanine DNA methyltransferase
MOS	medium overall survival
MRI	magnetic resonance imaging
mRNA	messenger ribonucleic acid
NAD	nicotinamide adenine dinucleotide
PBS	phosphate buffered saline
PCR	polymerase chain reaction
PGBM	primary glioblastoma multiforme
PML	promyelocytic leukemia gene
PN	proneural
RA	retinoic acid
RAS	retinoic acid signaling
RFS	relapse-free survival
RNA	ribonucleic acid
ROS	reactive oxygen species
RT-PCR	reverse transcriptase PCR
SDS	sodium dodecyl sulfate
SGBM	secondary glioblastoma multiforme

Contents

TMZ	temozolomide
TUM	Technische Universität München
UK	United Kingdom
USA	United States of America
WHO	World Health Organisation

1 Introduction

1.1 Human Glioblastoma multiforme

Glioblastoma multiforme (GBM) is the most common adult glioma with a medium overall survival (MOS) of 15 months (450 days) (Hau et al., 2007). The incidence of GBM in the USA is 3.19 in 1000000 (Vigneswaran et al., 2015). The median age at diagnosis is 64 years. Men are 1.6 times more often affected than women (Verhaak et al., 2010). The reason for this gender-specific preponderance is unclear. 95% of all GBM develop *de novo* (primary glioblastoma multiforme, PGBM), while 5% evolve out of low grade gliomas, for example astrocytomas, and are named secondary glioblastoma multiforme (SGBM) (Figure 1.1). Analysis of GBM genomics revealed multiple tumour suppressor and oncogenes that are inactive and active, respectively, during tumour progression and *de novo* formation (Figure 1.2). For example, in low grade gliomas and SGBM, mutations of isocitrate dehydrogenase (IDH1 and IDH2) are found most frequently, whereas PGBM never have these mutations. Genetic differences between SGBM and PGBM tumours are used in diagnostics (Nobusawa et al., 2009) and are relevant for the selection of the therapy. With immunohistochemistry (IHC), the expression of IDH1 in SGBM and low grade GBM can be detected easily (Figure 1.3).

Despite various efforts and combined therapy (Hau et al., 2007; Stupp et al., 2009), PGBM is still an incurable disease. At the moment, the standard therapy for patients

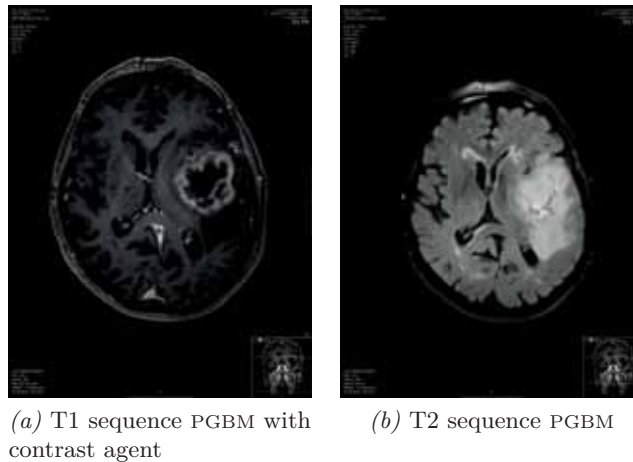


Figure 1.1: Magnetic resonance imaging from a PGBM patient, transversal sections. Tumour in the right hemisphere.

1 Introduction

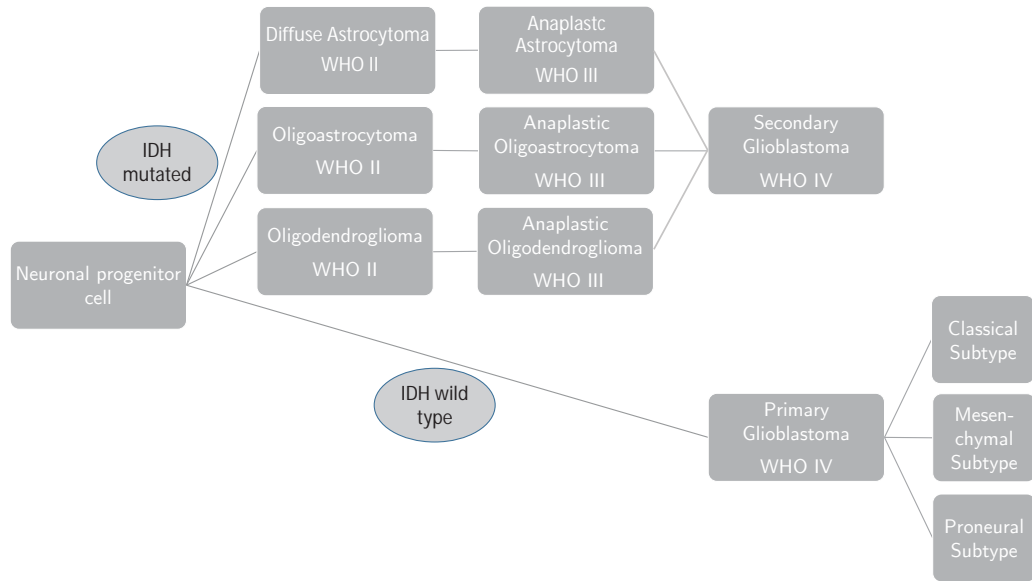
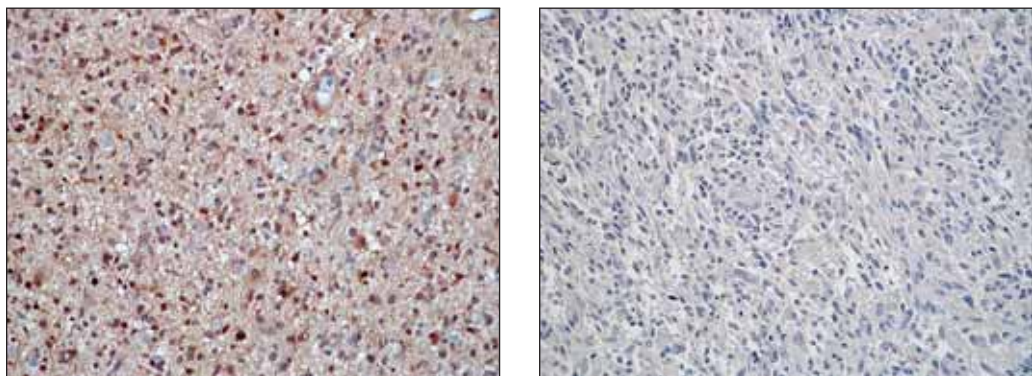


Figure 1.2: Development of PGBM and SGBM. IDH mutation as difference of low grade, SGBM and PGBM.



(a) IDH1 positive sample of SGBM patient

(b) IDH1 negative sample of PGBM patient

Figure 1.3: IHC, 200 x, IDH1. a) secondary glioblastoma multiforme, positive for the R132H point mutation, b) primary glioblastoma multiforme, negative for the R132H point mutation. Used for diagnosis of PGBM and SGBM.

1 Introduction

below the age of 70 years consists of: surgical resection, external beam irradiation five times a week for six weeks, as well as oral temozolomide (TMZ) daily. Relapse occurs frequently within approximately 7 months (210 days) (Alifieris and Trafalis, 2015) (Figure 1.4). This is due to the fact that a complete microscopic resection can never be achieved because of the diffuse infiltration of PGBM. If re-irradiation and re-resection of recurrent tumours are not eligible, other medications like carboplatin, irinotecan, carmustine, etoposide, or vincristine are used in clinical trials (Mrugala et al., 2012; Pallud et al., 2015). Even investigatory approaches like convection enhanced delivery, stem cell treatment, immunotherapy, and gene therapy might be available in the future to elongate the survival of PGBM patients (Arshad et al., 2015; Stangeland et al., 2015).

For the choice of medication, it is essential to have prognostic markers to predict the course of the disease, or to evaluate developed medications. At the moment there is only one stable predictive marker defined for PGBM therapy. The success of PGBM treatment with TMZ is depends on the methylation status of the O^6 -methylguanine DNA methyltransferase (MGMT) promoter (Hegi et al., 2008; Quillien et al., 2012; Stupp et al., 2009). TMZ is an alkylating agent, targeting the O^6 -position of guanine. This leads to DNA double strand breaks and finally results in apoptosis. MGMT, however, removes methyl adducts at the O^6 -guanine and works therefore as a DNA repair enzyme, antagonising TMZ. If the MGMT promoter is methylated, the enzyme is not produced and the alkylating agents can lead to DNA double strand breaks (Hegi et al., 2004). Patients with a high MGMT promoter methylation benefit more from a TMZ therapy and have a longer MOS than patients with low MGMT promoter methylation.

Histopathologically, PGBM are very heterogeneous (Bonavia et al., 2011). Modern pathology combines morphological patterns with molecular markers to manifest

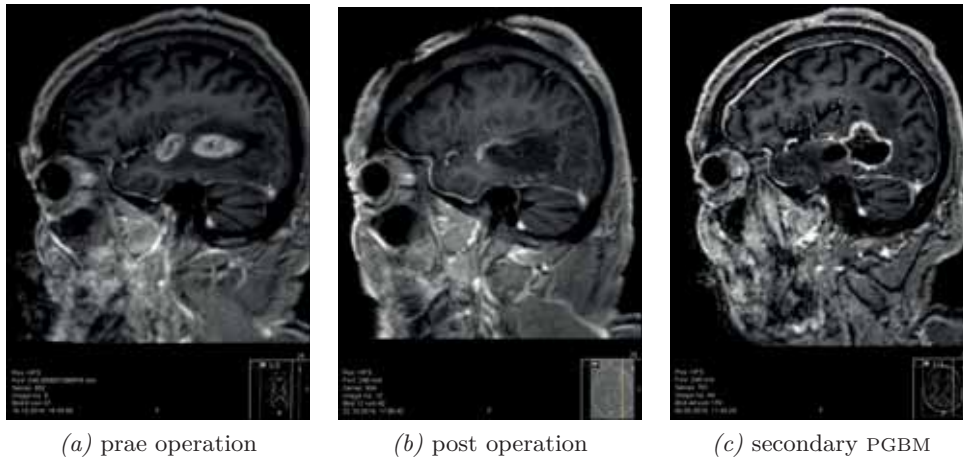


Figure 1.4: Magnetic resonance imaging from a PGBM patient, sagittal sections. a) before surgical resection, b) after surgical resection, c) 4 months after surgical resection, secondary PGBM visible.

diagnosis. However, PGBM grow infiltrative, lead to neovascularisation and necrosis, and show an enhanced mitotic activity and nuclear atypia (Vigneswaran et al., 2015) The tumour is usually surrounded by peritumoural edema and inflammation. Histological variants are: small cell PGBM, giant cell PGBM (Figure 1.5), and gliosarcomas (Louis et al., 2007).

Guan et al. (2014) and the National Human Genome Research Institute (USA) distinguish on the basis of expression profiling between classical, proneural (PN), mesenchymal (MES), and neural PGBM subtypes. There are other subclassification schemes such as Mao et al. (2013) who define only two subtypes, PN and MES PGBM. Although the exact number of subtypes is controversial, there is always an undisputed clear differentiation between PN and MES. MES are more resistant to radiotherapy than PN, which leads to a shorter MOS of patients with MES PGBM (Figure 1.6). As a possible reason for this difference, Mao et al. (2013) suggest a high expression level of genes responsible for DNA repair in MES PGBM. A summary of subtype specific markers can be found in Table 1.1. Verhaak et al. (2010) found, furthermore, that the subtypes MES and PN occur in at least twice as many men as women. A reason for this sex predominance has still not been found.

As it is still unclear how many subtypes of PGBM can be distinguished and little is known about the therapeutic advantages of specific types, there is a need to understand more about PGBM, especially about markers predictive for successful therapy and MOS. In addition to research on human material, there is a need for accurate and reproducible PGBM brain tumour animal models which should be ideally close to the human cancer. This includes kinetics and anti-tumour immune responses.

1.2 Models in GBM research

In cancer research a reliable model to investigate tumour growth, cell behaviour, and to test new therapies is a key to understand more about cancer and to be able

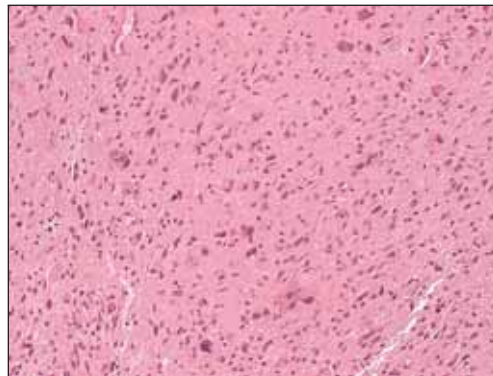


Figure 1.5: H&E, 200x. Example of histopathological PGBM variant: giant cell PGBM of patient No.47.

1 Introduction

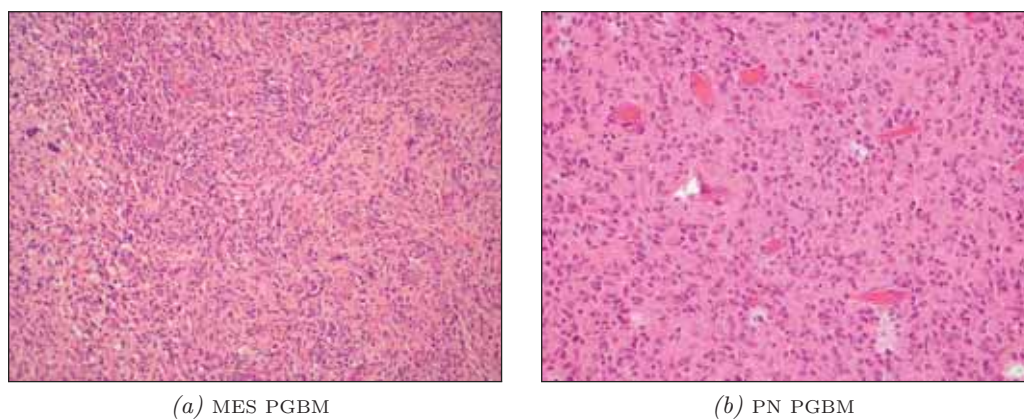


Figure 1.6: H&E, 200 x. Staining of PGBM subtypes: a) MES and b) PN. Subtypes of PGBM can be defined by genomic analysis or histopathological pattern.

Table 1.1: Subtypes of PGBM, modified after Mao et al. (2013) and Bhat et al. (2013).

Characteristics	PN	MES
frequency	60 %	40 %
sensitivity to therapy	relatively sensitive to radiation	radio resistant
stem cell markers	CD133, CD15	ALDH1A3
potential cell of origin	embryonic neonatal neural stem cell	adult neural stem cell differentiated astrocyte
altered signalling pathway	Notch, PDGFRA, GLUT3 mediated glucose uptake	NF- κ B, ALDH1A3, glycolysis, inflammasome

to improve patients live.

1.2.1 Mouse models in GBM research

Rodent models have been used for more than 30 years to investigate glioma morphology and to test preclinical therapies. It is common to implant human GBM cells subcutaneously or intracranially (xenograft model) into an immunocompromised mouse. These models are used for therapeutic preclinical trials to study for example angiogenesis, or invasion (Becker et al., 2015; Schmidt et al., 2004; Sun et al., 2015; Suzuki et al., 2014). For GBM immunotherapy trials syngeneic mouse models are used (Belcaid et al., 2014).

Histopathological features of mouse GBM models are (Candolfi et al., 2007): inflammation, hypercellularity, pleomorphism, nuclear atypia, and neovascularisation. In syngeneic GBM models in contrast to xenograft models you can find furthermore necrosis, hemorrhages, and pseudopalisading. Invasion of GBM cells into surrounding tissue is dependent on the chosen cell line.

Both GBM models stand out because of their high reproducibility, fast *in vivo* and *ex vivo* growth of tumours, and low costs. However, they do not fit for all experiments. Two of the widely used models in research are: the xenograft model with human U87-MG GBM cell line and the syngeneic model with the murine cells G1261.

The human PGBM cell line U87-MG was isolated in 1966 from a 44 years old male patient. G1261 cells were induced by methylcholanthrene in 1970s and serially implanted by Ausman et al. (1970). G1261 tumours resemble ependymoblastom (a tumour of the central nervous system of embryos) in histology, but closely mimic GBM phenotypes (Ausman et al., 1970). For example, they are positive for several GBM markers as vimentin and harbor mutations of the K-ras oncogene and p53 tumour suppressor gene (Szatmári et al., 2006). They grow invasively but will never metastasize. One advantage compared to other syngeneic models is that they never spontaneously regress (Vince et al., 2004). A characterisation of growth pattern was done by Szatmári et al. (2006).

A different approach using genetic engineering makes it possible to study tumour growth in mice with constitutive or conditional alleles of genes associated with GBM development and are summarized by Weiss et al. (2002).

The choice of the right model is not always easy. This thesis is going to compare two models in terms of suitability for ALDH research (Section 4.2).

1.2.2 Canine Glioblastoma multiforme

Not only in humans but also in dogs, GBM occur spontaneously and are one of the most common neoplasms of the canine central nervous system (Stoica et al., 2009). However, these tumours are very rare. Song et al. (2013) analysed necropsies and found a prevalence of 2-4% for GBM. A therapy consisting out of resection, radio-, and chemotherapy like in humans is uncommon. Clinical signs and prognosis of

dogs with GBM are quite similar to the ones of human PGBM patients (Candolfi et al., 2007), with a MOS of 176 days. Neuroimaging features of canine GBM seen in magnetic resonance imaging correlate well with human PGBM.

The canine GBM are common in brachycephalic breeds, in particular in Boxers and Boston Terriers (Beveridge and Sobin, 1974; Snyder et al., 2006). GBM are also found in cattle and pigs. Unlike as described in man, no sex predilection is found in dogs (Hayes et al., 1975). Many GBM of dogs occur in the subependymal plate (Palmer, 1976). The growth pattern and the heterogenous histology of canine GBM is quite similar to human PGBM. They are highly cellular, round in shape, and the nuclei are rich in chromatin and irregular in shape (Candolfi et al., 2007). The cells are often arranged in rows or in semicircles. The tumours grow infiltrative, are leading to neovascularisation, and show extensive mucinous degeneration and cyst formation. Necrosis is also found regularly (Beveridge and Sobin, 1974).

1.3 Theory of cancer growth

In general, cancer occurs, when the carefully controlled processes of cell growth and repair fall out of line. When cells divide in an uncontrolled way and form abnormal masses of cells, they are called cancer. The cause of this event are gene mutations. Mutations accumulate over time in our cells while they divide and age. In the end, certain combinations of mutations can lead to cancer.

Tumours consist of a mixture of different cell types. There are two main theories trying to explain how cancer grows and why cancer is heterogeneous: the stochastic model and the cancer stem cell (CSC) theory of cancer growth (López-Lázaro, 2015) (Figure 1.7).

The stochastic model suggests that every single tumour cell can function as a tumour founding cell. Tumour cells keep their ability to grow and divide although they differentiate. Any cell can contribute to the tumour growth because they all have the same intrinsic potential.

The CSC theory postulates that only a small subpopulation of the tumour cells can sustain the growth and proliferation of neoplastic clones. This model presumes that tumours are a well organised system with CSC giving rise to transient amplifying cells which form the majority of the tumour. Transient amplifying cells can divide a certain number of times and then become differentiated cells losing the ability to further divide.

There is no real proof in favour of either the theories. But since some cancer entities reoccur, it is widely accepted, that a particular subpopulation of tumour cells is not affected by conventional therapies and form new tumours. These cells are commonly called CSC or tumour initiating cells. Their presence has now been described in most cancers and is defined by two main characteristics: enhanced tumorigenicity, and capacity for self-renewal (Dalerba et al., 2007). These findings fit best with the CSC theory. Identification of the CSC population usually uses cell surface markers known from corresponding stem cell markers of the tissue of the

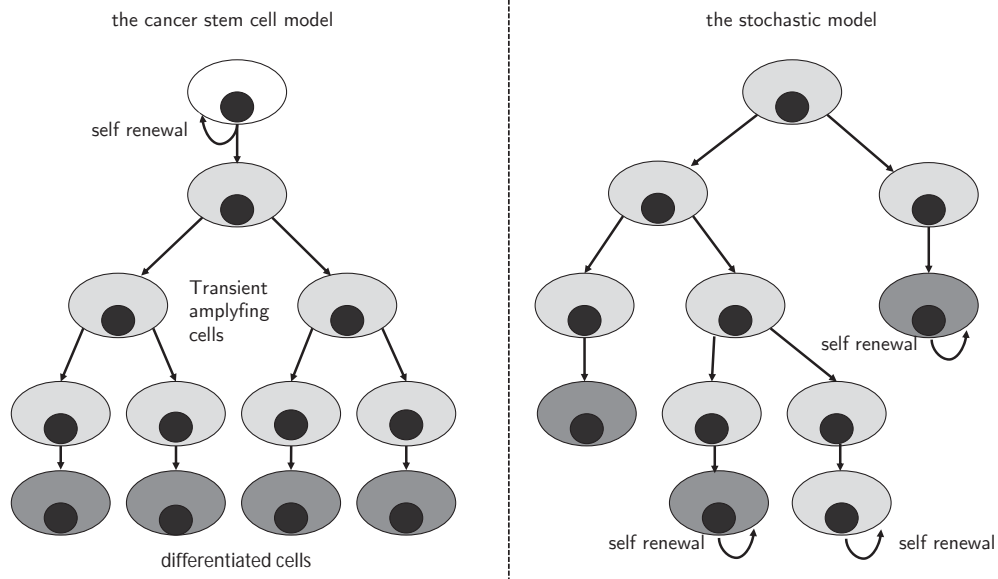


Figure 1.7: Models of cancer growth: CSC theory and stochastic model. Heterogeneity is maintained in both models.

tumour origin. Nevertheless, not all CSC are identified by such markers. Therefore, cells that might be considered as CSC need to show following abilities: giving rise to experimental tumours after xenotransplantation, recapitulate the tumour of origin morphologically and immunophenotypically, and allow serial xenotransplantation (Park et al., 2009). Important markers which are believed to detect CSC are: CD34, CD38, and aldehyde dehydrogenase 1 (ALDH1) (Choi et al., 2014; Raha et al., 2014). Recently, ALDH activity has been claimed as a marker for CSC in various organs like breast (Ginestier et al., 2007; Liu et al., 2014b), colon (Huang et al., 2009), bladder (Xu et al., 2015a), prostate (Li et al., 2010), and brain (Ni et al., 2015; Schäfer et al., 2012). When Ginestier et al. (2007) experimentally eliminated ALDH1 in mammary CSC, growth is inhibited and cells are sensitized to chemotherapy. The role of ALDH enzymes will be described in detail in Section 1.4.

Resistance of GBM CSC to currently used chemotherapy like temozolomide, carboplatin, etoposide, and others, is believed to be the major contributing factor in cancer recurrence and metastasis development. A therapy that kills CSC or induces differentiation and shrinks tumours, would possible cure patients. There are several suggested mechanisms how these cells escape chemo- and radiotherapy. The most important properties of CSC are: slow growth, increased activation of DNA damage repair enzymes (Bao et al., 2006; Singh et al., 2003), enhanced expression of efflux transporters, and overexpression of proteins which protect the cell from the toxic effects of elevated levels of reactive oxygen species, like ALDH1 (Hilton, 1984; Raha et al., 2014) (Figure 1.8).

1 Introduction

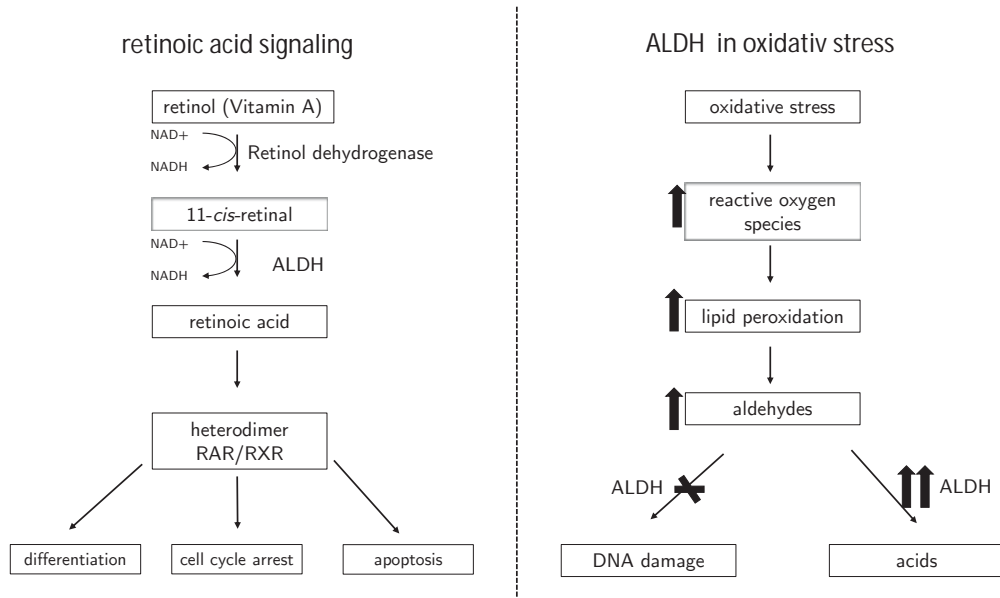


Figure 1.8: Schemes of the role of ALDH in the retinoic acid signaling (RAS) pathway and as a protective enzyme of reactive oxygen species. a) Retinol is oxidized by the retinol dehydrogenase to retinal. Retinal is the substrate of ALDH and is converted to retinoic acid (RA). RA acts on the heterodimer RAR and RXR in the nucleus. The RAR/ RXR complex regulates the expression of genes which are involved in cell differentiation, cell cycle arrest and apoptosis. RAR: retinoic acid receptor, RXR: retinoid “X” receptor. b) Oxidative stress increases reactive oxygen species in the tissue. They lead to lipid peroxidation and an increase of aldehydes. ALDH can catalyse the further oxidation to acids. If ALDH is blocked by any therapeutic agent, the increase of aldehydes leads to DNA damage and as a consequence to apoptosis.

1.4 Aldehyde dehydrogenase superfamily

The aldehyde dehydrogenase superfamily is a group of enzymes that catalyse the dehydrogenation of aldehydes and is preserved in all three taxonomic domains *archaea*, *bacteria*, and *eukarya* (Jackson et al., 2011). In mammals, ALDH enzymes of the same isotype are conserved up to 98 % on the amino acids sequence level.

Nineteen putatively different ALDH in 11 families and 4 subfamilies (Jackson et al., 2011; Ma and Allan, 2011; Vasiliou and Nebert, 2005) are known at the moment. This classification is based on the percentage of amino acid sequence identity between the enzymes (Marchitti et al., 2008; Vasiliou and Nebert, 2005). Proteins which are more than 40 % identical are assigned to a particular family, whereas proteins sharing more than 60 % amino acid identity are grouped into one subfamily (Vasiliou and Nebert, 2005).

In general, the ALDH enzymes catalyse nicotinamide adenine dinucleotide (NAD) dependent irreversible oxidation of a wide spectrum of endogenous and exogenous aldehydes (Marchitti et al., 2008). The ALDH proteins can be found in all cellular compartments (Marchitti et al., 2008) and have a wide tissue distribution. Normally, aldehydes arise from oxidative degradation of membrane lipids, amino acids, carbohydrates, and from neurotransmitter catabolism (Marcato et al., 2015). The isoforms ALDH1A1, ALDH1A2, ALDH1A3, and ALDH8A1 play a major role in retinoic acid signaling (RAS) (Figure 1.8). Retinoic acid (RA) is produced by oxidation of all-*trans*-retinal and 9-*cis*-retinal (Lane and Bailey, 2005; Raha et al., 2014), which is catalysed by the before named isoforms. This signal pathway has been identified as a important pathway for breast CSC (Ginestier et al., 2009). The gene transcription is induced by RA (Campos et al., 2011), and thus ALDH modulates a variety of biological processes like cell proliferation, differentiation, cell cycle arrest, and apoptosis (Muramoto et al., 2010; Raha et al., 2014). ALDH1 positive CSC are also more tolerant to drugs than ALDH1 negative CSC (Raha et al., 2014), due to the ability to keep the level of reactive oxygen species (ROS) sufficiently low to prevent apoptosis (Figure 1.8). ROS usually emerge from extrinsic and intrinsic stresses. These stresses influence the tumour cells all the time.

1.4.1 ALDH1A1

The gene for ALDH1A1 is located at 9q21.13 and is involved in multiple biological processes, for example: oxidative stress response (Marchitti et al., 2008), cell differentiation (Chute et al., 2006) and drug resistance (Hilton, 1984; Muramoto et al., 2010). The loss of *ALDH1A1* is usually associated with alcohol intolerance. The ALDH1A1 enzyme can be found in the cytosol of several organs like lung, liver, breast, brain, and pancreas. Rasper et al. (2010) introduced ALDH1A1 as a novel maker for PGBM cells with CSC characteristics. There is evidence that ALDH1A1 could be a prognostic marker for PGBM patients, but not to which extent (Adam et al., 2012; Schäfer et al., 2012). In other tumours like colon carcinoma and prostate cancer the isotype ALDH1A1 was correlated to poor clinical prognosis (Huang et al.,

2009; Li et al., 2010). In breast CSC, there is recently a shift in scientific opinion, whereas till 2011 it was believed that ALDH1A1 is predictive of metastasis, Marcato et al. (2011b) showed now, that ALDH1A3 is a more reliable marker.

1.4.2 ALDH1A3

The gene of ALDH1A3 is located at 15p26.2. The enzyme catalyses the conversion of acetate from acetaldehyde (Nakano, 2014). It can be found in the cytosol of the cells in many organs, like skeletal muscle, lung, breast, brain, liver, and kidney. Homozygous loss of the *ALDH1A3* leads to anophthalmia or microphthalmia and is autosomal recessive. An experimental inactivation of ALDH1A3 leads to perinatal death due to nasal defects (Dupé et al., 2003).

In PGBM, there is evidence that ALDH1A3 activity is increased in MES PGBM but not in PN PGBM (Mao et al., 2013; Nakano, 2014) and contributes to the radioresistance of MES PGBM. Experimental inhibition of ALDH1A3 by short hairpin RNA mediated gene silencing attenuates not only MES gene signature but also the *in vitro* growth and radioresistance (Nakano, 2014). Nakano (2014) and Ni et al. (2015) describe, that an increased proportion of ALDH1A3 positive cells correlates with malignancy of glioma and poor MOS of patients.

2 Objective

GBM is one of the devastating diseases in men. Medium overall survival of PGBM patients is, though aggressive therapy, approximately 15 months. Rarely full resection is achieved and tumour reoccurs regularly after 7 months. A therapy resistant sub-population of cells might be responsible for tumour re-growth. Reliable predictive markers and targets for PGBM therapy have yet not been found.

As described in Section 1.4, the protein expression of ALDH1A1 and ALDH1A3 are of special interest as a prognostic marker for human PGBM patients. The role of the ALDH superfamily in human PGBM and especially ALDH1 isoforms is re-evaluated (Section 4.1). A clear correlation between ALDH isoform expression and MOS of human PGBM patients, will make the inhibition of the enzyme activity interesting for targeted therapy. To assess which mouse PGBM model would be the best for ALDH enzyme activity measurements and inhibition, two different approaches are analysed and compared to cell culture conditions and PGBM patients material. In Section 4.2, a xenograft model and a syngeneic model will be studied.

3 Materials and Methods

3.1 Material

The statistical analysis was done with R 3.1.2 with the packages survival (version 2.38-3), tikzDevice (version 0.10-1), DBI (version 0.3.1). Pictures were arranged with GIMP 2 and Aperior ImageScope (v12.1.0.5029). Survival analysis was done with Kaplan-Meier estimator and Cox regression test. Used reagents and chemicals and technical devices can be found in Tables 3.1 and 3.2.

Table 3.1: Chemicals and reagents

Substances	Producer
25 bp DNA Ladder	Invitrogen™, Life Technologies Corp., Paisley, UK
Avidin / Biotin Blocking Kit	Vector Laboratories Inc., Burlingham, USA
Biozym LE Agarose	Biozym Scientific GmbH, Hessisch Oldenburg
Distilled water DNase/RNase Free	Life Technologies Corp., Paisley, UK
Citric acid mono hydrate $C_6H_8O_7 \cdot H_2O$	Merck KGaA, Darmstadt, Germany
Dulbecco's Modified Eagle Medium	Life Technologies, Darmstadt, Germany
Eagle's Minimum Essential Medium	Life Technologies, Darmstadt, Germany
Ethanol	Carl Roth GmbH & Co. KG, Karlsruhe, Germany
Ethidium bromide $C_{12}H_{20}BrN_9$	amresco International GmbH, Darmstadt, Germany
Ethylenediaminetetraacetic acid disodium salt solution	Sigma-Aldrich, Co., St.Louis, USA
Fetal bovine serum	Biochrom AG, Berlin, Germany
Formaldehyde	Carl Roth GmbH & Co. KG, Karlsruhe, Germany
Gelatine from cold water fish skin	Sigma-Aldrich Co., St. Louis, USA
High Pure RNA Paraffin Kit	Roche Diagnostics GmbH, Mannheim, Germany

3 Materials and Methods

Table 3.1: Chemicals and reagents

Substances	Producer
Horse serum	Vector Laboratories Inc., Burlingham, USA
Hydrogen peroxide H ₂ O ₂	Carl Roth GmbH & Co. KG, Karlsruhe, Germany
Hydrochloric acid HCl	Carl Roth GmbH & Co. KG, Karlsruhe, Germany
ImmPACT DAB	Vector Laboratories Inc., Burlingham, USA
Isopropanol	Carl Roth GmbH & Co. KG, Karlsruhe, Germany
Meyer's haematoxylin	Carl Roth GmbH & Co. KG, Karlsruhe, Germany
RevertAid H Minus First Strand cDNA Synthesis Kit #K1631	Thermo Fisher Scientific Inc., Waltham, USA
peqGOLD Taq-DNA-Polymerase "all inclusive"	Peqlab VWR International GmbH, Erlangen, Germany
PrimerScript™ RT reagent Kit (Perfect Real Time)	TAKARA Bio Inc., Otsu, Japan
Potassium chloride KCl	Carl Roth GmbH & Co. KG, Karlsruhe, Germany
Potassium dihydrogen phosphate KH ₂ PO ₄	Carl Roth GmbH & Co. KG, Karlsruhe, Germany
RNeasy™ Mini Kit	QIAGEN GmbH, Hilden, Germany
Sodium dodecyl sulfate (10 %, pH 7.3)	Sigma-Aldrich Co., St. Louis, USA
Sodium chloride NaCl	Carl Roth GmbH & Co. KG, Karlsruhe, Germany
Sodium hydroxide NaOH	Carl Roth GmbH & Co. KG, Karlsruhe, Germany
<i>di</i> Sodiumhydrogen phosphate dihydrate Na ₂ HPO ₄	Merck KGaA, Darmstadt, Germany
Triton X100	Carl Roth GmbH & Co. KG, Karlsruhe, Germany
Trizma® hydrochloride solution (1 M, pH 8.0) Tris-HCl	Sigma-Aldrich Co., St. Louis, USA
Vectastain ABC Kit	Vector Laboratories Inc., Burlingham, USA
Xylene	Carl Roth GmbH & Co. KG, Karlsruhe, Germany

3 Materials and Methods

Table 3.2: Technical Devices

Device	Model	Manufacturer
Centrifuges	5415D	Eppendorf AG, Hamburg, Germany
Gel imaging sytem	4K15	Sigma, Deisenhofen, Germany
	Eagle Eye™ II	Stratagene, Heidelberg, Germany
Magnetic stirrer	RCT basic	IKA®-Werke GmbH & Co. KG, Staufen, Germany
Microtome	HM355	Thermo Fisher Scientific Inc., Waltham, USA
pH meter	EL-30	Mettler-Toledo GmbH, Giessen, Germany
Power supply	Power PAC 300	Bio-Rad Laboratories, Inc., Hercules, USA
Shaker	Mini shaker MS1	IKA®-Werke GmbH & Co. KG, Staufen, Germany
Slide scanner	Aperio CS2	Leica Biosystems Nussloch GmbH, Nussloch, Germany
Spectrophotometers	NanoDrop 2000c	Thermo Fisher Scientific Inc., Waltham, USA
Steamer	TEFAL Steam cuisine	Groupe SEB Deutschland GmbH, Frankfurt am Main, Germany
Stereotaxis	Lab standard stereotaxic instrument	Stoelting Europe, Dublin, Ireland
Thermal cyclcer	GeneAmp™ PCR Sytem 9700	Applied Biosystems, Waltham, USA
Thermomixer	Thermomixer comfort	Eppendorf AG, Hamburg, Germany
Water bath	TFB 35.000	Medite Medizintechnik, Burgdorf, Germany

3.2 Methods

All experiments were done at Institut für Allgemeine Pathologie und Pathologische Anatomie der Technische Universität München (TUM), with the help of Sandra Baur and Christine Grubmüller.

3.2.1 Collection of GBM patients data

The specimens for this retrospective study were collected at the Klinikum rechts der Isar, TUM with patients' consent according to the TUM medical faculty's guidelines for tissue preservation. All patients had signed informed consent forms according to the local ethics committee. Tissue samples for histopathological diagnosis and molecular genetic analysis were acquired during tumour resection at the NeuroKopf-Zentrum, Klinikum rechts der Isar, TUM. Tumour diagnoses of glioblastoma multiforme, WHO IV (Louis et al., 2007), were established by standard light-microscopic evaluation of H&E sections, immunohistochemistry for IDH1 (R123H point mutation (Nobusawa et al., 2009)), glial fibrillary acidic protein (GFAP), Ki67, microtubule-associated protein 2, tumour suppressor protein p53, epidermal growth factor receptor, and MGMT promoter methylation, and verified by two independent neuropathologists (Prof. Dr. Jürgen Schlegel, Claire Delbridge) at Institute für Allgemeine Pathologie und Pathologische Anatomie der TUM. Data of 135 GBM patients were collected in this retrospective patient cohort study with a follow up of 3 years. For analysis, only PGBM patients receiving neurosurgery, chemotherapy and radiotherapy as described by Stupp et al. (2005) were included. 71 Patients were excluded from analysis because of: different therapy (only neurosurgery, only chemo- or only radiotherapy), incomplete data, bad tissue quality, IDH1 mutation. Neurosurgery on recurrent tumours is controversial (Sughrue et al., 2015) and therefore we are pleased to present data on 28 secondary tumours of PGBM patients. IHC analysis was performed blinded on FFPE tissue of primary and recurrent surgical specimens of patients diagnoses as PGBM, WHO IV (Louis et al., 2007).

Table 3.3: Patient characteristics

	female $n = 26$			male $n = 39$		
	min	mean	max	min	mean	max
Age (in years)	40	60	78	20	59	80
overall survival (in days)	37	463	1437	22	607	2904

3.2.2 Canine GBM samples

As described in Stoica et al. (2009), the incidence of canine GBM is unclear. There is no routine therapy like tumour resection, chemo- and radiotherapy available like in humans. Necropsies of the dog brain are not usually performed in detail. Biopsies from one female, 12 years old Cocker Spaniel and one German Shepherd dog with unknown age and sex diagnosed in 2014 in the neuropathological laboratory of the Tierpathologie der Ludwig-Maximilians Universität as canine GBM, are analysed. Both tumour samples show a tumour of the glia with necrosis, mitosis, atypic nuclei, and neovascularisation comparable with the human GBM WHO IV.

IHC as described in Section 3.2.3 was performed on both biopsies. As positive control for IHC served a liver of a 6 months old autopsied pug with hydrocephalus.

3.2.3 Immunohistochemistry analysis

Immunohistochemical method

Tissue sections of 2 μm thickness are deparaffinised. All incubation steps are performed in a humidified chamber. Epitope unmasking is performed with citric acid based buffer (pH 6.0) or with EDTA (pH 8.0) for 30 min in a steamer. The endogenous peroxidase is quenched with 3% H_2O_2 for 20 min at room temperature. To minimize non-specific staining resulting from endogenous avidin-biotin activity it is blocked with Avidin/Biotin blocking kit for 30 min. Non-specific binding sites are blocked with the blocking buffer described in Table 3.4. Each tissue section is incubated in a humidified chamber with the in Table 3.5 described dilution of the

Table 3.4: Buffers and solutions

Buffer	Ingredients
Blocking buffer	1 x PBS 1 % Bovine serum albumin 0.1 % Triton X100 0.2 % Gelatin from cold water fish skin 2.5 % Normal Horse Serum
PBS 10 x pH 7.4	140 mM NaCl 2.7 mM KCl 20 mM Na_2HPO_4 1.8 mM KH_2PO_4
Citrate buffer pH 6.0	2.1 g citric acid monohydrate add up to 500 ml H_2O
10 x Tris buffer	60.5 g Tris 90 g NaCl add up to 1000 ml H_2O

3 Materials and Methods

Table 3.5: Antibodies used for IHC and IFC

Antibody	Clone	Company	Dilution
ALDH1	44/ALDH	BD, Heidelberg, Germany	1:50
ALDH1A1	EP1933Y	Novus Biologicals Europe, Cambridge, UK	1:1000
ALDH1A3	PA5-29188	Thermo Fisher Scientific Inc., Waltham, USA	1:1000
Alexa flour [®] 488 donkey-anti mouse		Life technologies Carlsbad, USA	1:500
Alexa flour [®] 568 donkey-anti rabbit		Life technologies Carlsbad, USA	1:500
Anti-human Ki67	mib1	Dako Deutschland GmbH, Hamburg, Germany	1:50
biotinylated horse Anti-mouse IgG		Vector Laboratories Inc., Burlingham, USA	1:200
biotinylated horse Anti-Rabbit IgG		Vector Laboratories Inc., Burlingham, USA	1:200
biotinylated goat Anti-Rabbit IgG		Kirkegaard & Perry Laboratories Inc., Maryland USA	1:1

3 Materials and Methods

AB in blocking buffer overnight at 4°C. Followed by the incubation with the corresponding biotinylated secondary AB for 30 min at room temperature. Afterwards the ABC-Kit is applied for 30 min. Finally, tissues slides are incubated with ImmPACT DAB chromogen working solution for 4 to 8 min and counter stained with Meyer's haematoxlin. Liver tissue serves as positive control for all ALDH isoforms. Negative controls for all ALDH isoforms were obtained by substituting primary AB with blocking buffer.

All routine stainings and IHC of ALDH1 are performed during routine diagnosis and were done with an automated staining system.

Immunofluorescence method

For the immunofluorescence staining specimens are deparaffinized. The epitope unmasking with EDTA (*pH* 8.0) for 30 min is performed in a steamer. Followed by blocking with Blocking buffer for 30 min at room temperature. After washing twice in 1 x PBS the in Blocking buffer prediluted AB is applied (Table 3.5) to the sample and incubated overnight at 4°C. The next day the slide is wahsed twice with 1 x PBS and then incubated with the prediluted secondary fluorescence labeled AB (Table 3.5) for 45 min at room temperature. Before adding prediluted Hoechst dye to the tissue sections, it is washed twice with 1 x PBS.

Immunohistochemistry Score

The IHC reaction was rated in cooperation with Claire Delbridge. The percentage of tumour cell with stained cytoplasm was scored, intensity of the staining was taken into account. We defined two categories of IHC reaction: none and up to 10 % positive cells count as no IHC reactivity, more than 10 % positive cells as IHC reactivity.

3.2.4 Analysis of ALDH isoforms on the mRNA level

Isolation of mRNA

FFPE Material Expression of different ALDH isoforms on mRNA level is analyzed with reverse transcription PCR (RT-PCR) with Taq Polymerase. The specimens are the same as for the IHC. For extraction of the RNA of formalin-fixed paraffin-embedded tissue the High Pure RNA Paraffin Kit from Roche Diagnostics GmbH is used. The guidelines of the producer are followed. The paraffin embedded tissue is cut into 10 µm thick sections. After drying the tissue and following deparaffinisation, sections are microdissected from the slide with a new sterile single-use scalpel and placed in an RNase free reaction tube. 100 µm Tissue Lysis Buffer, 16 µl 10 % SDS and 40 µl Proteinase K working solution is poured to each sample and incubated overnight with brief vortex in several intervals at 55°C. The next day, 325 µl Binding Buffer and 325 µl ethanol absolute is added. Than the lysate is transferred into a combined High Pure Tube and a collection tube. After centrifugation for 30 sec at

3 Materials and Methods

Table 3.6: Oligonucleotide sequences for RT-PCR

Gene	Accession number (NM_)	Sequences (5'-3') f: forward, r: reverse	T_m (°C)	Product size (bp)
<i>ALDH1A1</i>	000689	f TGTTAGCTGATGCCGACTTG r CTGGCCCTGGTGGTAGAATA	58.27 58.49	71
<i>ALDH1A2</i>	001206897	f AGTGGGAGAGTGTTCCTGT r TATCTGCCTTGCTGCTTCTTGA	60.10 59.74	79
<i>ALDH1A3</i>	000693	f TCGACCTGGAGGGCTGTATTA r GTTGTCATCTGTGGGGATGGT	60.06 60.00	89
<i>ALDH2</i>	000690.3	f GGAAAACATTCCCCACCGTC r GCCTTGTCACATCTTCCTTGT	59.11 60.82	85
<i>ALDH3A1</i>	001135168.1	f TACATAGCCCCACCATCCT r GGCCCGAAGATCTCCTCTTG	59.73 59.89	71
<i>ALDH7A1</i>	001201377.1	f ACTGCGAGGCGACTGTTTAT r TTCCCAACTCGGATCTGTGC	59.75 60.04	89
<i>ALDH8A1</i>	022568.3	f GCACATTTGGAGAAAGTCAGAAGT r TTATCCACTCCCTCACCGCA	59.72 60.62	83
<i>GFAP</i>	002055	f GCAGATTCGAGAAACCAGCC r GGTCTTCACCACGATGTTCCCT	59.27 60.00	76
<i>GAPDH</i>	002046.5	f CTCTGCTCCTCCTGTTTCGAC r ATGGTGTCTGAGCGATGTGG	59.83 60.11	75

3 Materials and Methods

8000 g the flow through is discarded. Repeated centrifugation dries the filter fleece completely. 500 μ l Wash Buffer 1 working solution is given to the upper reservoir, followed by another centrifugation (15 sec at 8000 g) and the discharging of the flow through. 300 μ l of Wash Buffer 2 working solution is added. The sample is centrifugated at 8000 g for 15 sec. After ward discard the flow through. The High Pure Filter Tube is centrifugated at 13000 g for 2 min. Than the High Pure Filter Tube is placed into a fresh 1.5 ml reaction tube. 90 μ l of the Elution Buffer is poured in before centrifugation at 8000 g for 15 sec. After adding 10 μ l DNase Incubation Buffer and 1 μ l DNase 1 working solution to the eluate and mixing it, samples are incubated for 45 min at 37°C. Followed by adding 20 μ l Tissue Lysis Buffer, 18 μ l 10 % SDS and 40 μ l Proteinase K working solution and an incubation for 1 h at 55°C. The reaction tube is replaced. Afterwards first steps are repeated as following: 325 μ l Binding Buffer and 325 μ l ethanol absolute is added to the sample. Than the lysate is transferred into a combined High Pure Tube and a collection tube. After centrifugation for 30 sec at 8000 g the flow through is discarded. The centrifugation is repeated to dry the filter fleece completely. 500 μ l Wash Buffer 1 working solution is given to the upper reservoir followed by another centrifugation (15 sec at 8000 g) and the discarding of the flow through. 300 μ l of Wash Buffer 2 working solution is added. The sample is centrifugation at 8000 g for 15 sec, and the flow through is discarded. The High Pure Filter Tube is again centrifugated at 13000 g for 2 min. The High Pure Filter Tube is placed into a fresh 1.5 ml reaction tube. 90 μ l Elution Buffer is given into the tube before centrifugation at 8000 g for 15 sec. The High Pure Filter Tube is again placed into a fresh reaction tube. To the sample 50 μ l of the Elution Buffer is added. After incubating for 1 min at room temperature and centrifugation for the last time for 1 min at 8000 g the eluted RNA is collected. RNA is measured by NanoDrop, and stored at -80°C or directly transferred into cDNA by the RevertAid H Minus First Strand cDNA Synthesis Kit from Thermo Fisher Scientific. Protocol as following. The following reagents are mixed within a sterile, nuclease-free tube on ice: Template RNA (0.01-0.1 ng), 1 μ l random hexamer primer and nuclease-free water up to 12 μ l and than incubated for 5 min at 65°C. The sample is placed on ice after spin down. 4 μ l 5 x Reaction Buffer, 1 μ l RiboLock RNase Inhibitor (20 U/ μ l), 1 μ l RevertAid H Minus M-MuLV Reverse Transcriptase (200 U/ μ l) is given to the sample, mixed and incubated first for 5 min at room temperature and than for 60 min at 42°C. The reaction is terminated by heating up to 70°C for 5 min. The cDNA is stored at -20°C for short term and for long term at -80°C .

Cell line LN18 The Glioblastoma cell line LN18 was used as a positive control for all ALDH isoforms, GFAP, and GAPDH. LN18 cells were bought at ATCC™ and was isolated from a 65 years old male patient with PGBM grade WHO IV (Diserens et al., 1981).

The RNA isolation is done with the RNeasy™ Mini Kit. The cells are harvested, when grown to 80 % confluency in medium. After washing the cells twice with cold PBS, 600 μ l RLT Lysis Buffer and 10 μ l *beta* Mercaptoethanol is given to the cells.

3 Materials and Methods

The cells are collected with a sterile cell scraper, transferred into a reaction tube and resuspended 5x with a 20 G needle. 600 μl 70% Ethanol is added to the sample and mixed gently. Sample is transferred into a High Pure Tube, and centrifugated at 200 g for 15 sec before discarding the flow through. Carefully 10 μl DNase 1 and 70 μl Buffer RDD is added and following incubation for 15 min at room temperature. 350 μl Buffer RW1 is added thereafter samples are centrifugated at 200 g for 15 sec. After discarding flow through reaction tube is replaced with a new one. 500 μl RPE Buffer is added again and centrifugated at 200 g for 2 min, before discarding the flow through. Membrane is dried with another centrifugation at 1300 g 1 min. 100 μl DNase/RNase-Free Water is pipetted to the sample before centrifugation at 200 g for 1 min at 4°C to collect eluted RNA. The with the NanoDrop measured RNA is stored at -80°C or directly transferred into cDNA.

The reverse transcription is done following the instruction of PrimerScript™ RT reagent Kit (Perfect Real Time) of TAKARA Bio Inc.. Briefly: mixed 2 μl 5x PrimeScript Buffer, 0.5 μl PrimeScript RT Enzyme Mix 1, 0.5 μl Oligo dT Primer 50 μM , 0.5 μl Random hexamers 100 μM , and the isolated RNA (max 500 ng) and filled up to 10 μl with DNase/RNase free water is incubated for 15 min at 37°C, than 5 sec at 85°C and than cooled down to 4°C. cDNA is stored at -20°C .

Polymerase chain reaction

All Primers are designed with the help of Primer-Blast (Ye et al., 2012) and purchased by Sigma-Aldrich. The annealing temperatures for RT-PCR for respective primer pairs are described in Table 3.6. PCR Mastermix for RT-PCR was prepared as described in Table 3.7. Program of RT-PCR is summarized in Table 3.8.

Quantification of MGMT promoter methylation The quantification of MGMT promoter methylation was assessed by specific relative quantitative real time PCR technique named MethyQESD, as described by Bettstetter et al. (2008) and performed during routine diagnosis. In short, the endonucleases Hin61 (methylation-

Table 3.7: PCR Mastermix for RT-PCR

Substance	Volume (μl)
H ₂ O	31.2
10 x buffer	5
Enhancer	10
dNTPS	1
Forward primer (10 μM)	1
Reverse primer (10 μM)	1
Taq Polymerase	0.5
cDNA (from 500 ng RNA)	0.3

3 Materials and Methods

Table 3.8: RT-PCR Program

	Temp. (°C)	Duration	
Denaturation	95	5 min	single
Denaturation	95	30 s	35 cycles
Primer annealing	59 or 56	30 s	
Elongation	72	30 s	
Elongation	72	7 min	single
Cooling	4		single

quantification digestion) and XbaI/DraI (methylation independent calibrator digestion) were applied. After the digestion, MGMT promoter methylation status was determined by relative quantitative real-time PCR using the LightCycler 480. For positive control digested DNA of SW48 was used, for negative control non-methylated blood DNA. The proportion of methylated template was calculated from the difference of the cycle threshold values from the two endonucleases. MGMT negative are patients with less than 8% MGMT promoter methylation and MGMT positive are patients with more than 8% MGMT promoter methylation (Quillien et al., 2012).

Gel electrophoresis Following PCR, mix 5 μ l products with 1 μ l DNA loading dye and separate on 2.5% Agarose gel. A 25 bp DNA ladder is used to distinguish between specific and unspecific bands. Human universal gene and LN18 served as positive control. Normal brain and liver were evaluated as well.

3.2.5 Mouse experiments

The U87-MG implantation into the NMRI-nude mouse (HsdCpb:NMRI-Foxn1^{nu}, $n = 14$) were done by Dr. Velia Hülsmeier and implantation of G1261 cells into C57BL/6JRj mice ($n = 10$) were done by myself. Both experiments were done at the Institut für Allgemeine Pathologie und Pathologische Anatomie der TUM and were approved by the Veterinäramt München and in accordance to the German welfare law (Az. 55.2-1-54-2532-6-11 and Az. 55.2.1-45-2532.0-83-14). Mice were housed under specific pathogen-free conditions.

Table 3.9: summary of mouse experiments

	C57BL/6JRj	NMRI-nude
control	10	7
treated with DSF	0	7

Orthotopic implantation

The orthotopic implantation into the brain was done following the descriptions for stereotactical implantation of Yamada et al. (2004). In short, the mouse is anaesthetised with a combination of fentanyl (0.05 mg/kg bodyweight), medetomidin (0.5 mg/kg bodyweight), and midazolam (5 mg/kg bodyweight). The mouse is prepared for the surgical intervention including shearing, cleaning of the operation area, and fixation into the stereotaxic instrument (Figure 3.1). Before opening the skin, local anaesthesia with bupivacain is applied. For correct implantation the coordinates of bregma and lambda are recorded. The height of bregma and lambda were adjusted to the same level to ensure correct perpendicular injection of tumour cells. The injection site was calculated from bregma. 2 mm lateral and 0.5 mm anterior of bregma a 0.47 mm wide hole is drilled. A Hamilton syringe (26 GS) containing the tumour cells is fixed to the stereotactical frame and guardedly inserted over 5 min to a depth of 3 mm. Over 7 min tumour cells are injected and after waiting another 2 min the syringe is carefully removed over 7 min. After sewing with a absorbable thread, mouse is taken out of stereotactic frame. Atipamezol (2.5 mg/kg bodyweight), flumazenil (0.5 mg/kg bodyweight), and naloxon (1.2 mg/kg bodyweight) are injected to antagonize the anaesthesia. The recovery period is short because of quick inhibition of fentanyl, medetomidin, and midazolam.



(a) Stereotaxic instrument



(b) Mouse fixed in stereotaxic instrument

Figure 3.1: a) Used stereotaxic instrument for mouse operation to assure correct implantation into the striatum. b) Mouse fixed and with opened cutis. Sutures of cranium are visible: sutura coronalis, sutura sagitalis, sutura occipitalis.

3 Materials and Methods

Termination criteria and plan of action

Mice were controlled regularly, in the first week after implantation every 6 to 8 hours, following weeks every day and if mouse condition impaired more frequently. An examination of fitness and general performance was done according to the Table 3.10 and if needed action was followed described in Table 3.11.

Table 3.10: Termination criteria for intracranial implantation

degree of strain	0	I	II	III
points per symptom complex	0	1	2	3
central nervous system symptoms	none	ataxie, starting head tilt	ataxie, head tilt	paralysis, seizures, not eating
behaviour	active, curios	hyperactive or hypoactive, reduced conciseness	hyperkinesia, reduced conciseness even after stimulus, reluctant to move	isolation, paresis, plegia, torti collis, seizures, autoaggressive, vocalisation, tremor
appearance	shiny and flat coat, clean eyes	dull eyes, no grooming, too much grooming	truncated coat, no grooming	dirty, truncated coat, rapid breathing, skin tone reduced
weight change in %	0-5	6-10	11-19	>19
pain symptoms	none	starting head tilt, nystagmus	abnormal body posture, bent back, normal after stimulus	vocalisation, agression, automutilation, bent back

3 Materials and Methods

Table 3.11: Action: for intracranial implantation

degree of strain	additive symptom points	intensity of strain	action
0	0	none	none
I	1-3	light	daily check, if aggravate sacrifice
II	4-6	moderate	daily check, therapeutic intervention if possible without influence of experiment
III	>7	high	immediate termination, sacrifice

After 8 weeks NMRI-nude mice and after 2 weeks C57BL/6JRj mice were sacrificed with a lethal doses of pentobarbital-natrium (600 mg/kg bodyweight) after narcosis with fentanyl (0.05 mg/kg bodyweight), medetomidin (0.5 mg/kg bodyweight), and midazolam (5 mg/kg bodyweight).

Experimental inhibition of ALDH

Disulfiram (DSF) is a known ALDH inhibitor (Eneanya et al., 1981), effecting the tumour growth (Loo and Clarke, 2000; Wang et al., 2013; Yakisich et al., 2001). In clinical trails it is used for PGBM therapy (Kast et al., 2014), without any success. To evaluate the effect of DSF treatment on GBM *in vivo*, 7 NMRI-nude mice were treated intraperitoneal 7 days after tumour implantation with 100 mg/kg bodyweight DSF per day.

Magnetic resonance imaging of mice

To ensure tumour growth mice are checked with MRI 7 Tesla. While scanning mice are anaesthetized with isoflurane, a general inhalation anaesthetic, enabling a rapid onset and a rapid recovery without any analgesic effect. Mouse is placed into a chamber which is floated with isoflurane. Withdrawl reflex is checked to assure depth of anaesthesia. Mouse is placed onto a heated bed within the MRI for 30 min to perform scan (Figure 3.2).

Perfusion of mouse

Cardialgic perfusion is performed to accelerate fixation of organs before autolysis can begin. Another advantage of perfused organs is that they are less likely develop artefact and are not sensitive to handling. The performed perfusion uses the vascular

3 Materials and Methods

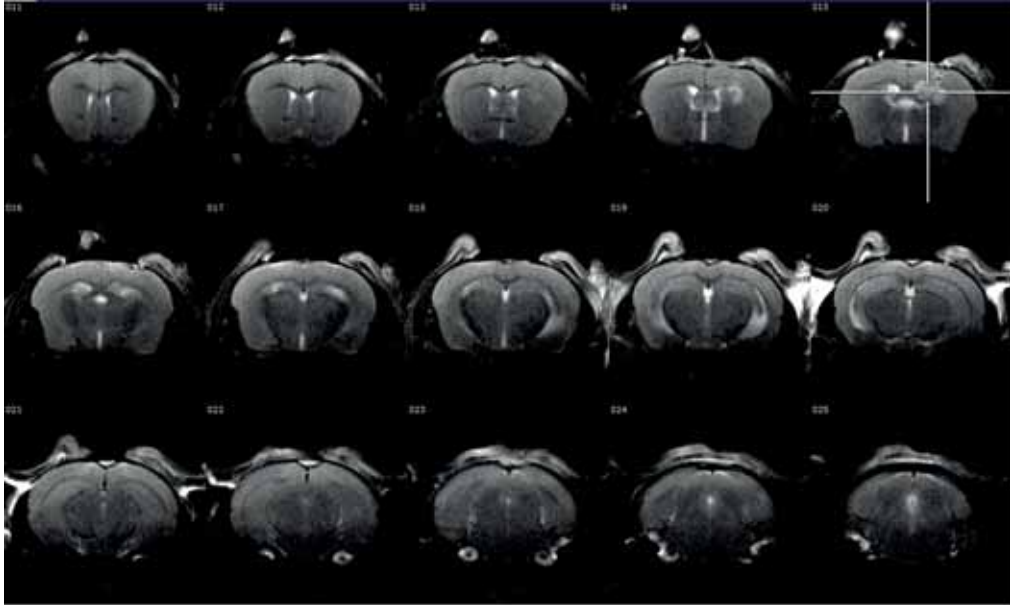


Figure 3.2: MRI pictures of a C75BL/6JRj mice with G1261 tumour at the right hemisphere. Coronal sections of T1 weighted images. Tumour marked with cross.

system of the sacrificed animal (Figure 3.3). The sacrificed animal is fixed on its back with each limb fixed to Styrofoam. To open the abdomen an incision of the midline skin is made from the pelvis to the thoracic inlet. Abdomen is carefully opened so intestines are not opened. The xyphoid process is gasped with forceps and the diaphragm is opened to allow lung to collapse. A collapsed lung reduces risk of incise it during the opening of the thorax. A butterfly is placed into the left ventricle and fixed to the Styrofoam. 1 x PBS perfusion is started. The right auricle of the heart is opened when liquid accumulated. Blanching of the liver and the spleen are taken as sign for good perfusion. When liquid is dripping out of nose, perfusion pressure is to high.

Preparation of the brain

After pefusion the skull is opened beginning at the foramen magnum. With forceps and a dull scissors the os occipitale and the os frontale are removed. When the dorsal brain is completely visible the nervi optici and the bulbi olfactori are cut with a spatula. The brain is fixed overnight in 4% formalin on shaker for immersion fixation. The next day, fixation is checked and tissue is placed into the dewatering machine to be embedded afterwards in paraffin.

3 Materials and Methods

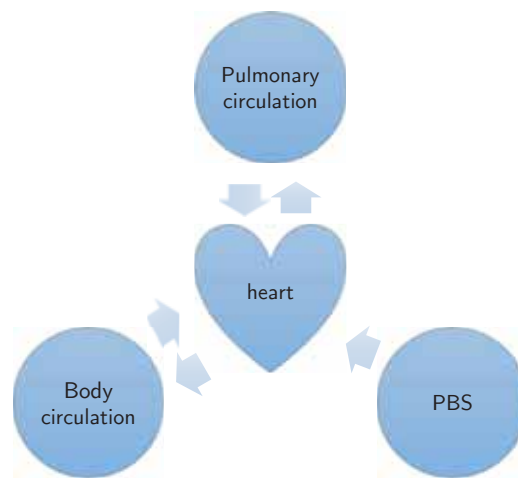


Figure 3.3: Schema of perfusion. A butterfly is placed into the left ventricle of the heart. With 1 x PBS the all vessels of the body circulation and the pulmonary circulation are flushed. Blanching of the liver and the spleen are taken as reference for perfusion status.

3.2.6 Culture of cell line LN18, U87-MG, G1261, C6, and F98

All cells are cultured at 37°C at 5% CO₂. Growing medium for LN18 and U87-MG is the Eagle's Minimum Essential Medium with 10% fetal bovine serum, for G1261, C6, and F98 the Dulbecco's Modified Eagle Medium with 10% fetal bovine serum. Medium renewal is done twice or three times a week. When cells are grown confluent, a subcultivation ratio between 1:3 and 1:5 is chosen. Mycoplasma test are done regularly on a quarterly period basis.

3.2.7 Cell pellet

The cells are harvested with trypsin and than fixed in 4% formalin for 15 min. After centrifugation at 1800 g for 10 min at room temperature, the supernatant is decanted, and cells are resuspended in 5 ml 70% ethanol for 30 min and than 100% ethanol. The fixed cells are resuspended in 1% agarose and chilled on ice. Afterwards sample is prepared like routine FFPE material.

3.3 Summary of samples

Table 3.12: Summary of samples and methods

method	specification	type	species	number of samples
IHC	PGBM	tissue	human	65
		tissue	human	28
		tissue	canine	2
		tissue	mouse	24
		cellpellet	human	1
		cellpellet	mouse	1
		cellpellet	rat	2
IFC	PGBM	tissue	human	65
PCR	PGBM	tissue	human	28

4 Results

4.1 Human PGBM cohort analysis

The aim of this study was to investigate the immunoreactivity of the ALDH isoforms and their power as prognostic factor for the survival of PGBM patients. In this retrospective study, patients with following properties were included:

1. primary glioblastoma multiforme WHO IV (Louis et al., 2007)
2. resection between 2003 and 2013
3. IDH1 wild type
4. treatment
 - surgical resection of primary tumour
 - radiotherapy
 - chemotherapy with TMZ
 - resection of secondary tumour (28 patients)
5. good follow-up.

Primary tumour tissue samples were obtained by surgical resection before radiation and chemotherapy, secondary afterwards. The patient cohort consists after exclusion of 65 patients (exclusion criteria in Section 3.2.1). We enrolled 26 female and 39 male patients with a mean age at diagnosis of 60 years and 59 years, respectively. The MOS were 15.4 months for female and 20.2 months for male patients, respectively. 11 patients lived another 2.5 years after diagnosis and count therefore as long-time survivors defined by Smoll et al. (2013). Further characteristics are summarised in Table 3.3 (p. 16) and an overview of patients data can be found in Table 9.1 (p. 68).

4.1.1 Immunohistochemistry

IHC staining was performed as described in Section 3. We defined two categories of IHC reaction: none or up to 10 % positive cells count as no IHC reactivity, more than 10 % positive cells as IHC reactivity. Scoring was done blinded without knowledge of patients data.

4 Results

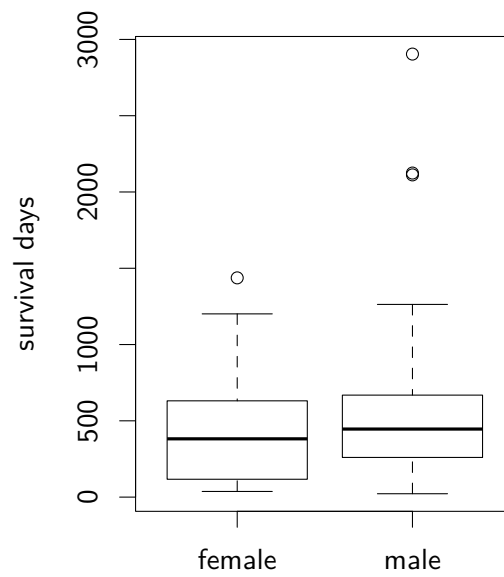
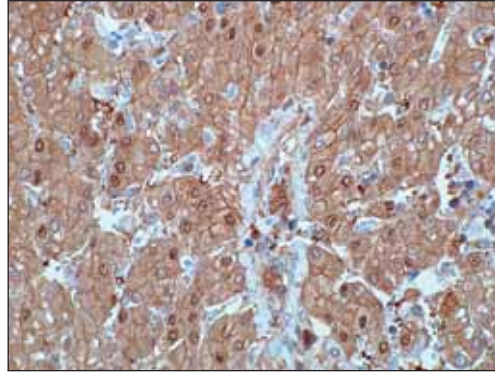
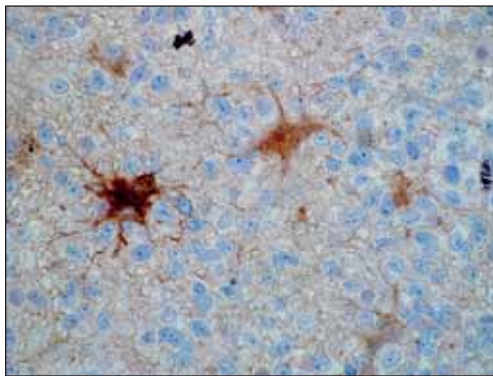


Figure 4.1: Survival distribution of female ($n = 26$) and male ($n = 39$) PGBM patients. Three male and one female patient differ in survival more than 1.5 times to the interquartile range and are shown as cycles.

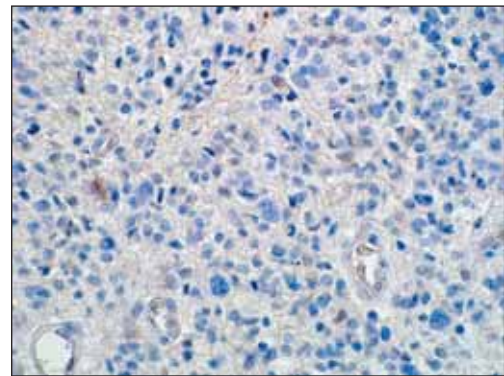
4 Results



(a) IHC ALDH1 liver



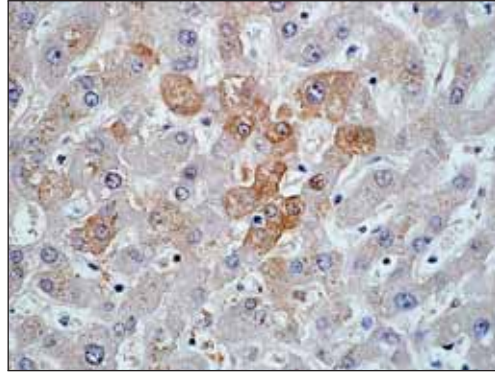
(b) IHC ALDH1 positive



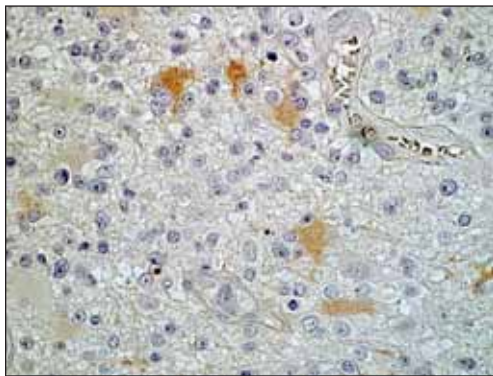
(c) IHC ALDH1 negative

Figure 4.2: IHC, 400x, ALDH1. FFPE sections of human liver served as positive control for all ALDH isoforms. Positive primary PGBM with >10% expression of patient No. 95, negative primary PGBM with <10% reactivity of patient No. 9 respectively.

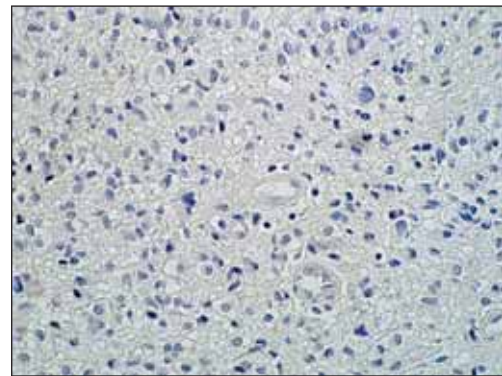
4 Results



(a) IHC ALDH1A1 liver



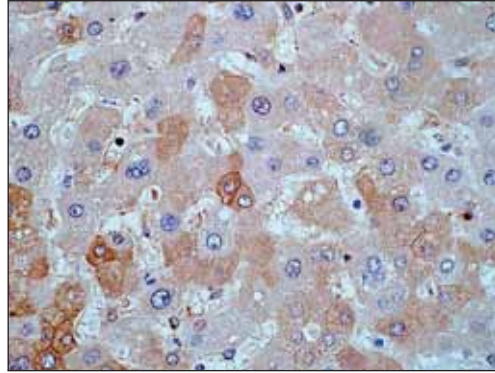
(b) IHC ALDH1A1 positive



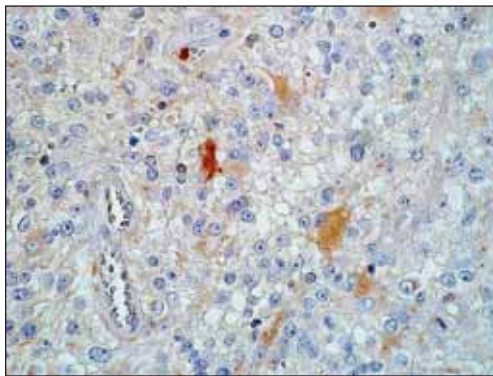
(c) IHC ALDH1A1 negative

Figure 4.3: IHC, 400 x, ALDH1A1. FFPE sections of human liver served as positive control for all ALDH isoforms. Positive primary PGBM with >10% expression of patient No. 95, negative primary PGBM with <10% reactivity of patient No. 9 respectively.

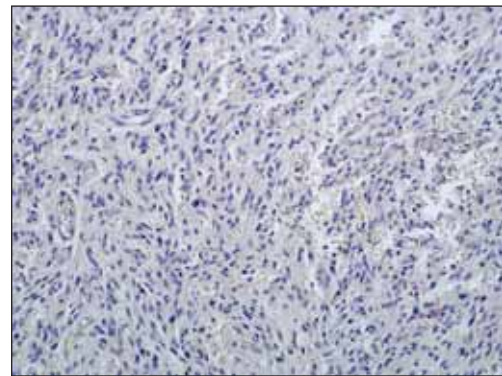
4 Results



(a) IHC ALDH1A3 liver



(b) IHC ALDH1A3 positive



(c) IHC ALDH1A3 negative

Figure 4.4: IHC, 400 x, ALDH1A3. FFPE sections of human liver served as positive control for all ALDH isoforms. Positive primary PGBM with >10% expression of patient No. 95, negative primary PGBM with <10% reactivity of patient No. 9 respectively.

Immunohistochemistry of primary PGBM

In the IHC staining of the PGBM tumours for ALDH1, ALDH1A1 and ALDH1A3, at least two different cell types can be identified (Figure 4.5). ALDH1A1 positive cells are multipolar and star-like. Their end-feet tend to terminate on blood vessel walls, and they can mostly be found in the tumour surrounding tissue. The epithelium of the blood vessel itself reacts positive, as well as macrophages. In contrast, ALDH1A3 positive cells are widely distributed in the tumour area. They are multipolar and star-like, like the ALDH1A1 positive cells. ALDH1 staining does stain both cell types.

The IHC staining pattern of ALDH1 was unevenly disseminated among the tumour tissue. In detail: 55 (84.6%) patients had an ALDH1 expression, 10 (15.4%) did not. In general the ALDH1A1 expression was low. Most ($n = 43$, 66.2%) of the patients were ALDH1A1 negative, only 22 (33.8%) patients had protein expression of ALDH1A1. For ALDH1A3, 16 (24.6%) patients showed no immunoreactivity in contrast to 49 (75.4%) showing expression.

The MOS of PGBM for the ALDH isoforms is shown in Figures 4.6, 9.1, 9.2. Only the ALDH1 expression can confidently be correlated with the MOS. The adjusted hazard ratio for mortality associated with being ALDH1 positive ($n = 55$, MOS = 366 days) was 3.06 ($p = 0.0042$). Patients without ALDH1 ($n = 10$) had a MOS of 922 days. The differences in MOS between ALDH1A1 positive patients ($n = 22$, MOS = 382 days) and ALDH1A1 negative patients ($n = 43$, MOS = 446 days), and ALDH1A3 positive patients ($n = 49$, MOS = 373 days) and ALDH1A3 negative patients ($n = 16$, MOS = 495 days) do not show significance with a odds ratio of 1.23 ($p = 0.43$) and 1.17 ($p = 0.59$), respectively (Figure 9.2).

ALDH1A1 and ALDH1A3, are not predictive for the MOS of PGBM patients by themselves, but might be in combination (Figure 4.7). Double positive (ALDH1A1 and

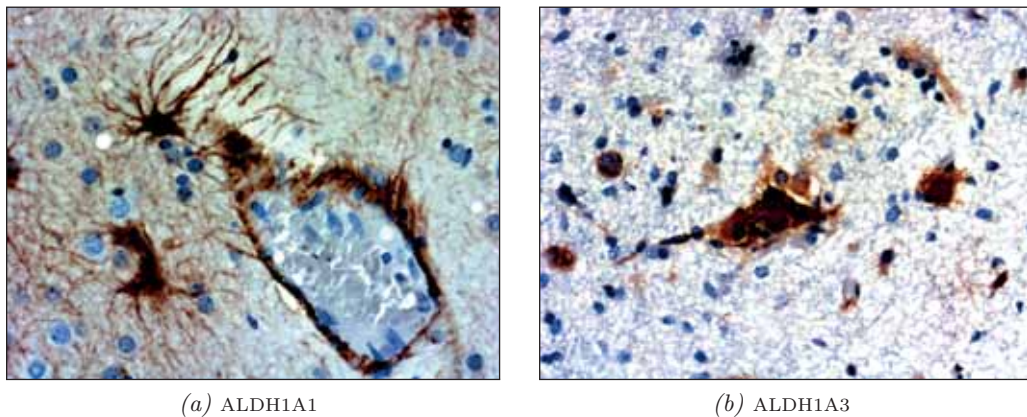


Figure 4.5: IHC, 400 x, ALDH1A1 and ALDH1A3. Staining of primary PGBM of patient No. 106. Different cell types are reacting with the ALDH isotype antibody. ALDH1A1 positive cells have end feet, ending on vessels. ALDH1A3 cells have often two nuclei.

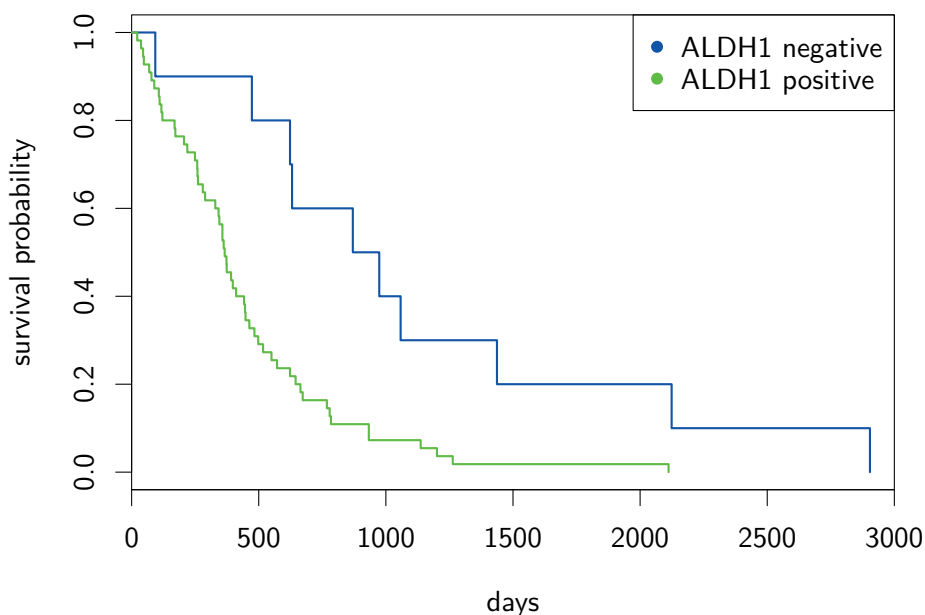


Figure 4.6: Survival of patients with different ALDH1 expression in primary PGBM. ALDH1 positive ($n = 55$) patients have a MOS of 366 days, ALDH1 negative ($n = 10$) patients have a MOS of 922 days.

ALDH1A3) patients ($n=6$) have a MOS of 516 days in contrast to totally negative patients ($n=5$) with a MOS of 870 days. The multiple Cox regression analysis while adjusting for age showed that double positive PGBM patients have a risk of disease progression with a hazard ratio 3.5 ($p = 0.091$).

We could not predict the RFS of 28 patients with secondary PGBM with one of the scorings of ALDH isoforms or in combination of the primary PGBM (Figure 9.3, 9.4, 9.5).

Evaluation of longtime survivors Long time survivors are from special interest because of their obvious different tumour reaction to therapy. 11 longtime survivors were analysed in terms of ALDH expression. Every category of expression is present but no difference in MOS is striking.

Table 4.1: Immunoreactivity of primary PGBM of longtime survivors

	ALDH1	ALDH1A1	ALDH1A3
positive	5	2	8
negative	6	9	3

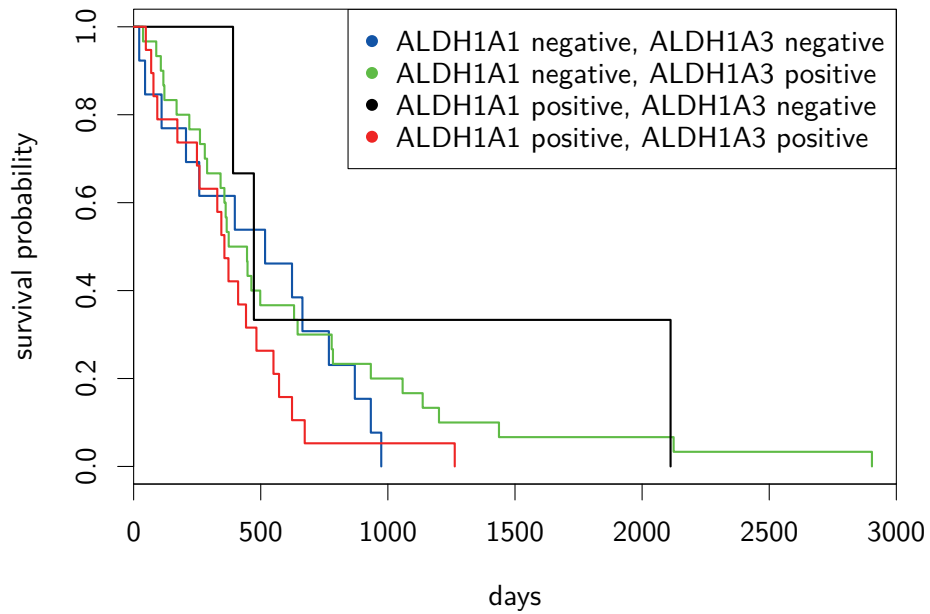


Figure 4.7: Survival of primary PGBM patients with different combinations of ALDH1A1 and ALDH1A3: double negative patients ($n = 15$) have a MOS of 517 days, double positive patients ($n = 19$) have a MOS of 357 days, ALDH1A1 positive and ALDH1A3 negative patients ($n = 3$) have a MOS of 473 days, ALDH1A1 negative and ALDH1A3 positive patients ($n = 28$) have a MOS of 410 days.

Gender separated analysis Another aspect of this study was, to have a look into gender differences. In general, women in this cohort analysis have a shorter overall survival than men. The Cox regression analysis while adjusting for age showed that ALDH1 positive female PGBM patients have a risk of disease progression with a hazard ratio 4.7 ($p = 0.021$), male PGBM patients a hazard ratio 3.5 ($p = 0.023$) (Figure 4.8).

However, isotype specific analysis of ALDH reveals striking differences. The Cox regression for the hazard function of ALDH1A1 expression revealed that female PGBM patients with a ALDH1A1 expression ($n = 7$, MOS = 329 days) have a 2.81 ($p = 0.048$) higher risk for disease progression than female patients without ALDH1A1 expression ($n = 19$, MOS = 448 days, adjusted for age, Figure 4.9). The mutiple Cox regression analysis after adjusting to the age showed that double positive for ALDH1A1 and ALDH1A3 female PGBM patients have a risk of disease progression with a hazard ratio 3.6 ($p = 0.018$).

MOS of male PGBM patients is not affected by the ALDH1A1 expression, but ALDH1A3 is important. ALDH1A3 expressing ($n = 28$, MOS = 370 days) was in males associated with a shorter live (ALDH1A3 negative $n = 11$, MOS = 623 days, Figure 9.9), albeit insignificant (Odds ratio 1.30, $p = 0.46$).

Immunohistochemistry of secondary PGBM

The IHC stainings of the recurrent PGBM tumours for ALDH1, ALDH1A1, and ALDH1A3 were intended as a test if the intensity, the amount of cells, or the reacting cell fraction itself changes in comparison to the primary tumour, but no difference was seen. Even the distribution between negatively and positively reacting patients did not change compared to the primary tumour stainings. 22 (78.6%) samples had an ALDH1 expression, 6 (21.4%) did not. ALDH1A1 expression was seen in 10 (35.7%) patients. For ALDH1A3, 23 (82.1%) patients showed IHC reactivity.

The IHC score of each protein and each patient in the primary and recurrent tumours changes usually not, but in some cases to a higher and less often to a lower score (Table 4.2). No trend can be derived.

The staining of the relapse tumours regarding the IHC expression of ALDH did not show any correlation to the MOS (Figures 9.6, 9.7, 9.8).

Table 4.2: IHC reactivity changes from primary to secondary PGBM.

Protein	less reactivity	same reactivity	higher reactivity
ALDH1	4	19	5
ALDH1A1	3	21	4
ALDH1A3	2	21	5

4 Results

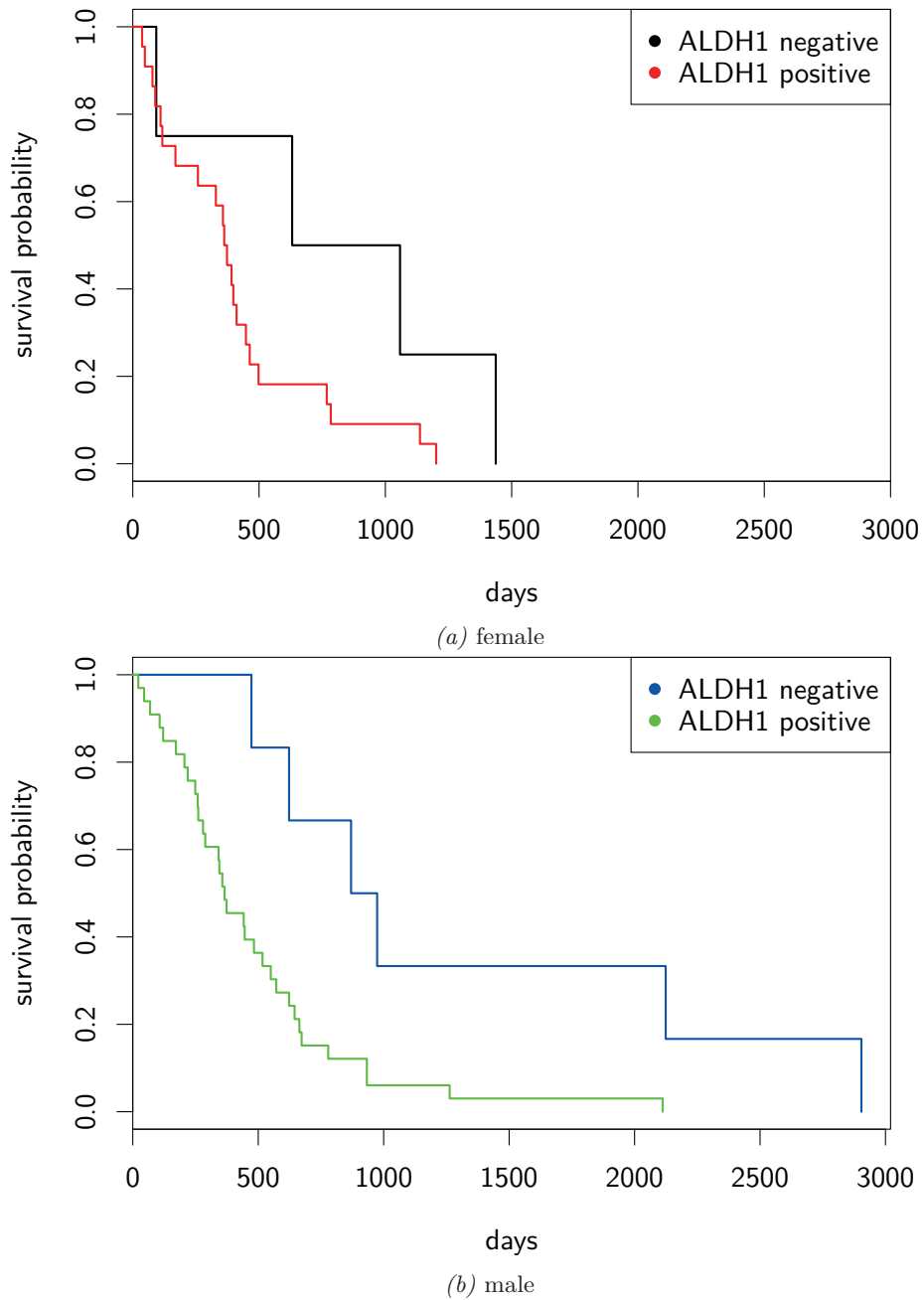


Figure 4.8: Survival of PGBM patients separated by sex and ALDH1 expression. female: ALDH1 positive ($n = 22$) have a MOS of 368 days ALDH1 negative ($n = 4$) have a MOS of 844 days. male: ALDH1 positive ($n = 33$) have a MOS of 366 days ALDH1 negative ($n = 6$) have a MOS of 922 days.

4 Results

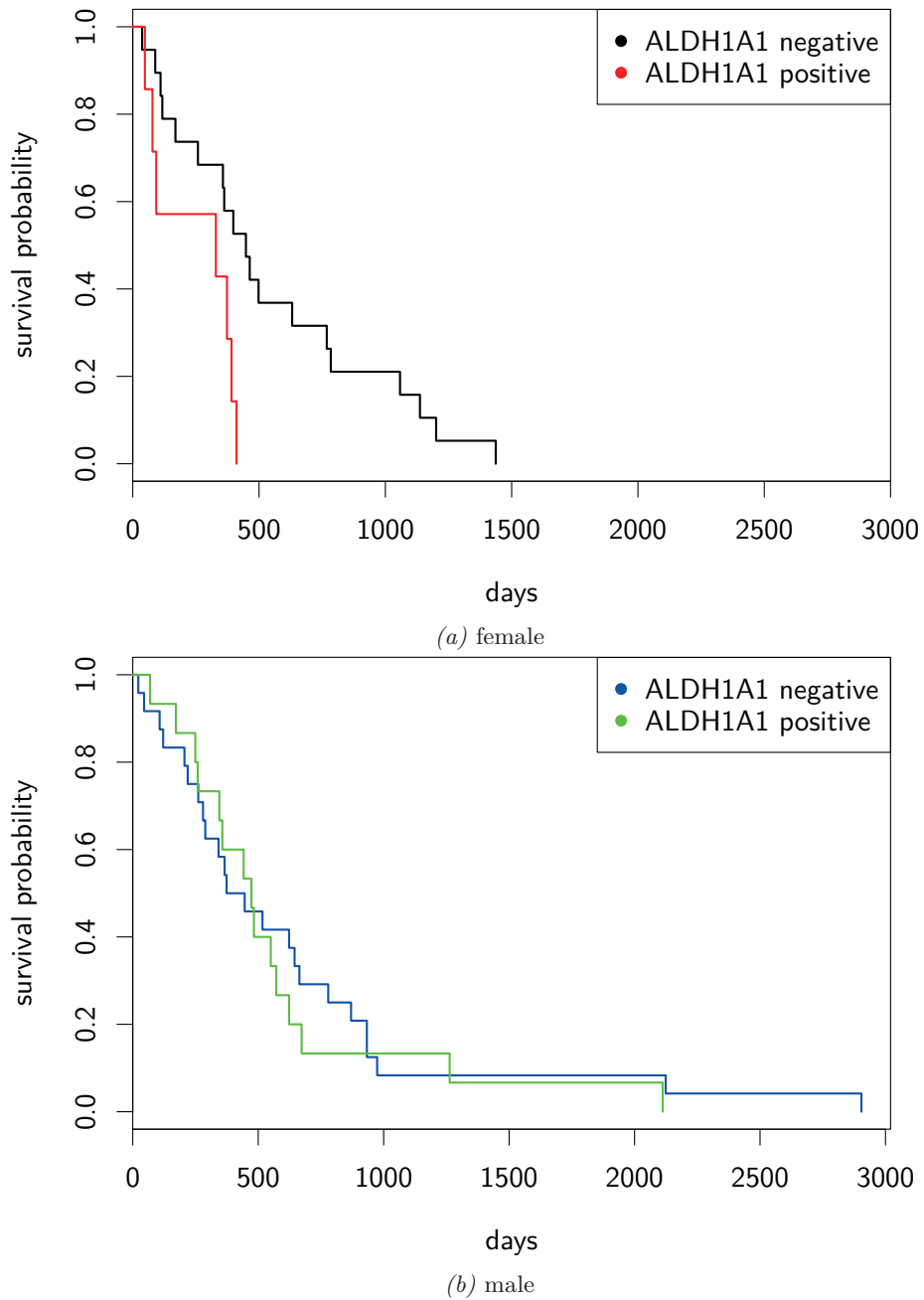


Figure 4.9: Survival of PGBM patients separated by sex and ALDH1A1 expression. female: ALDH1A1 positive ($n = 7$) have a MOS of 329 days ALDH1A1 negative ($n = 19$) have a MOS of 448 days. male: ALDH1A1 positive ($n = 15$) have a MOS of 473 days ALDH1A1 negative ($n = 24$) have a MOS of 410 days.

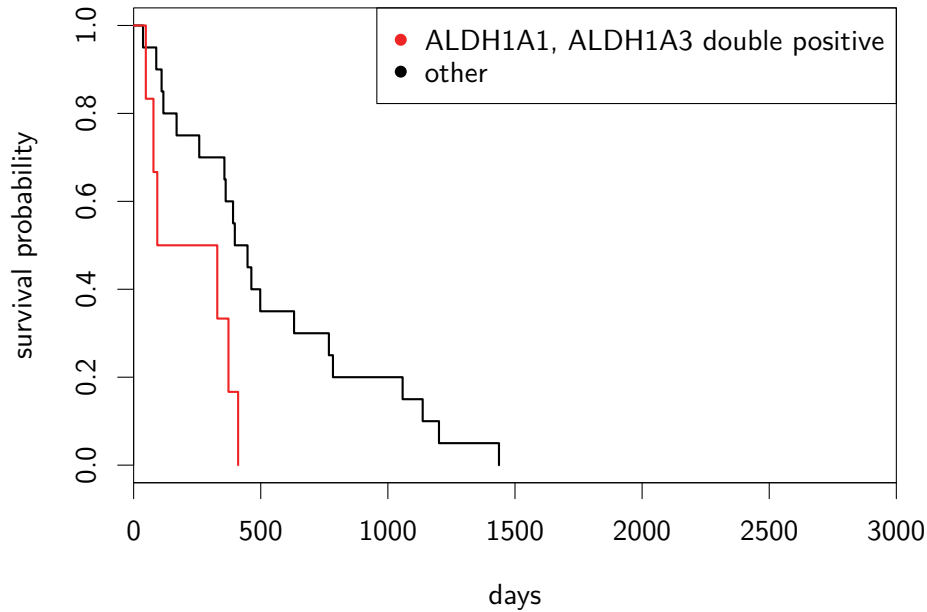


Figure 4.10: Survival of female primary PGBM patients. Double positive patients for ALDH1A1 and ALDH1A3 ($n = 6$) have a MOS of 211 days, all other combinations ($n = 20$) have a MOS of 423 days.

4.1.2 Double immunofluorescence for ALDH1A1 and ALDH1A3 with Ki67

To further investigate the mitotic activity of ALDH1A1 and ALDH1A3 positive cells, we performed a double staining. The double IFC was performed on the same tissues of the PGBM patients cohort as the IHC stainings. The combinations ALDH1A1 and Ki67, and ALDH1A3 and Ki67 were performed (Section 3). We saw more double reactive cells for ALDH1A3 and Ki67 than for ALDH1A1 and Ki67, as shown in Figure 4.11 and Figure 4.12.

4.1.3 MGMT methylation status and expression of different ALDH1 isoforms

As mentioned in Section 1.1, the stable prognostic marker for PGBM is the MGMT promoter methylation status. Patients with methylated MGMT promoter respond better to standard therapy (Stupp et al., 2009). The MGMT promoter methylation of the patients was determined during diagnosis. Cut off for MGMT promoter methylation was set to below 8% for non methylated and above of 8% for methylated, accordingly to Quillien et al. (2012).

To investigate if one of the ALDH1 isoforms is another reliable marker for MOS of GBM patients as described by Schäfer et al. (2012), we analysed IHC expression of ALDH1, ALDH1A1, and ALDH1A3 together with the MGMT status. The general opinion of the favorable outcome of MGMT promoter methylated patients can be

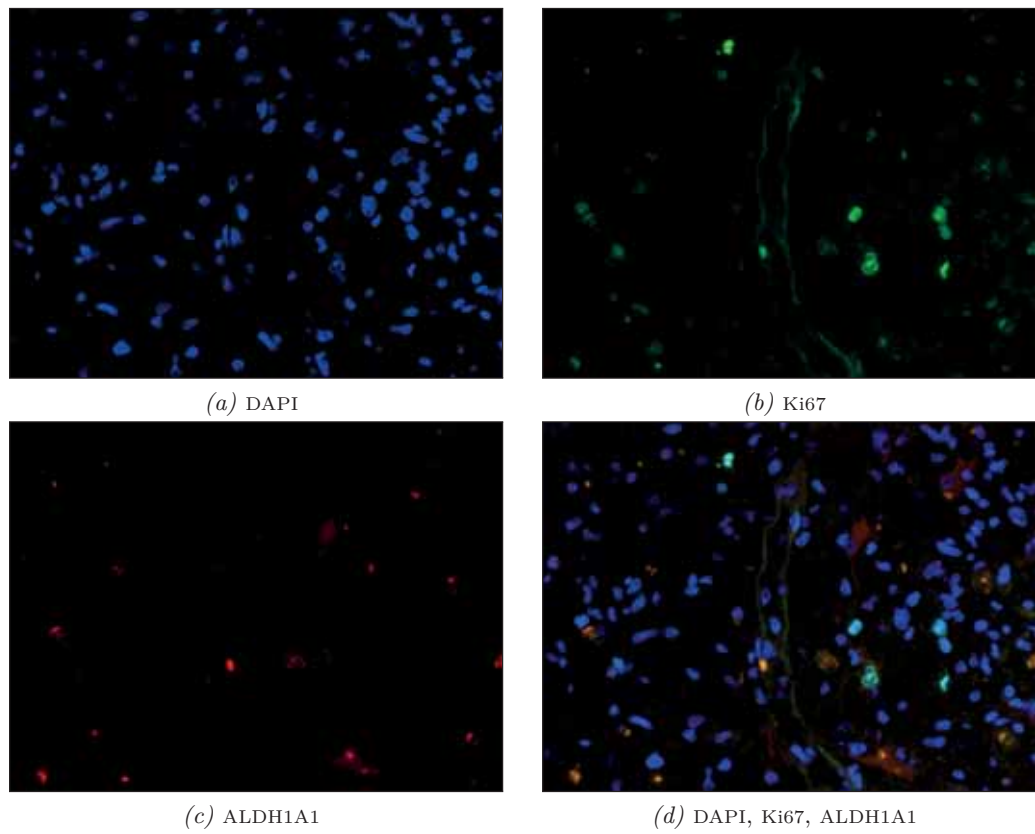


Figure 4.11: IFC, 400x, DAPI, Ki67, ALDH1A1. Secondary PGBM sample of patient No. 50. ALDH1A1 positive cells are not positive for Ki67.

4 Results

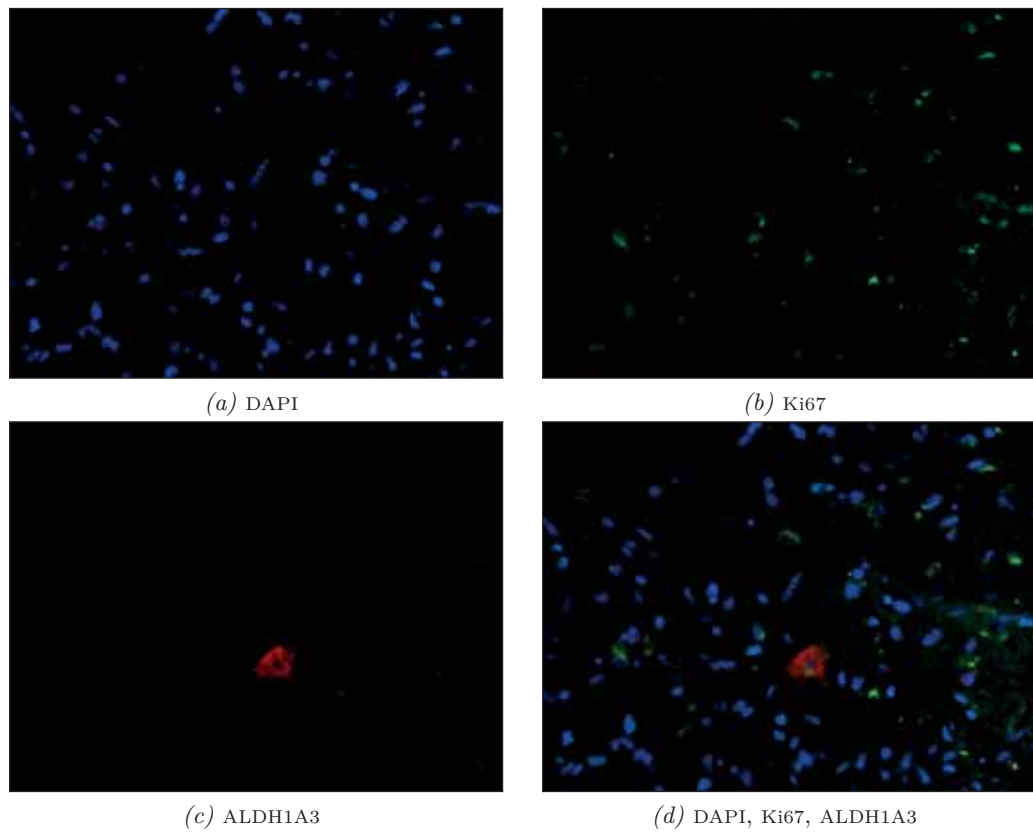


Figure 4.12: IFC, 400 x, abbreviationstylecommandDAPI, Ki67, ALDH1A3. Secondary PGBM sample of patient No. 50. Double positive cell for ALDH1A3 and Ki67.

supported by our data (Figure 4.13) (Stupp et al., 2009).

The combined analysis (Figures 4.14, 9.10 9.11) of the expression of ALDH isoforms and MGMT promoter methylation status show that the combination of MGMT promoter methylated and ALDH1 IHC negative status elongates MOS (Figure 4.14) which is in consent with the data from Schäfer et al. (2012). The Risk of patients to die with MGMT promoter methylation and being ALDH1 positive ($n = 19$, MOS = 463 days) is 2.68 times ($p = 0.047$) higher than ALDH1 negative patients ($n = 5$, MOS = 870 days).

The observations of the survival of PGBM patients with MGMT promoter methylation, ALDH1A1 positive ($n = 9$, MOS = 373 days) show that they live shorter than ALDH1A1 negative patients ($n = 15$, MOS = 664 days), although the number of observation is not sufficient to gain statistical significance (odds ratio 1.85, $p = 0.188$). For ALDH1A1 expression in combination without MGMT promoter methylation, there is no difference (positive $n = 28$, MOS = 391 days, negative $n = 13$, MOS = 350 days, Figure 9.10b).

There is also no difference in MOS of patients with different ALDH1A3 expression and MGMT promoter methylation status: patients without MGMT promoter methylation and with ALDH1A3 ($n = 28$) have a MOS of 344 days and patients without ALDH1A3 ($n = 13$) MOS of 473 days; patients with MGMT promoter methylation and with ALDH1A3 ($n = 21$, MOS = 498 days) do not live shorter than patients without ALDH1A3 ($n = 3$, MOS = 664 days), due to small number of patients, no significance was analysed.

4.1.4 ALDH expression by RT-PCR

RT-PCR was performed out of the same patient tissue as the IHC, as described in Section 3.2.4, with primers listed in Table 3.6. As a positive control for all ALDH proteins LN18 and human universal gene were used (Table 4.4). Liver and normal brain tissue were analyzed as reference. We isolated RNA out of 36 FFPE primary PGBM tumour samples. We could not isolate a sufficient amount of material out of two samples due to the small size of available tumour tissue. GFAP and GAPDH were used as house keeping genes to evaluate cDNA content. Negative samples were excluded from further analysis (Figure 4.15).

Table 4.3: MGMT and ALDH1

	ALDH1	
	positive	negative
MGMT promotor methylated	19	5
MGMT promoter not methylated	36	5

4 Results

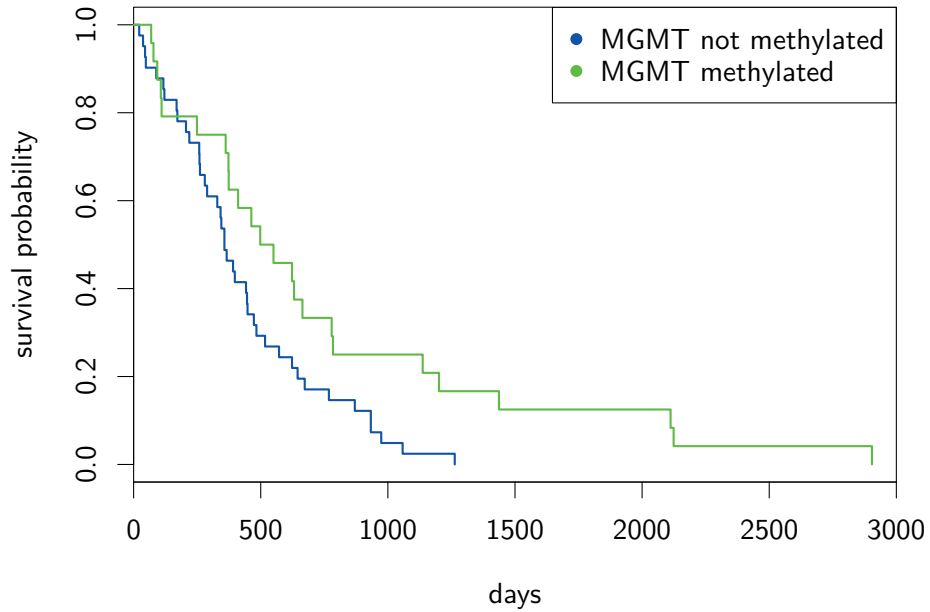
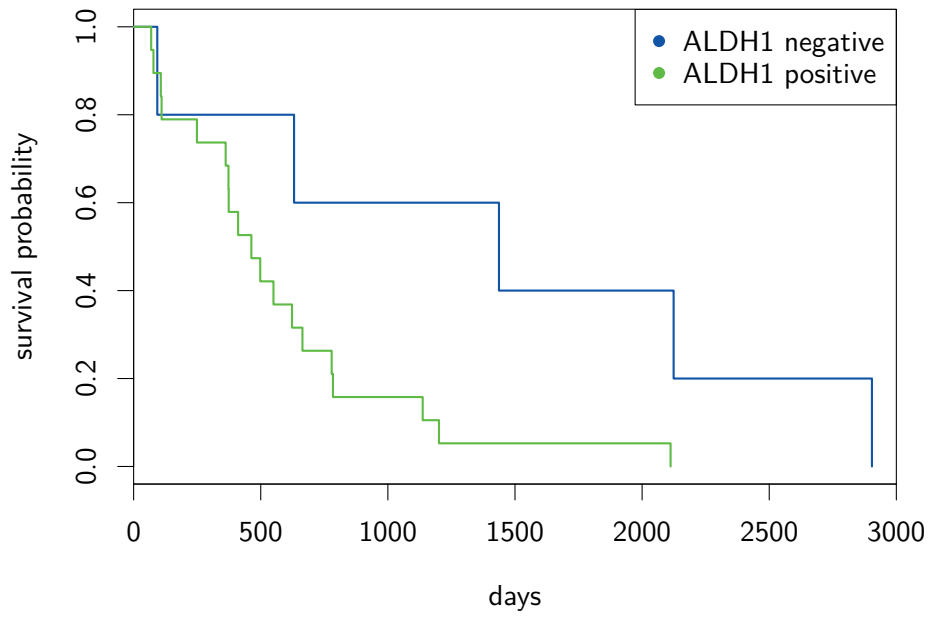


Figure 4.13: Survival of patients MGMT promoter methylated ($n = 24$, MOS = 524 days) and MGMT promoter not methylated ($n = 41$, MOS = 357 days) in primary PGBM. The risk of death of MGMT promoter methylated PGBM patients is 0.57 times ($p = 0.048$) smaller than counterpart.

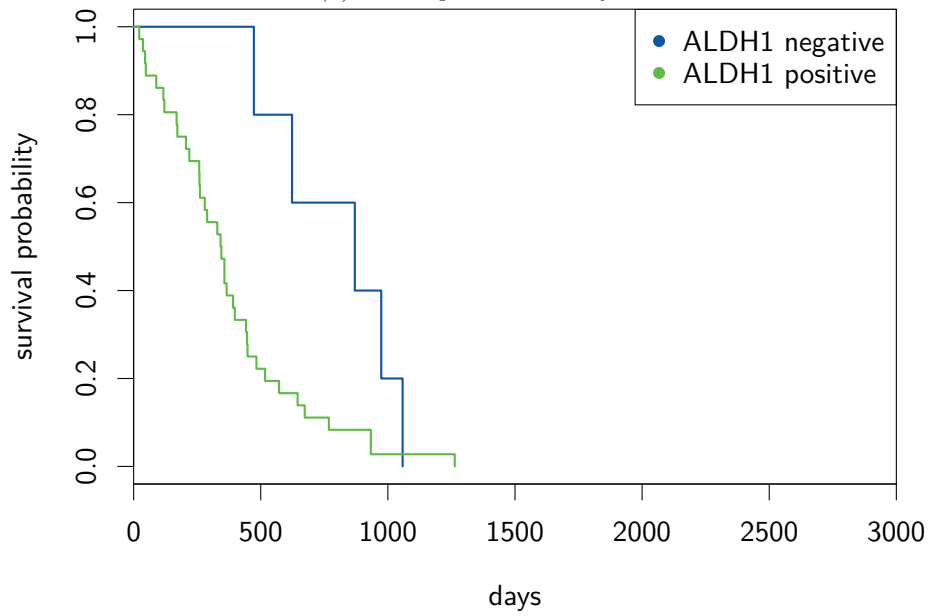
Table 4.4: RT-PCR of controls

Specimen	GFAP	GAPDH	ALDH						
			1A1	1A2	1A3	2	3A1	7A1	8A1
LN18	+	+	+	+	+	+	+	+	+
Liver	-	-	-	-	-	-	-	-	-
human ref. gen	+	+	+	+	+	+	+	+	+
brain	+	+	-	-	-	-	-	-	-

4 Results



(a) MGMT promoter methylated



(b) MGMT promoter not methylated

Figure 4.14: Survival of patients with or without MGMT promoter methylation in combination with ALDH1 expression in primary PGBM. No MGMT promoter methylation ALDH1 positive patients ($n = 36$) have a MOS of 344 days compared to ALDH1 negative patients ($n = 5$) with a MOS of 870 days. With MGMT promoter methylation ALDH1 positive patients ($n = 19$) have a MOS of 463 days compared to ALDH1 negative patients ($n = 5$) with a MOS of 1437 days.

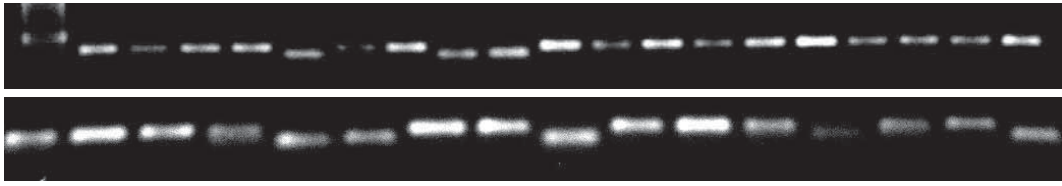


Figure 4.15: RT-PCR of primary PGBM with GFAP of all patients with secondary PGBM. Patients with non specific binding of primers were excluded from analysis due to insufficient extraction or degenerated mRNA.

Except 6 (25%) patients all are ALDH1A1 positive, which is in contrast to the IHC expression of ALDH1A1. 66.2% of patients did show no or less than 10% immunoreactivity to ALDH1A1. ALDH1A2 was detectable in 7 cases. 17 (60%) patients are positive for ALDH1A3, which is in accordance to the IHC staining. 3 out of 24 samples were ALDH2 positive, 9 (37%) for ALDH7A1. In the collective only one sample was positive for ALDH3A1, one sample for ALDH8A1. No pattern of combinations of different ALDH isoforms can be detected (Table 9.4).

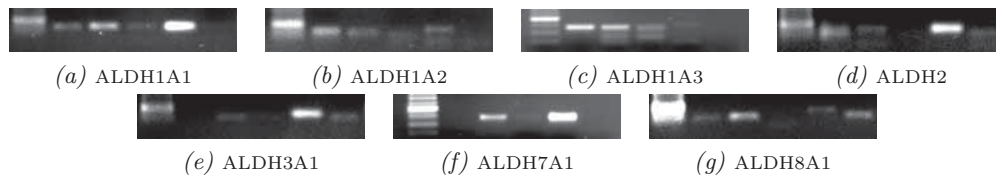


Figure 4.16: RT-PCR of ALDH isoforms (25 bp marker, Patient No. 2, 25, and 47, as positive control LN18 and the non template control). ALDH1A1: Patient No. 2, 25, 47, LN18 positive. ALDH1A2: Patient No. 2, 25, LN18 positive, patient No. 47 negative. ALDH1A3: patient No. 2, 25, No. 47, LN18 positive. ALDH2: No. 25, LN18 positive, patient No. 2, 47 negative. ALDH3A1: LN18 positive, patient No. 2, 25, 47 negative. ALDH7A1: patient No. 25 and LN18 positive, patient No. 2, 47 negative. ALDH8A1: patient No. 2, 25, 47 and LN18 negative.

4.2 Comparative analysis of ALDH in a xenograft and a syngeneic model for GBM

For future experiments it is necessary to find a suitable model with ALDH1A1 and ALDH1A3 expression. To evaluate a xenograft mouse model and a syngeneic model for ALDH1A1 and ALDH1A3 expression IHC was performed. Mouse experiments were done in accordance with the German welfare law. A human PGBM cell line (U87-MG) and a mouse PGBM cell line (G1261) were orthotopically implanted into mice as described in Section 3.2.5.

Procedure of IHC staining can be found in Section 3. As positive control for both ALDH isoforms in IHC analysis served a mouse liver (C57BL/6JRj, Figure 4.17).

4.2.1 U87-MG xenograft model

The U87-MG cells are ALDH1A3 positive and ALDH1A1 negative according to The Human Protein Atlas (Uhlén et al., 2005) and verified in cell pellet analysis shown in Figure 4.18.

The U87-MG cells implanted orthotopically into a NMRI-nude mice do not grow infiltrative. The tumour consists of pleomorphic cells with irregular shaped nuclei and numerous mitosis. The histopathological examination revealed no neovascularisation or necrotic areas within the tumour. Macroscopical screening of the animals for metastasis were negative.

In the histopathologically analysed mouse brains, however, no cell can be found positively stained for ALDH1A1. The immunoreactivity for ALDH1A3 is non-uniform. In the group of disulfiram treated mice ($n = 7$); 3 mice show no reactivity, 2 show scattered positively stained tumour cells, and 2 show more than 50 % immunoreactivity for ALDH1A3 (Figure 4.19). In the untreated control group ($n = 7$) two mice developed no tumour. The tumour of the other mice consist of scattered positively stained tumour cells for ALDH1A3 and none for ALDH1A1.

4.2.2 G1261 syngeneic model

The G1261 cells implanted orthotopically into a C57BL/6JRj mice show cellular pleomorphism and irregular shaped nuclei. Neovascularisation is frequently found within the tumour. No necrotic areas can be found due to tumour size. The tumour did not grow infiltrative and did not metastasise in other organs.

There is no characterisation of G1261 in terms of ALDH isotype expression. The

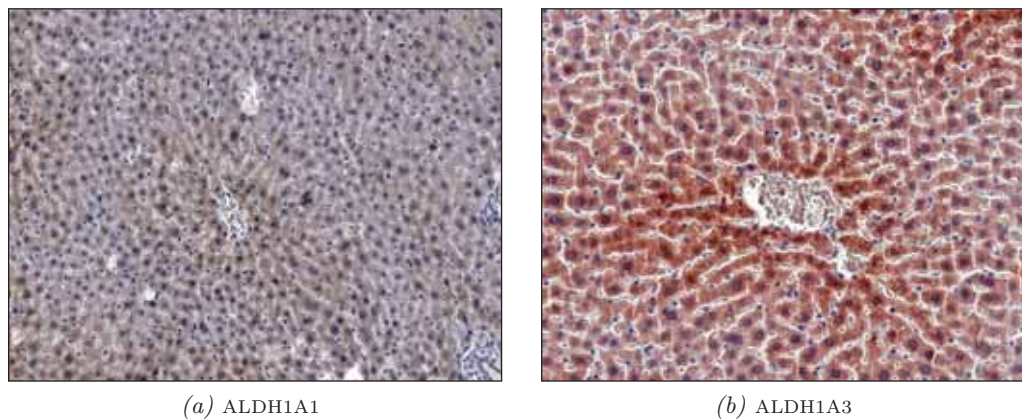


Figure 4.17: IHC, 200 x, ALDH1A1 and ALDH1A3. The mouse liver (C57BL/6JRj) served as positive control for both ALDH antibody.

4 Results

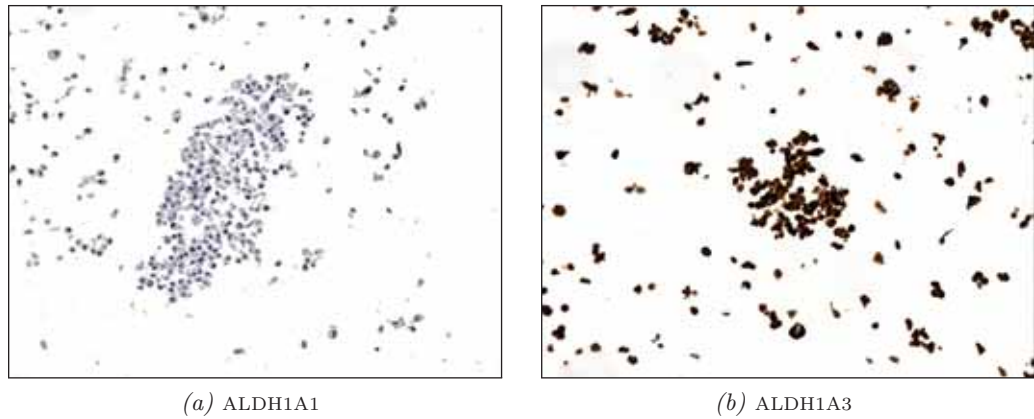


Figure 4.18: IHC, 200 x, ALDH1A1 and ALDH1A3. U87-MG PGBM cells show no IHC expression for ALDH1A1 but high expression for ALDH1A3.

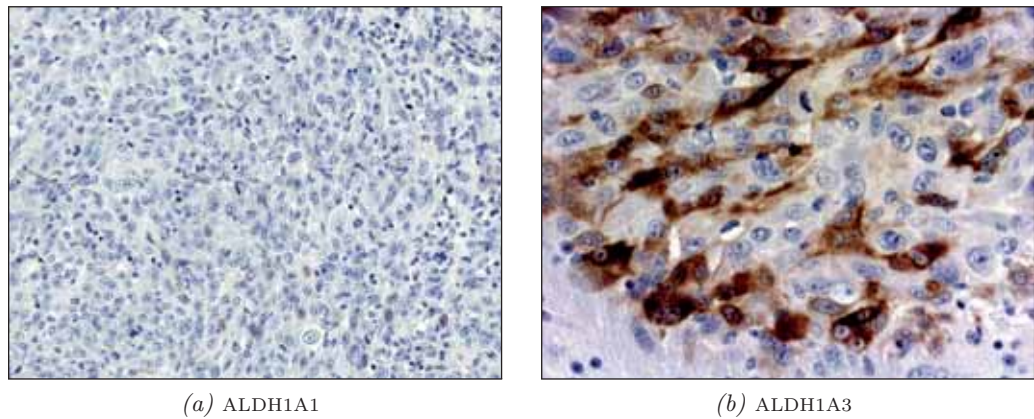


Figure 4.19: IHC , ALDH1A1 200 x and ALDH1A3 400 x. IHC expression in a NMRI-nude mouse with implanted U87-MG PGBM cells. No IHC expression for ALDH1A1 but high expression for ALDH1A3.

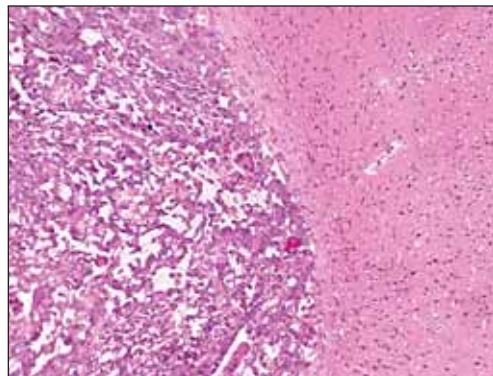


Figure 4.20: H&E, 200 x. Section of G1261 PGBM cells implanted into a C57BL/6JRj mice.

4 Results

cell pellet of G1261 stains positively for ALDH1A3, but is negative for ALDH1A1 (Figure 4.21). The implanted G1261 cell show light immunoreactivity for ALDH1A3 (Figure 4.22). ALDH1A1 expression was not detectable.

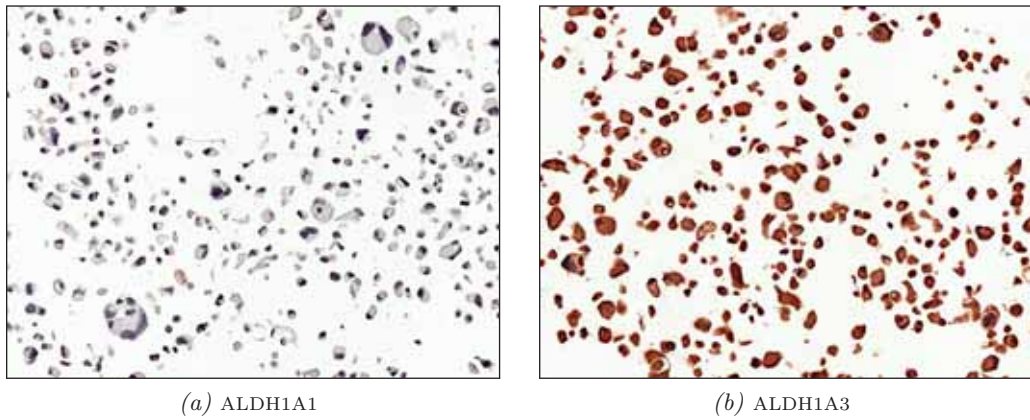


Figure 4.21: IHC 200 x, ALDH1A1 and ALDH1A3. G1261 PGBM cells do not express ALDH1A1 but ALDH1A3.

4.3 Evaluation of ALDH isoforms in rat GBM cells

The rat GBM cell line C6 and F98 were analysed for ALDH expression as well. IHC was performed according to the protocol (Section 3). A rat (Wistar) liver served as positive control for ALDH1A1 and ALDH1A3. Stained rat GBM cells show IHC reactivity against ALDH1A3 but not against ALDH1A1 (Figure 4.23, 4.24).

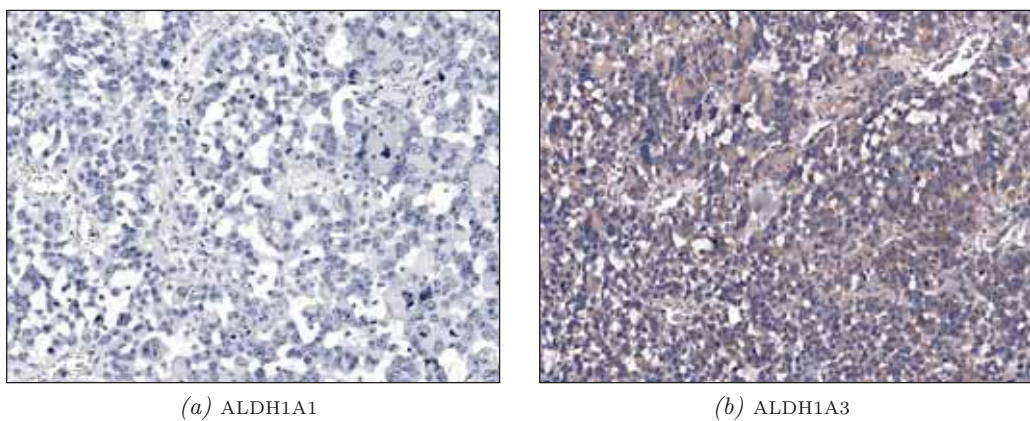
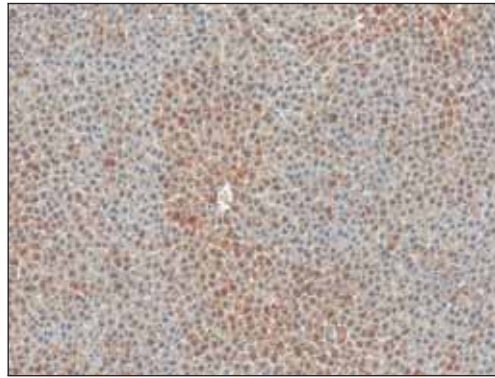
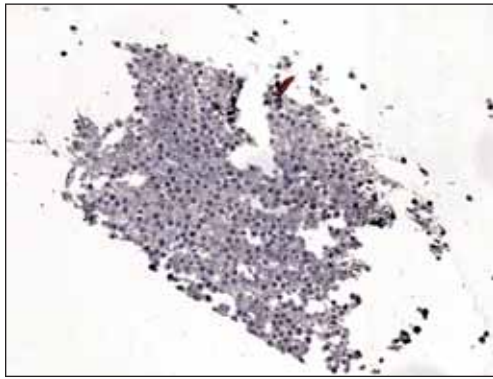


Figure 4.22: IHC, 200 x, ALDH1A1 and ALDH1A3. ALDH expression in an C57BL/6JRj mouse with implanted G1261 PGBM cells.

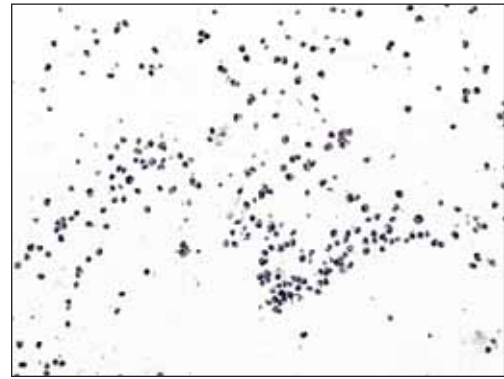
4 Results



(a) rat liver



(b) C6



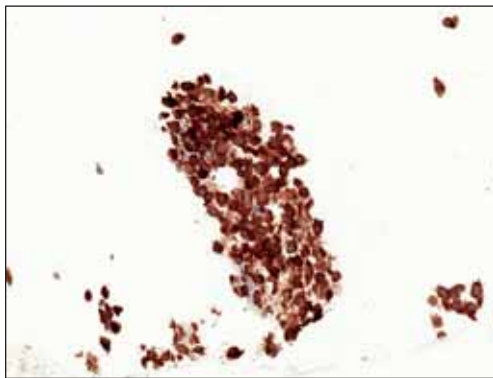
(c) F98

Figure 4.23: IHC, ALDH1A1. ALDH1A1 expression of rat liver (100 x), C6 (200 x), and F98 (200 x) GBM cells. The rat (Wistar) liver served as positive control for ALDH1A1 AB. C6 and F98 do not show any reactivity to the ALDH1A1 antibody.

4 Results



(a) rat liver



(b) C6



(c) F98

Figure 4.24: IHC, ALDH1A3 expression of rat liver (100 x), C6 (200 x), and F98 (200 x) GBM cells. The rat (Wistar) liver served as positive control for the ALDH1A3 AB. C6 and F98 show a great reactivity to the ALDH1A3 antibody.

4.4 Immunohistochemistry analysis of ALDH expression in canine GBM

As a investigative approach two biopsies of Cocker Spaniel and one German Shepherd dog are analysed for ALDH1A1 and ALDH1A3 expression. The Cocker Spaniels is female and 12 years old. From the German Shepherd age and sex is unknown. GBM in dogs are rare and because they occasionally under go surgery. Both biopsies show necrosis, neovascularisation, and cellular pleomorphism (Figure 4.25). Numerous mitotic figures can be found.

Biopsies were analysed with the same antibody as the human PGBM patients cohort (Table 3.5). Analysis is possible because proteins are up to 93% (ALDH1A3) identical. Canine liver served as control for the isotype specific AB against ALDH1A1 and ALDH1A3 (Figure 4.26). IHC staining was carried out according to the protocol (Section 3). ALDH1A3 IHC expression was detected in large parts of the GBM tumours (Figure 4.26). Preponderantly tumour cells stained positive for ALDH1A3. ALDH1A1 expression was not found in one of the cases (Figure 4.26).

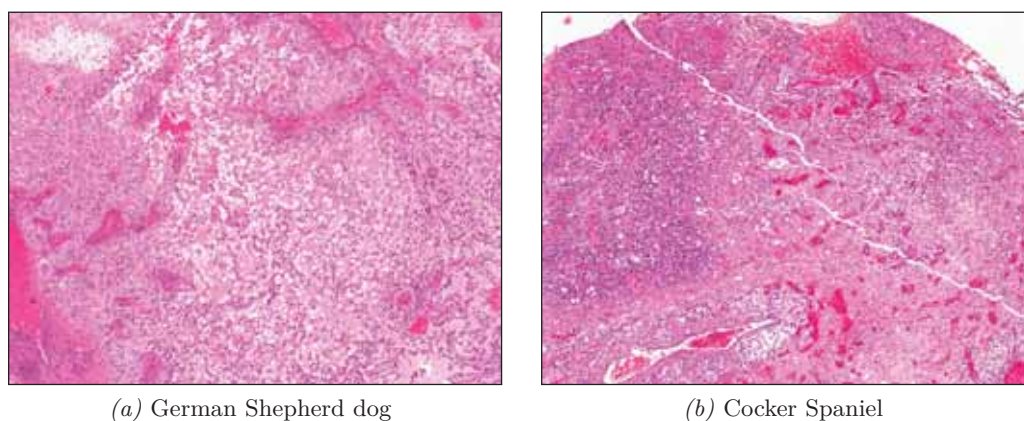


Figure 4.25: H&E, 50x. Sections of canine GBM samples: a) German Shepherd dog unknown sex and age. b) 7 years old, female Cocker Spaniel.

4 Results

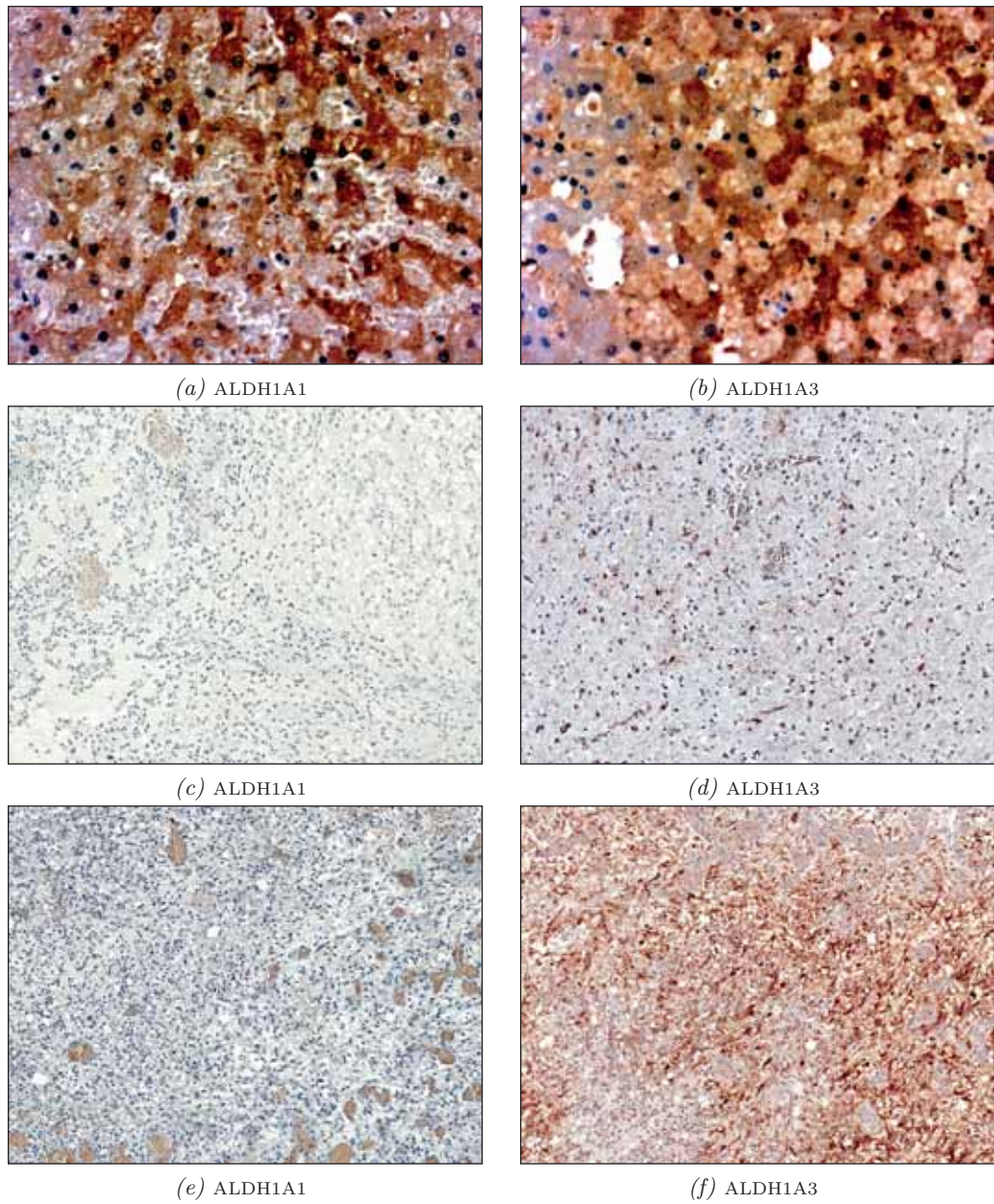


Figure 4.26: IHC, ALDH1A1 and ALDH1A3. a + b) Liver of a 6 months old pug as positive control for ALDH1A1 and ALDH1A3 (50x). c + d) German Shepherd dog (100x) e + f) Cocker Spaniel (100x). Canine GBM show no ALDH1A1 expression but ALDH1A2 positive cells are distributed among the tumour cells.

5 Discussion

5.1 Analysis of the distribution of ALDH in human PGBM

Glioblastoma multiforme is one of the most devastating diseases. 15 months after diagnosis, despite all therapy, only half of the patients are still alive. PGBM are normally resected and afterwards treated with TMZ and radiotherapy. Due to the morphology of the tumour, a complete resection is rarely achieved. To understand PGBM CSC and their ability to evade therapy, it is essential to learn more about genetic alterations and molecular markers. In this thesis, the ALDH isoform specific expression in GBM tissue was analysed with IHC and RT-PCR. The findings point out that there is a striking need of isotype specific investigations.

5.1.1 Primary PGBM

ALDH1A3 is a marker for tumour cells and ALDH1A1 is a marker for reactive astrocytes. This is supported by the staining pattern of ALDH1A1 and ALDH1A3 and the performed double IFC with Ki67. ALDH1A1 positive cells were found more often in the tumour adjacent region than in the tumour itself, in accordance to Xu et al. (2015b).

ALDH1 The observations in this thesis show a correlation between ALDH1 IHC expression and patient survival (Figure 4.6, p. 36). Cox regression analysis revealed that ALDH1 negative patients live longer than positive patients (odds ratio 3.06, $p = 0.0042$, adjusted for age). The presented findings are in accordance with Schäfer et al. (2012) showing that ALDH1 is an independent marker for PGBM outcome. Only data published by Adam et al. (2012), suggesting ALDH1 as a prognostic maker for better outcome of GBM patients, stays in contrast. Adam et al. (2012) analysed 56 tumour resections and 37 biopsies of GBM patients, without differentiation by IDH mutation between PGBM and SGBM and with different therapy regimens. Altogether, the comparability of these studies to the observation in this thesis is limited and has to be elucidated in further investigations.

ALDH1A1 A clear correlation of the survival of ALDH1A1 positive and negative patients could not be observed in this thesis (Figure 9.1, p. 70). The MOS of ALDH1A1 positive and negative patients suggests a correlation, but this could be only by chance (odds ratio 1.23, $p = 0.43$). Campos et al. (2011) report of an increased intratumoural retinoid availability and ALDH1A1 overexpression, associated with an unfavorable outcome of GBM patients. This stays in contrast to the function of

ALDH1A1 in RAS as a pro-differentiation enzyme, leading to cells, which should be sensitive to chemo- and radiotherapy. In acute promyelocytic leukemia, for example, patients are treated with RA and achieve a complete remission in 70%. RA targets PML, a retinoic acid receptor fusion protein, and is therefore regarded as molecular-targeted therapy. PML expression is inversely correlated with cell proliferation in acute promyelocytic leukemia as well as in GBM (Iwanami et al., 2013). Former *ex vivo* and *in vivo* studies showed inhibition of GBM CSC tumour growth and xenograft mouse model tumours when treated with RA (Campos et al., 2011, 2010). Mouse tumours showed moderate signs of angiogenic activity, impaired migration, and growth inhibition. GBM CSC treated with RA showed higher differentiation compared to untreated CSC. However, preclinical trials with RA given to GBM patients, only including those with recurrent disease, show only limited effects (Defer et al., 1997; Kaba et al., 1997; Phuphanich et al., 1997). In a phase II study, promising effects can be seen, using 13-*cis* retinoic acid for long time treatment (Wismeth et al., 2004). Further studies determining the mechanism of PML promoting drug resistance in GBM and the seemingly inconclusive role of ALDH1A1 in RA are needed.

ALDH1A3 Another result presented in this thesis (Figure 9.2, p. 70) shows a difference in MOS of PGBM patients with and without ALDH1A3 expression, although not statistically significant (odds ratio 1.17, $p = 0.59$). This analysis was performed to substantiate Mao et al. (2013) and Ni et al. (2015) findings that ALDH1A3 is a predictive marker for MOS of PGBM. In the single center study of Ni et al. (2015), a correlation between both the promoter methylation of *ALDH1A3* and the IHC expression, and a longer survival of GBM patients was found. Limitations of their study are the differences in treatment of the analysed GBM patients and the unified evaluation of PGBM and SGBM patients. In this thesis, only PGBM patients were analysed with the same treatment, but no significant prognostic correlation of ALDH1A3 and MOS of patients was observed. An increase of observations and a separate analysis of SGBM is intended to validate or reject the supposed differences. With the help of transcriptome array analyses, Mao et al. (2013) investigated low and high grade gliomas and saw an increase of the latter in ALDH1A3 expression. Furthermore, a significant up regulation of *ALDH1A3* was associated with the MES subtype and a down regulation in PN GBM. Pharmacological inhibition of ALDH1 or shRNA knock-down of *ALDH1A3* attenuates PN to MES transformation and *in vitro* growth of MES GBM CSC (Mao et al., 2013).

Long time survivors

Long time survivors are interesting for research because of the obvious difference to the shorter living patients (Section 4.1.1). The separate analysis of PGBM long term survivors ($n = 11$) in this thesis did not show any distinction for shorter living PGBM patients in ALDH IHC expression. A genomic alteration or difference in metabolism leading to this advantage in therapy response has not yet been found. Indications of altered signaling pathways have been described lately by Fazi et al. (2015), showing

that long time survivors ($n = 4$) differ in TGF- β expression compared to shorter living PGBM patients ($n = 9$). A collection of a larger cohort of long time survivors could reveal more information about beneficially altered signaling.

Gender analysis

Gender differences in incidence, like in GBM, and progression of human disease are mechanistically important to understand varying response to treatment. In metabolic diseases, inflammation, and some cancers, sex-specific divergences are observed. The results presented in this thesis (Section 4.1.1) suggest a difference of female and male patients in terms of ALDH1A1 IHC expression, next to the described ALDH1 correlation to survival (Figure 4.8). Female patients significantly profit from the lack of ALDH1A1 expression (odds ratio 2.81, $p = 0.048$), while men seem not to be influenced by this isotype (Figure 4.9). The multiple Cox regression analysis after adjusting to the age showed that double positive for ALDH1A1 and ALDH1A3 female PGBM patients even have a risk of disease progression with a hazard ratio 3.6 ($p = 0.018$). The reasons for this gender differences in PGBM are unknown. Observations of other diseases suggest that estrogen influences the expression of *ALDH1A1*, suppresses *ALDH1A2* and *ALDH1A3*, following a female-specific mechanism of retinoic acid signaling (RAS) (Petrosino et al., 2014). The RAS pathway, for example in adipose tissue, is described to be influenced by estrogen. In breast cancer, Isfoss et al. (2013) could show an increased ALDH1A1 positive cell proportion in breast ductules in women with a familial risk for breast cancer. As estrogen regulated ALDH expression is tissue dependent (Duester et al., 2003); a possible effect on PGBM tumour cells cannot be excluded. Another explanation for the observed correlation could be found in studies of neurodegenerative diseases showing a protective action of estradiol and estrogen receptors in the female and male brain. These receptors are cooperating in multiple signaling mechanisms (Arevalo et al., 2015; Dhandapani and Brann, 2002; Hatch et al., 2005). Aromatase, the enzyme that converts androgens into estrogens, is physiologically expressed in neurons from different brain regions and is rapidly regulated (Cornil et al., 2012). After brain injury, however, reactive astrocytes show increased aromatase expression, reducing reactive gliosis and protecting neurons (Azcoitia et al., 2001; McCullough et al., 2003). Estrogen receptor α , estrogen receptor β , and G protein-coupled estrogen receptor trigger parallel neuroprotective mechanisms by activation of extracellular signal-regulated kinase 1 and 2 as well as phosphatidylinositide 3-kinases signaling and pro-apoptotic c-Jun N-terminal kinase signaling (Wu et al., 2005; Yang et al., 2010; Zhao and Brinton, 2007). However, most knowledge of neuroprotective estrogen signaling is only based on acute models of neurodegeneration. Data on continuous influences of female hormones in chronic, slowly progressing diseases is missing. A large cohort study suggests that only exogenous hormones have a protective effect on gliomas (Felini et al., 2009). The data presented in this thesis, the gender separated analysis, shows striking differences between female and male in survival and ALDH1A1 IHC expression in PGBM samples (Figure 4.9). In general, the MOS of female and male PGBM

patients differ by 144 days (Table 3.3). Furthermore, female ALDH1A1 positive patients live shorter than female ALDH1A1 negative patients (Figure 4.9). In former ALDH studies, the differentiation between male and female human PGBM was not analysed. Only one orthotopic GBM rat model identifies a survival advantage of female, estrogen treated, ovariectomized nude rats (Plunkett et al., 1999). In the future, the four core genotypes model could help to find out if sex chromosome or gonadal hormones are responsible for the observed gender differences (Arnold and Chen, 2009; De Vries et al., 2002). With the help of this model, answers to the question if gender differences are associated with neuroprotective mechanisms or if ALDH interferes with estrogen in RAS like in adipose tissue, due to the chromosomal influences, or due to random chance, might be found. GBM subtype specific analysis showed that males are categorized more often into the MES subtype than female patients (Sun et al., 2014). Furthermore, male MES GBM astrocytes showed greater growth and colony forming capacity than female ones and could be correlated to retinoblastoma signaling inactivation. MES GBM are in general the unfavourable subtype, being insensitive to standard therapy. The in this thesis presented data presented was not subclassified and can therefore not be compared to the data from Sun et al. (2014). In general, a subclassification based on biopsies or small tumour samples is not representative for the whole tumour and is usually made without respect to the heterogenous nature of GBM. Therefore, subclassification of PGBM was not performed in this thesis.

MGMT and different IHC expression of ALDH1 subtypes

The hypothesis that MGMT promoter methylation status and ALDH1 IHC expression are independent markers for MOS of PGBM is corroborated with the data presented in this thesis (Section 4.1.3). Following new recommendations, the cut-off for the MGMT promoter methylation status was set to a much lower percentage in this thesis (Quillien et al., 2012) than in former studies by Schäfer et al. (2012). Corroborating this well known marker with the presented data indicates representativeness with respect to MGMT promoter methylation and response to TMZ.

The hypermethylation of *ALDH1A3*, leading to a low IHC expression of ALDH1A3, results in a significantly favourable outcome of PGBM patients without MGMT promoter methylation (Zhang et al., 2013). The data presented here is leading in the same direction but requires a higher number of observation to gain significance (Figure 9.11).

RT-PCR of human PGBM samples

The RT-PCR was performed to relevance of *ALDH1A1*, *ALDH1A2*, *ALDH1A3*, *ALDH2*, *ALDH3A1*, *ALDH7A1*, and *ALDH8A1* (p. 41) in PGBM.

No specific pattern of ALDH expression was seen in analysed microdissected samples. The mRNA level of *ALDH1A3* can be directly associated to the IHC expression. The *ALDH1A1* mRNA levels were surprisingly high with 75% positive PGBM in the

investigated patients. This is evidence for strict post transcriptional or post translational regulation. The promoter of *ALDH1A1* contains a positive regulatory region (−91 to 53 bp) (Yanagawa et al., 1995), and post translational regulation through acetylation or deacetylation of lysin was found in breast cancer (Zhao et al., 2014). A study dealing with PGBM CSC and *ALDH* regulation has not been performed, but it can be estimated that regulatory systems could be found.

5.1.2 Secondary PGBM

This thesis challenges the findings of Schäfer et al. (2012). The claimed change of the immunoreactive fraction of ALDH1 increase in secondary PGBM compared to corresponding primary tissue (Table 4.2, p. 38) was not reproduced. This raises the question if ALDH1 detects CSC or differentiated cells. Keeping the CSC theory in mind and the proclaimed insensitivity of CSC to therapy, the equal proportion of ALDH1 expression in primary and secondary PGBM observed by IHC in this thesis suggests that the differentiated cell population expresses ALDH1.

5.1.3 Conclusion of human PGBM analysis

Taken together, the heterogeneity of PGBM is a main complication in GBM studies. The investigated specimens represent only small pieces and are not from the same place within the tumours. A comparison of defined tumour regions, or ideally of whole tumours, could help to find the reason for recurrence of PGBM. Another approach would be a separate analysis of the described subgroups of PGBM tumours. As proposed by Mao et al. (2013), *ALDH1A3* is up-regulated only in MES but not in PN PGBM.

CSC detection in terms of a reliable routine prognostic marker is usually based on IHC of FFPE material. ALDH isotype specific research in PGBM is challenging because the proteins are up to 70 % identical, this is also discussed for breast cancer (Marcato et al., 2011a). RT-PCR analysis does not give any hint for enzyme activity or relevance after post transcriptional regulation. A combined analysis with IHC, enzyme activity measurements (Aldeflour), and RT-PCR or methylation assays would give a general view on ALDH presence on all levels and might help to find a new therapy target of PGBM tumours.

5.2 Evaluation of the syngeneic and the xenograft PGBM mouse model

In this thesis, a syngeneic and a xenograft orthotopic mouse model were used. The decision to take an orthotopic model was made because of two reasons: the orthotopic implantation of cells enables the host to build up a microenvironment, closely mimicking the situation seen in humans. Disadvantages, especially with intracranial models, are that the operation is challenging and a higher animal morbidity than

in easily performed subcutaneous injection has to be taken into account (Sano and Myers, 2009). The advantages of the orthotopic model outweigh the disadvantages.

Inoculation of cells into the brain of a mouse is a well established model to investigate neuronal tumours (Ozawa and James, 2010; Yamada et al., 2004). The cranial hemispheres were chosen for inoculation because, even by a great increase of tumour volume, epileptic seizures are rarely observed. The stereotactic implantation makes it possible to securely inject into the parenchyma and not into the ventricles or the subarachnoid space. For the injection a dulled syringe was used, so brain tissue was only separated but not punched. The break between injection and removal of the syringe prevents the cell suspension to be sucked out immediately. No extra cranial tumour growth could be observed. Injection volume was set to $2\ \mu\text{l}$ to minimise brain pressure increase even though cell suspension is viscous and preparing the syringe needs some practice. The anaesthesia was well controllable, so no mice was lost due to anaesthesia. The recovery period after anaesthesia was about 30 min, before the mice started grooming and eating. The antagonizable anaesthesia with combination of fentanyl, medetomidin, and midazolam is superior to the use of the long effective ketamin and xylazin (Flecknell and Mitchell, 1984; Green, 1975; Zuurbier et al., 2014). The main difference is the fact that the triple anaesthesia is easy to handle (Kirihara et al., 2014) and can be antagonised after intervention to minimize effect on the animals. Postoperative analgesia was performed with Buprenorphin and showed good effectively, corroborating findings of Matsumiya et al. (2012). The intervals between clinical checkups were sufficient to see any potential changes in behavior, appearance, or central nervous system symptoms. Intervention according to the Table 3.11 was fast and ensured that animals did not suffer.

Tumour screening is helpful to identify critical checkpoints or therapeutic effects during experiment. In subcutaneous tumour models, the use of sliding calliper is standard. In intracranial models, only an MRI can be performed for a *in vivo* measurement of tumour growth. The short isoflurane anaesthesia is feasible to minimize the anaesthetic effect of physiological behavior, though it has an effect on neurocognitive functions (Liu et al., 2014a). Scanning without immobilizing animals is not eligible according to animal welfare.

Histopathological workup showed a reasonable tumour uptake, with only 2 mice without detectable tumor. The tumours were well defined and did not grow into the injection canal. No metastasis of tumours were found in the syngeneic and the xenograft models.

5.2.1 ALDH expression in mouse models

The antibody shows a good and specific staining for ALDH isotypes in the positive control (liver, Figure 4.17, p. 48). The xenograft and the syngeneic mouse model, with U87-MG and G1261 cells, respectively, did not show any ALDH1A1 immunoreactivity (Figures 4.19, 4.22). The analysis of the cells in culture did not show any ALDH1A1 reactivity as well (Figures 4.18, 4.21). Reactive astrocytes can normally be found after stroke and brain injury (Bardehle et al., 2013). The reason for this

activation is unclear. The absence of ALDH1A1 cells in the compared mouse model approaches can be due to different reasons. The reactivation of astrocytes should have been in the normal brain parenchyma surrounding the artificial tumour. One hypothesis for the missing ALDH1A1 expression would be that the immunocompromised status of the mice in xenografts and the low immunogenic nature of G1261 cells in C57BL/6JRj do not lead to an activation of astrocytes.

In the xenograft model, the ALDH1A3 staining is scattered throughout the tumours. While untreated mice only show a small amount of positive cells, two of the DSF treated mice show a great immunoreactivity. The C57BL/6JRj mice show scattered positive cells for ALDH1A3 in the G1261 tumours (Figures 4.19, p. 49, Figure 4.22, p. 50). Both observations stay in contrast to the cell pellet analysis of the same cells where cells showed more than 80 % reactivity to the ALDH1A3 antibody (Figures 4.18, 4.21). A phenotypical shift between cell culture and *in vivo* takes place. Different conditions must be the reason.

The presence of ALDH1A3 expression in the DSF treated xenograft mice ($n = 7$) is ambiguous. While two mice show only minor reactivity, three no reactivity, and two mice show an exceptional amount (above 50 %) of ALDH1A3 positive cells. These results are not conclusive. Differences in this group can be due to the different cutting levels of the tumours investigated. The investigated sections show only a small part of the whole tumour. Serial sections of the tumour would give a complemented view and may show a different distribution of ALDH1A3 expression throughout the tumour. A functional isotype specific assay for ALDH isoforms could reveal more information about the enzyme activity and the actual total number of ALDH1A3 positive cells in cell culture conditions and *in vivo* growth. However, available assays, like the flow cytometric analysis named Aldefluor assay (Jones et al., 1995), are not isotype specific.

Further research is needed to understand the meaning of ALDH expression in cell culture conditions and the lack of expression in mouse experiments.

5.3 Evaluation of rat GBM cells

The C6 and F98 rat GBM cells did not show any specific immunoreactivity to the utilised ALDH1A1 antibody, but they did against ALDH1A3 (Figures 4.23, 4.24). An intracranial implantation into rats would be interesting to see if the phenotypical shift, observed in mice, is repeatable in rats.

5.4 Evaluation of the canine GBM model

The antibody designed primarily for human material for ALDH1A1 and ALDH1A3 detects the enzymes specifically as well in canine samples, as shown by the positive controls used in this study. At least for the small number of investigated samples of canine GBM, only ALDH1A3 is present in GBM tumour cells (Figure 4.26, p. 54). To further analyse the relevance of ALDH in canine GBM, it is necessary to increase the

number of investigations and to provide complete patient data including survival and therapy.

The natural presence of ALDH1A3 in canine GBM is a scientific advantage over the evaluated mouse models. Therefore, dogs are potential candidates for further ALDH enzyme analysis. One advantage of using dogs in therapeutic studies is the appropriate size of the skull for surgical resection. Furthermore, dogs develop GBM spontaneously, allegorizing the events that lead to GBM in humans (York et al., 2012). The heterogeneity of human tumours in morphology, histology, and growth pattern is well represented by the canine tumours. In contrast, mouse tumours are homogenous, highly artificial, and do not grow infiltrative. Another important factor is that immunologically naive mice do not show comparable immunoreactivity to tumours as humans or dogs. This is a considerable advantage in favour of canine models, as the immunological response is targeted by newly developed medications (Xiong et al., 2010). Genetic alterations of canine GBM are comparable in most of the cases to the ones found in human GBM (Olin et al., 2014). However using privately owned dogs has a lot of disadvantages as a model for human GBM: lack of reproducibility, unclear environmental conditions, non-uniform cohort, and owner compliance. The costs of preclinical trials would increase because of the scale-up for producing the required amount of preclinical drugs. An elongation of preclinical trials to 1–3 years, according to Hansen and Khanna (2004), is reasonable to estimate. One successful trial in dogs was done by Stubbs et al. (2002) who evaluated a new device to deliver brachytherapy to the margins of resected brain tumours.

Irrespective of the potential use of canine GBM models for further research, the presence of ALDH1A3 expression in canine GBM suggests a preservation of this enzyme and its relevance in tumour growth. Dogs could therefore profit from novel medication targeting ALDH1A3.

Another interesting approach could be a genome analysis of canine GBM patients. As mentioned, Boxers and Boston Terriers are over represented in canine GBM patients (Beveridge and Sobin, 1974; Snyder et al., 2006). A breed-based analysis, as done for other diseases (Erich et al., 2013), could reveal interesting genetic alterations. The genetic pool of the dog breeds is preserved by the strictly closed breeding programs in order to get typical phenotypes (Davis and Ostrander, 2014). Hence, the number of deleterious alleles in a single dog breed is limited (Karlsson et al., 2007). In this respect, dog breeds allegorise the outbred mouse stocks in terms of heterogeneity. These characteristics make pet dogs ideal models, with the above mentioned restrictions, to analyse genetic driver mutations and to test preclinical medications.

5.5 Conclusion of animal model analysis

Summing up, the ability to use the same antibody for human, murine, rat, and canine samples made it possible to directly compare results. However, the suitability of the presented rodent models for ALDH isotype specific research is not satisfactory. There

5 Discussion

is a need to understand why ALDH1A3 is important for the survival of the GBM cells in culture, but expression is down regulated after implantation. ALDH1A1 expression does not seem to be important for rat and mouse GBM cells in cell culture conditions. In any case, the results indicate that ALDH1A3 is more important for GBM CSC than ALDH1A1.

The absence of typical ALDH1A1 staining pattern for reactive astrocytes in the investigated mice with a implantation of murine and human GBM cells gives rise to more questions than answers. In canine samples, ALDH1A1 was absent as well. Hypotheses could be: no reactivation of astrocytes takes place, or reactive astrocytes of mice and dogs do not express ALDH1A1.

The reported ALDH1A3 expression in canine GBM is promising and will be investigated in more samples to substantiate findings. The canine ALDH1A3 immunohistochemical expressions of tumour cells indicate another similarity, next to the known parallels to the human GBM counterpart.

6 Outlook

Recapitulating the results presented in this thesis, ALDH1A1 immunohistochemical expression is associated with the reactive astrocyte staining pattern while ALDH1A3 immunohistochemical expression is more related to the tumour cells.

MOS of PGBM patients can only be predicted with ALDH1. Gender separated analysis of human PGBM for ALDH1 immunohistochemical expression revealed an unexpected difference in prognostic value of isotypes. Female PGBM patients with a combination of ALDH1A1 and ALDH1A3 live significantly shorter than double negative female PGBM patients. The mentioned four core genotypes model (Arnold and Chen, 2009; De Vries et al., 2002) could substantiate findings and help to understand the gender-specific preponderance and value of ALDH expression in GBM.

The number of canine GBM samples analysed for ALDH1 expression has to be increased in further research. However, found similarities of human and canine GBM can help to understand more about ALDH1A3 functions and improve therapy of canine GBM. Moreover, dogs could serve as a good model for human PGBM in the future, naturally expressing ALDH1A3 in tumour cells.

The mouse models investigated in this thesis seem not to be suitable to reproduce the whole situation for ALDH1 expression in human PGBM. A rat orthotopic GBM model with the characterized C6 and F98 cells is a possible alternative. Moreover, it would be interesting to see whether rat cells also change expression profile between *in vitro* and *in vivo* conditions, as observed for GL261 and U87-MG cells. This rat model would also be a syngeneic approach, the presence or absence of ALDH1A1 expressing cells in IHC will be interesting.

The perfect model for ALDH expression in GBM has not yet been found. An easy method to survey ALDH enzyme activity can be the inoculation of PGBM cells into the chicken chorioallantoic membrane (Strojnik et al., 2010). In principle, this model stands out with high turn over rates (7 days), inexpensiveness, comparable expression of immunohistochemical markers, and less ethical concerns than mouse and rat experiments. A comparison to human GBM is missing and would refine this model.

To sum up, the data presented data on human, mouse, rat, and canine GBM samples, emphasize the necessity of isotype specific ALDH research. Though proteins are up to 70% identical, results indicate that the different isotypes carry out diverse functions. Differences in expression of ALDH *in vitro* and *in vivo* conditions impede the transfer of research. Reasonable and convincing explanations for this phenomenon are only speculative. To gain further expertise in ALDH expression, cell culture research and animal model based investigations are needed. However, these are dependent on further characterisation of enzyme activity, knowledge about the functional differences of ALDH isotypes, and better isotype specific analytic methods.

7 Summary

Glioblastoma multiforme (GBM) is the most common malignant primary brain tumour in adults with a median survival, despite of multimodal aggressive therapy, of only 15 months. Relapse occurs inevitably because of the infiltrative nature of GBM. To date, only the MGMT promoter methylation is a reliable marker for therapy sensitivity. Survival-associated prognostic factors as well as novel therapy targets are urgently needed. Multiple genetic and metabolic pathway alterations contribute to tumour progression and therapy resistance. Recently proposed CSC markers for solid cancers include the aldehyde dehydrogenase (ALDH) superfamily. This cytoplasmic enzyme family consists of 19 different isoforms. The ALDH enzymes act upon oxidative stress and participate in proliferation, differentiation, and cell cycle arrest. The evolutionary conservation of the protein family enables comparative considerations of different species.

In the presented study, isotype specific expression of ALDH is analysed in human GBM tumours and in two commonly used mouse GBM models. Expression of ALDH in the mouse models is then compared with the human GBM to find a suitable model for further research.

The presented results indicate that there is, though challenging, a necessity for isotype specific analysis of ALDH expression. ALDH1A1 immunohistochemical expression in human PGBM was found primarily in the tumour adjacent region, whereas ALDH1A3 positive cells were more frequently found among tumour cells. Prognostic relevance for PGBM patients' outcome was found for the ALDH1 immunohistochemical expression. Moreover, female PGBM patients were shown to have prolonged survival if neither ALDH1A1 nor ALDH1A3 expression is present. For male PGBM patients, ALDH1A1 and ALDH1A3 immunohistochemical expression could not be correlated to the medium overall survival. The reasons for this gender difference remain yet undetermined.

Both the murine and the human GBM cells analysed in this thesis did not show ALDH1A1 immunohistochemical expression in cell culture or after implantation. The expression of ALDH1A3 is inhomogeneous in the analysed groups, raising further questions, which will be investigated in the future. The investigative approach of this thesis showed that the analysed canine GBM samples express ALDH1A3 but not ALDH1A1. This difference to human PGBM tumours in ALDH expression can help to understand more about the metabolic processes in tumour cells and the reactions to the tumour cells in the surrounding tissue.

Finally, there are two particularly promising research subjects for future investigations: the gender specific prognostic power of ALDH expression in PGBM patients and the reason for the change in ALDH1A3 expression between *in vitro* and *in vivo* conditions. This knowledge can contribute to finding new targets for PGBM therapy and to prolonging patient survival.

8 Zusammenfassung

Das Glioblastoma multiforme (GBM) ist der häufigste maligne hirneigene Tumor des erwachsenen Menschen, mit einem mittleren Überleben, trotz aggressiver multimodaler Therapie, von nur 15 Monaten. Aufgrund der infiltrativen Natur des GBM treten Rezidive unvermeidlich auf. Zur Zeit gibt es nur einen zuverlässigen Marker für das Ansprechen der Therapie, die MGMT Promoter Methylierung. Mit dem Überleben assoziierte Marker und neue Therapieziele werden dringend benötigt. Viele genetische und metabolische Veränderungen führen zu Tumorwachstum und Therapieresistenz. Zu den vorgeschlagenen neuen Markern für CSC der soliden Tumoren gehört die Aldehyddehydrogenase-Superfamilie (ALDH-Superfamilie). Diese Enzymfamilie besteht aus 19 verschiedenen, im Zytoplasma lokalisierten Isoformen. Die ALDH-Enzyme sind beteiligt an der Reaktion auf oxidativen Stress, an Proliferation, Differenzierung, und Zellzyklus-Arrest. Die evolutionäre Konserviertheit der Proteinfamilie lässt eine vergleichende Betrachtung zwischen verschiedenen Spezies zu.

Diese Arbeit vergleicht isotypenspezifisch die ALDH Expression von menschlichen GBM Tumoren mit zwei weitverbreiteten Tierversuchssmodellen. Die ALDH Expression der Maus tumoren wird verglichen mit der der menschlichen GBM, um für zukünftige Untersuchungen ein geeignetes Modell zu finden.

Die vorliegenden Resultate deuten darauf hin, dass die isotypenspezifische Analyse der ALDH notwendig, jedoch herausfordernd ist. Die immunhistochemische Expression von ALDH1A1 in humanen GBM Tumoren wurde hauptsächlich in der an den Tumor angrenzenden Region detektiert, während ALDH1A3 positive Zellen häufiger unter den Tumorzellen gefunden wurden. Eine prognostische Relevanz für das Überleben der PGBM Patienten konnte für die ALDH1 Expression nachgewiesen werden. Darüber hinaus zeigte sich, dass weibliche PGBM Patienten einen Überlebensvorteil haben, falls weder ALDH1A1 noch ALDH1A3 Expression vorliegt. Für männliche PGBM Patienten konnte keine Korrelation der ALDH1A1 und ALDH1A3 Expression mit der mittleren Überlebenszeit gefunden werden. Die Gründe für die geschlechtsspezifischen Unterschiede sind unbekannt und bedürfen weiterer Forschung.

Die in der vorliegenden Arbeit untersuchten murinen und humanen GBM Zellen zeigten in der Zellkultur und nach Implantation keine ALDH1A1 Expression. Die Expression von ALDH1A3 ist uneinheitlich in den untersuchten Gruppen, welches neue Fragen aufwirft, die in späteren Studien untersucht werden sollen. Die hier durchgeführte investigative Untersuchung von caninen GBM Tumoren zeigte, dass nur ALDH1A3, nicht jedoch ALDH1A1 exprimiert wird. Dieser Unterschied in der ALDH Expression zum menschlichen PGBM kann in weiteren Studien helfen, die metabolischen Prozesse im Tumor und die Reaktion des umliegenden Gewebes auf

8 Zusammenfassung

die Tumorzellen besser zu verstehen.

Abschließend sind im Hinblick auf weitere Untersuchungen vor allem zwei vielversprechende Ansatzpunkte zu nennen: die geschlechtsspezifisch unterschiedliche Eignung der ALDH Expression in PGBM als prognostischer Marker sowie die Ursache für die Veränderung der ALDH1A3 Expression zwischen *in vitro* und *in vivo* Bedingungen. Das gewonnene Verständnis kann in der Zukunft benutzt werden, um Angriffsziele für neue PGBM Therapien zu finden und zu einer Verlängerung des Lebens von Patienten beizutragen.

9 Supplemental Data

Table 9.1: Clinical characteristics of GBM patients enrolled in this study

Patient No	sex	age at time of diagnosis	survival days	relapse free survival
1	m	56	1263	791
2	m	39	357	183
7	m	79	410	
8	f	47	362	220
9	m	50	974	613
10	m	64	2112	606
11	f	69	391	150
13	m	62	673	626
17	m	58	259	179
18	m	62	2904	159
22	m	62	442	369
25	f	56	631	383
27	m	49	870	219
30	f	50	373	238
31	f	50	258	139
32	f	57	1437	16
40	f	50	1137	606
41	m	42	2124	1658
42	m	74	219	133
44	m	20	779	515
45	f	42	1707	24
47	m	53	933	
49	m	68	933	414
50	f	55	498	402
53	m	70	374	92
54	f	48	1201	721
57	m	63	664	531
58	m	42	473	110
65	f	55	784	525
67	m	65	572	454
76	m	59	623	293
88	m	66	550	290
91	f	69	1058	555

9 Supplemental Data

Table 9.1: Clinical characteristics of PGBM patients enrolled in this study

Patient No	sex	age at time of diagnosis	survival days	relapse free survival
95	m	53	483	292
96	m	62	289	
97	m	76	446	
98	f	78	78	
99	m	74	172	
100	f	50	411	
101	f	70	93	
102	f	71	37	
103	f	78	110	
104	f	68	74	
106	f	66	169	
107	m	79	22	
108	f	50	768	
109	f	40	89	
112	m	62	206	
113	m	31	342	
114	f	65	463	
115	m	56	261	
116	m	48	366	
117	m	79	121	
118	f	73	398	
119	m	67	280	
120	m	45	345	
121	f	55	357	
122	f	55	448	
123	f	71	603	
124	m	33	645	
125	m	70	517	
126	m	47	623	
128	m	53	107	
129	f	63	117	
130	m	77	249	
131	m	71	69	
132	f	70	329	
133	f	72	48	
134	m	80	45	

9 Supplemental Data

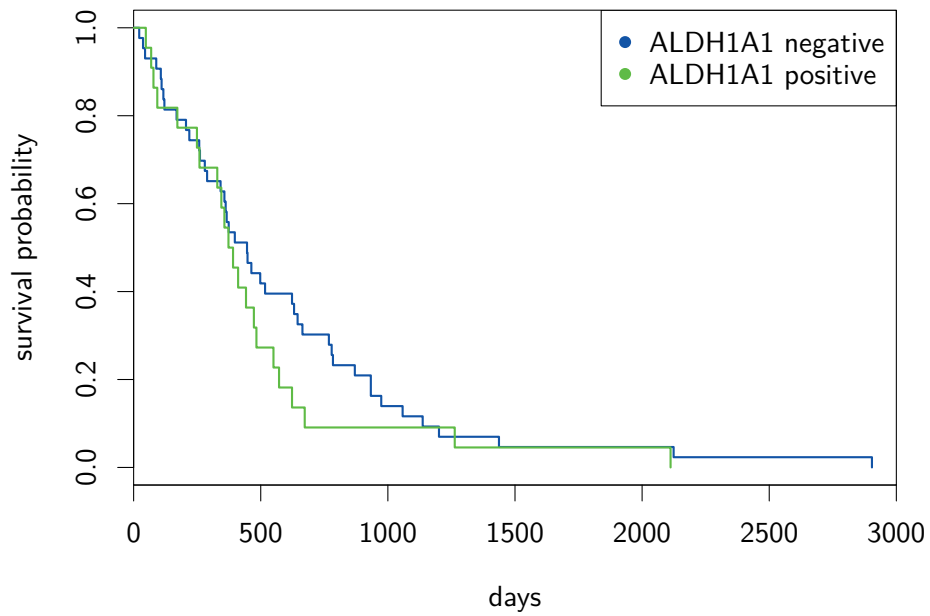


Figure 9.1: Survival of patients with different ALDH1A1 expression in primary PGBM. ALDH1A1 positive ($n = 22$) with a MOS of 382 days, ALDH1A1 negative ($n = 43$) with a MOS of 446 days.

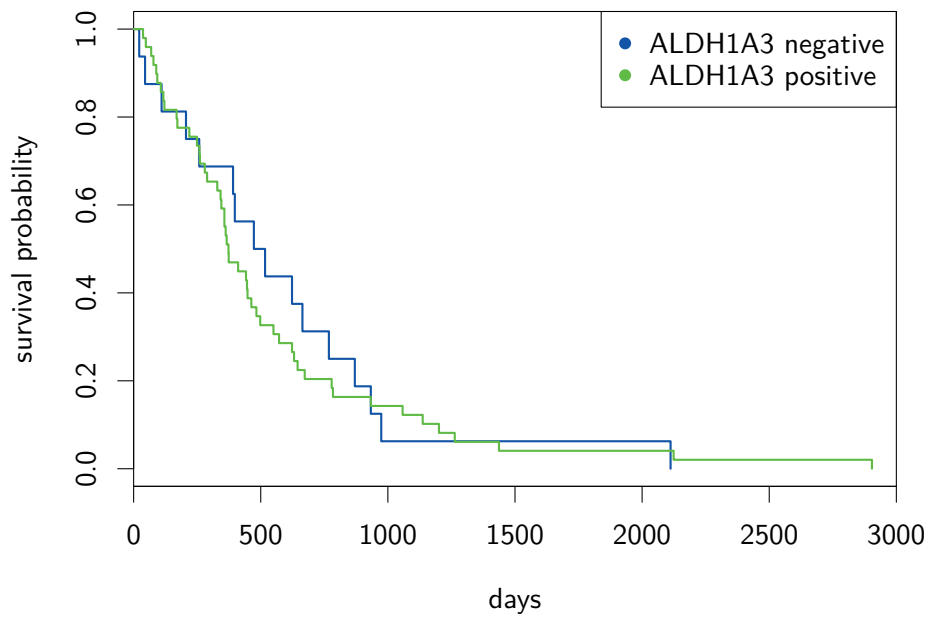


Figure 9.2: Survival of patients with different ALDH1A3 expression in primary PGBM. ALDH1A3 positive ($n = 49$) with a MOS of 373 days, ALDH1A3 negative ($n = 16$) with a MOS of 495 days.

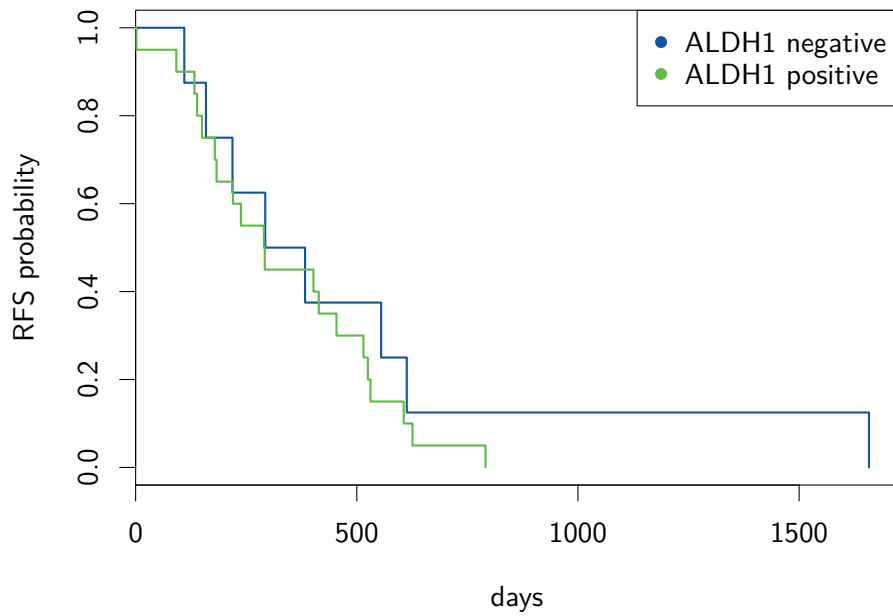


Figure 9.3: RFS with different ALDH1 expression in primary PGBM. ALDH1 positive ($n = 20$) with a medium RFS of 291 days, ALDH1 negative ($n = 8$) with a medium RFS of 338 days.

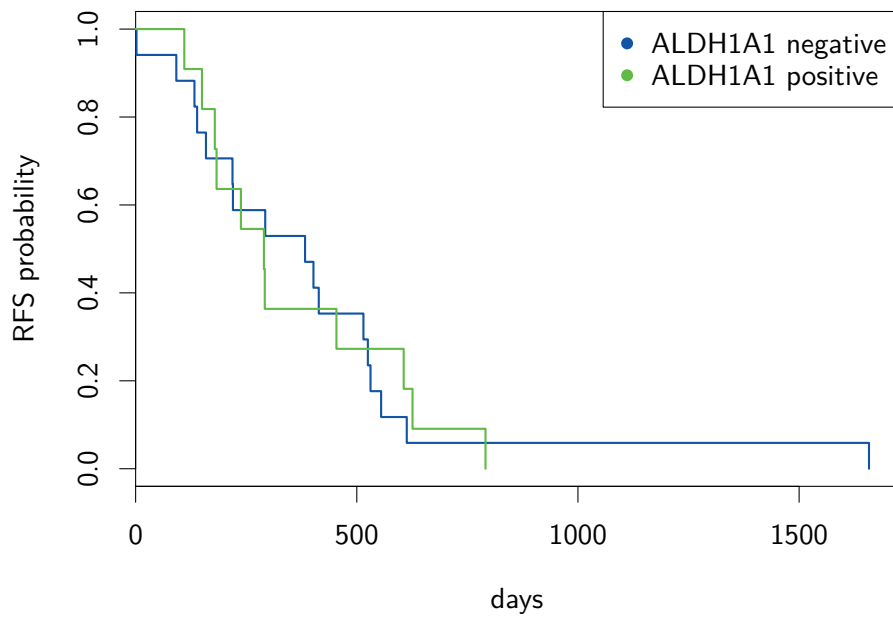


Figure 9.4: RFS with different ALDH1A1 expression in primary PGBM. ALDH1A1 positive ($n = 11$) with a medium RFS of 290 days, ALDH1A1 negative ($n = 17$) with a medium RFS of 383 days.

9 Supplemental Data

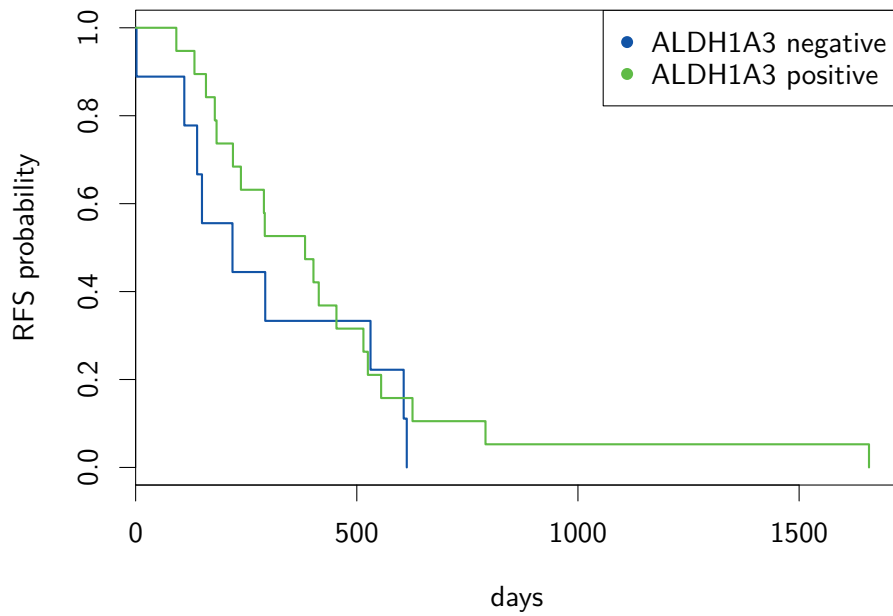


Figure 9.5: RFS with different ALDH1A3 expression in primary PGBM. ALDH1A3 positive ($n = 19$) with a medium RFS of 382 days, ALDH1A3 negative ($n = 9$) with a medium RFS of 219 days.

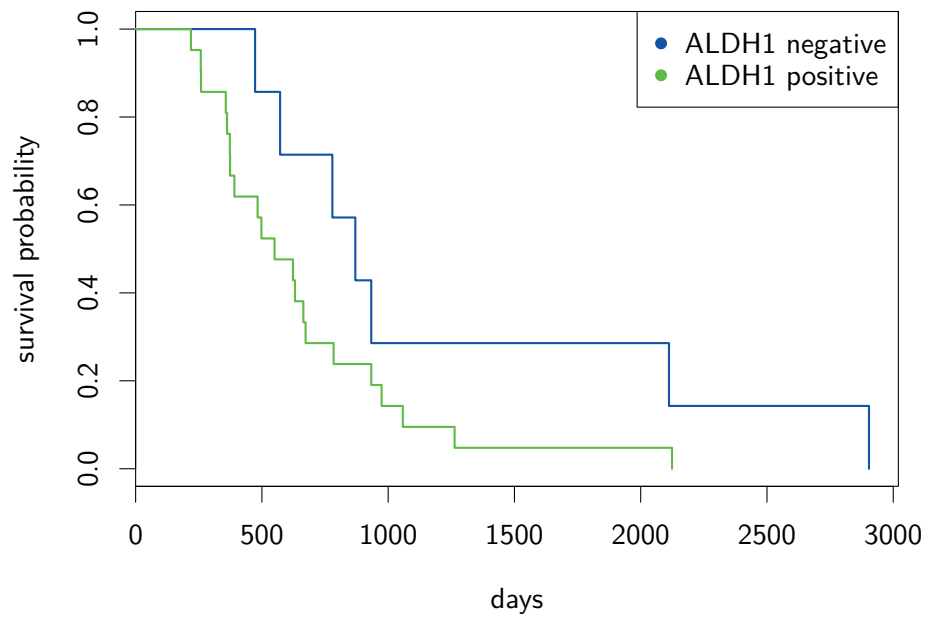


Figure 9.6: Survival of patients with different ALDH1 expression in secondary PGBM. ALDH1 positive patients ($n = 21$) have a MOS of 550 days compared to ALDH1 negative patients ($n = 7$) with a MOS of 870 days.

9 Supplemental Data

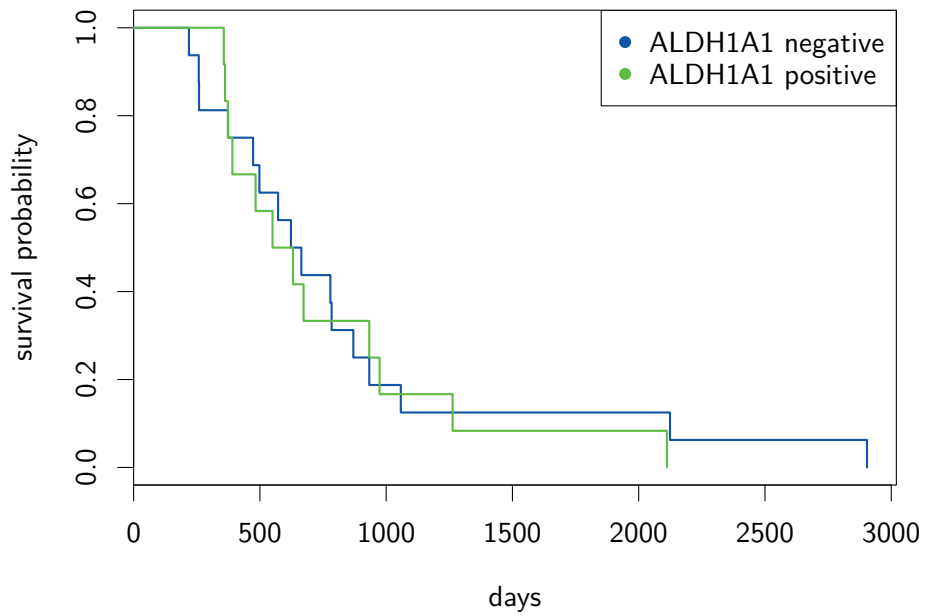


Figure 9.7: Survival of patients with different ALDH1A1 expression in secondary PGBM. ALDH1A1 positive patients ($n = 12$) have a MOS of 590 days compared to ALDH1A1 negative patients ($n = 16$) with a MOS of 644 days.

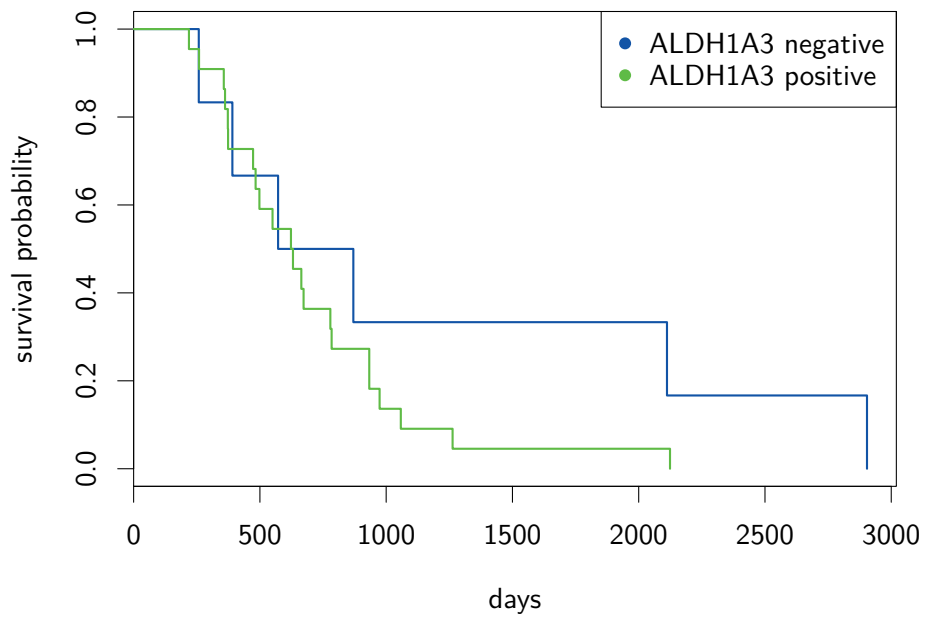


Figure 9.8: Survival of patients with different ALDH1A3 expression in secondary PGBM. ALDH1A3 positive patients ($n = 22$) have a MOS of 627 days compared to ALDH1A3 negative patients ($n = 6$) with a MOS of 721 days.

9 Supplemental Data

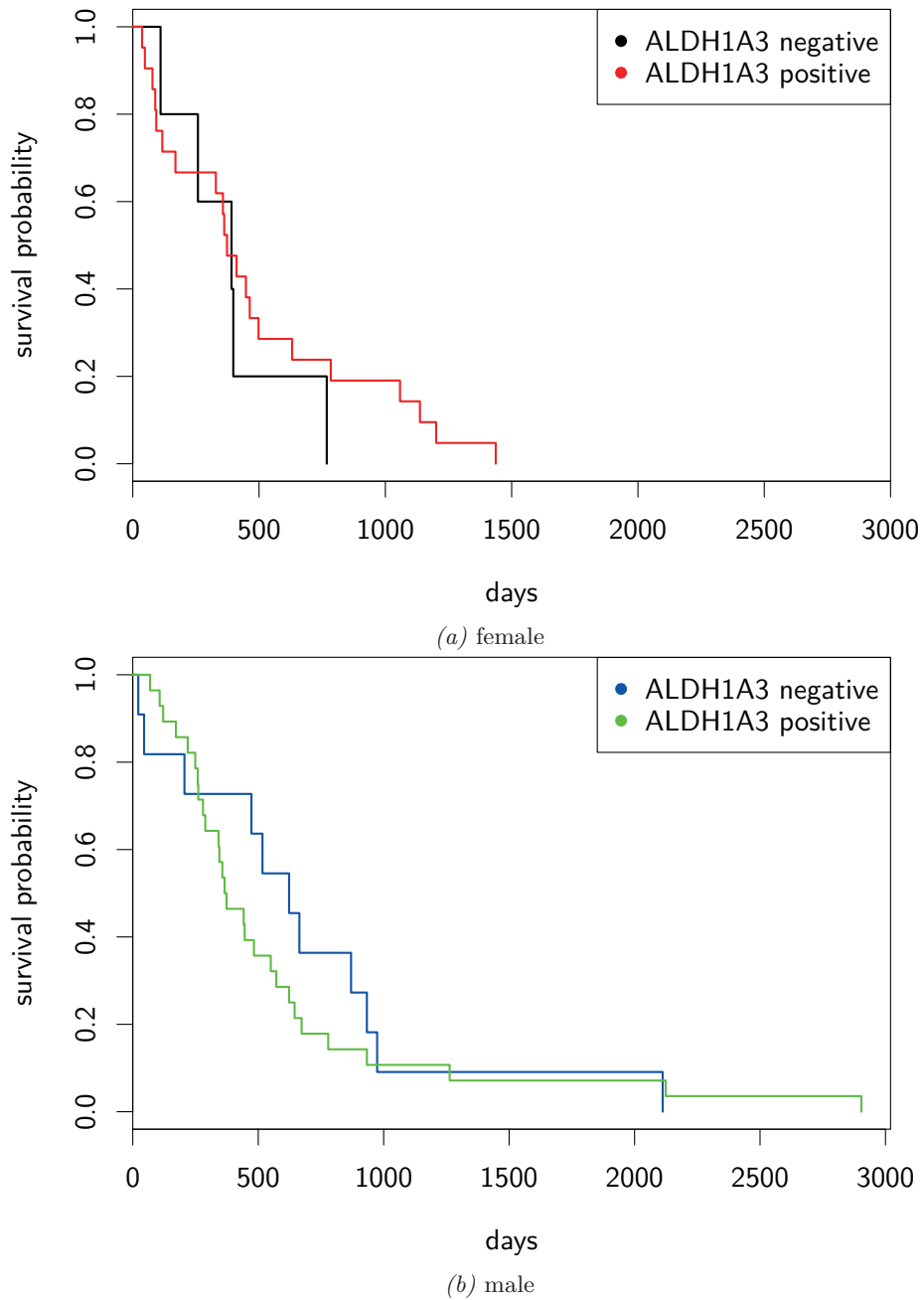
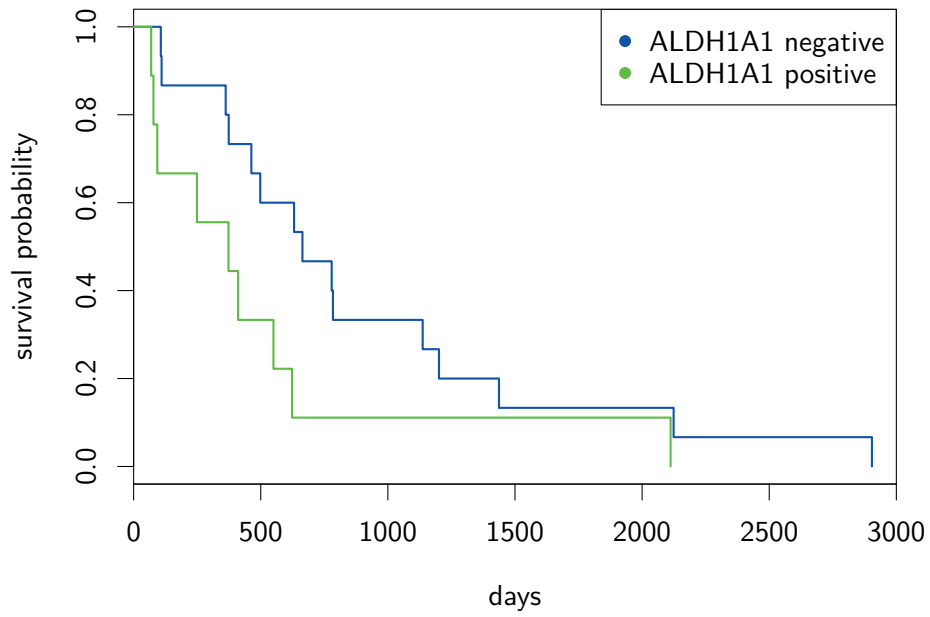
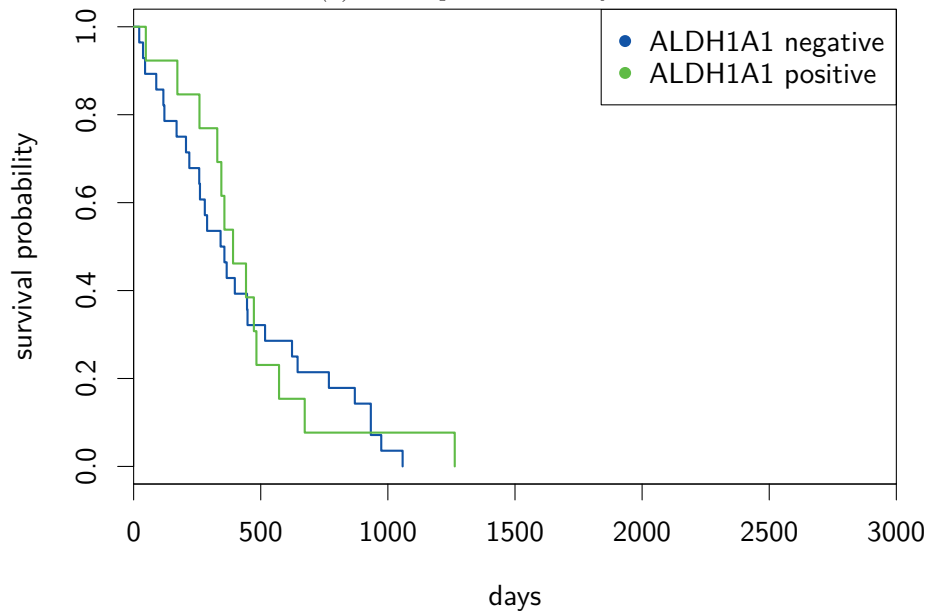


Figure 9.9: Survival of PGBM patients separated by sex and ALDH1A3 expression. female: ALDH1A3 positive ($n = 21$) have a MOS of 373 days ALDH1A3 negative ($n = 5$) have a MOS of 391 days. male: ALDH1A3 positive ($n = 28$) have a MOS of 370 days ALDH1A3 negative ($n = 11$) have a MOS of 623 days.

9 Supplemental Data



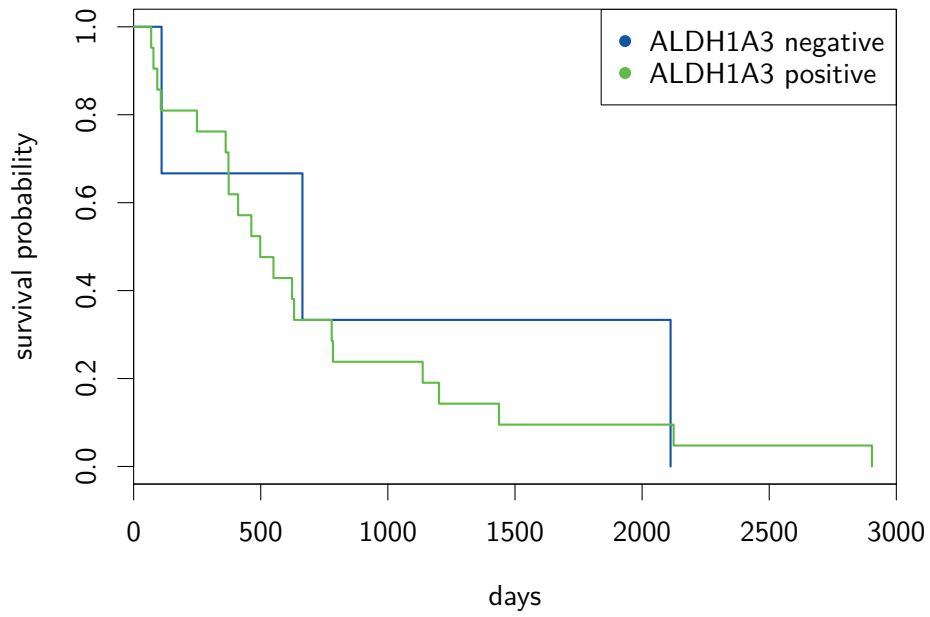
(a) MGMT promoter methylated



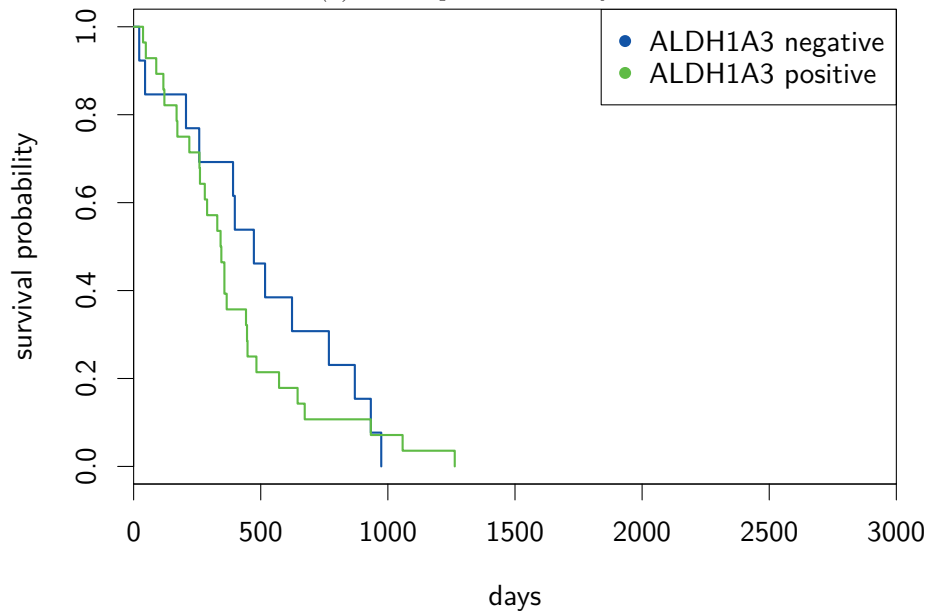
(b) MGMT promoter not methylated

Figure 9.10: Survival of patients with or without MGMT promoter methylation in combination with ALDH1A1 expression in primary PGBM. With MGMT promoter methylation ALDH1A1 positive patients ($n = 9$) have a MOS of 373 days compared to ALDH1A1 negative patients ($n = 15$) with a MOS of 664 days. No MGMT promoter methylation ALDH1A1 positive patients ($n = 13$) have a MOS of 391 days compared to ALDH1A1 negative patients ($n = 28$) with a MOS of 350 days.

9 Supplemental Data



(a) MGMT promoter methylated



(b) MGMT promoter not methylated

Figure 9.11: Survival of patients with and without MGMT promoter methylation in combination with ALDH1A3. With MGMT promoter methylation ALDH1A3 positive patients ($n = 21$) have a MOS of 498 days compared to ALDH1A3 negative patients ($n = 3$) with a MOS of 664 days. No MGMT promoter methylation ALDH1A3 positive patients ($n = 28$) have a MOS of 344 days compared to ALDH1A3 negative patients ($n = 13$) with a MOS of 473 days.

9 Supplemental Data

Table 9.2: MGMT and ALDH1A1

	ALDH1A1	
	positive	negative
MGMT promotor methylated	9	15
MGMT promoter not methylated	13	28

Table 9.3: MGMT and ALDH1A3

	ALDH1A3	
	positive	negative
MGMT promotor methylated	21	3
MGMT promoter not methylated	28	13

9 Supplemental Data

Table 9.4: Results of RT-PCR

Patients No.	GFAP	GAPDH	ALDH						
			1A1	1A2	1A3	2	3A1	7A1	8A1
1	+	+	+	-	+	-	-	+	-
2	+	+	+	+	+	-	-	-	-
8	+	+	+	+	+	-	-	+	-
9	+	+	+	-	-	-	-	+	-
10	+	+	+	-	-	-	-	-	-
13	+	+	-	-	+	-	-	-	-
17	+	+	-	-	+	-	-	+	-
25	+	+	+	+	+	+	-	+	-
30	+	+	+	+	+	+	-	-	-
32	+	+	-	+	+	+	-	+	-
41	+	+	+	+	+	-	+	-	-
42	+	+	+	-	+	-	-	-	-
44	+	+	-	-	+	-	-	+	-
47	+	+	+	-	-	-	-	-	-
49	+	+	+	-	+	-	-	+	+
50	+	+	-	-	+	-	-	-	-
53	+	+	+	-	+	-	-	-	-
57	+	+	-	-	-	-	-	-	-
65	+	+	+	-	-	-	-	-	-
67	+	+	+	+	-	-	-	-	-
71	+	+	+	-	+	-	-	-	-
88	+	+	+	-	-	-	-	-	-
91	+	+	+	-	+	-	-	-	-
95	+	+	+	-	+	-	-	+	-
number of positive patients	23	23	17	8	15	3	1	8	1

Bibliography

- S. A. Adam, O. Schnell, J. Pöschl, S. Eigenbrod, H. A. Kretschmar, J. C. Tonn, U. Schüller, ALDH1A1 is a marker of astrocytic differentiation during brain development and correlates with better survival in glioblastoma patients. *Brain Pathol*, 22(6), 788–97, **2012**.
- C. Alifieris, D. T. Trafalis, Glioblastoma multiforme: Pathogenesis and treatment. *Pharmacol Ther*, 152, 63–82, **2015**.
- M. A. Arevalo, I. Azcoitia, L. M. Garcia-Segura, The neuroprotective actions of oestradiol and oestrogen receptors. *Nat Rev Neurosci*, 16(1), 17–29, **2015**.
- A. P. Arnold, X. Chen, What does the "four core genotypes" mouse model tell us about sex differences in the brain and other tissues? *Front Neuroendocrinol*, 30(1), 1–9, **2009**.
- A. Arshad, B. Yang, A. S. Bienemann, N. U. Barua, M. J. Wyatt, M. Woolley, D. E. Johnson, K. J. Edler, S. S. Gill, Convection-enhanced delivery of carboplatin PLGA nanoparticles for the treatment of glioblastoma. *PLoS One*, 10(7), e0132266, **2015**.
- J. I. Ausman, W. R. Shapiro, D. P. Rall, Studies on the chemotherapy of experimental brain tumors: development of an experimental model. *Cancer Res*, 30(9), 2394–400, **1970**.
- I. Azcoitia, A. Sierra, S. Veiga, S. Honda, N. Harada, L. M. Garcia-Segura, Brain aromatase is neuroprotective. *J Neurobiol*, 47(4), 318–329, **2001**.
- S. Bao, Q. Wu, R. E. McLendon, Y. Hao, Q. Shi, A. B. Hjelmeland, M. W. Dewhirst, D. D. Bigner, J. N. Rich, Glioma stem cells promote radioresistance by preferential activation of the DNA damage response. *Nature*, 444(7120), 756–60, **2006**.
- S. Bardehle, M. Krüger, F. Buggenthin, J. Schwausch, J. Ninkovic, H. Clevers, H. J. Snippert, F. J. Theis, M. Meyer-Luehmann, I. Bechmann, L. Dimou, M. Götz, Live imaging of astrocyte responses to acute injury reveals selective juxtavascular proliferation. *Nat Neurosci*, 16(5), 580–586, **2013**.
- C. M. Becker, R. K. Oberoi, S. J. McFarren, D. M. Muldoon, D. H. Pafundi, J. L. Pokorny, D. H. Brinkmann, J. R. Ohlfest, J. N. Sarkaria, D. A. Largaespada, W. F. Elmquist, Decreased affinity for efflux transporters increases brain penetration and molecular targeting of a PI3K/mTOR inhibitor in a mouse model of glioblastoma. *Neuro Oncol*, 17(9), 1210–1219, **2015**.

Bibliography

- Z. Belcaid, J. A. Phallen, J. Zeng, A. P. See, D. Mathios, C. Gottschalk, S. Nicholas, M. Kellett, J. Ruzevick, C. Jackson, E. Albesiano, N. M. Durham, X. Ye, P. T. Tran, B. Tyler, J. W. Wong, H. Brem, D. M. Pardoll, C. G. Drake, M. Lim, Focal radiation therapy combined with 4-1BB activation and CTLA-4 blockade yields long-term survival and a protective antigen-specific memory response in a murine glioma model. *PLoS One*, 9(7), e101764, **2014**.
- M. Bettstetter, S. Dechant, P. Ruummele, C. Vogel, K. Kurz, M. Morak, G. Keller, E. Holinski-Feder, F. Hofstaedter, W. Dietmaier, MethyQESD, a robust and fast method for quantitative methylation analyses in HNPCC diagnostics using formalin-fixed and paraffin-embedded tissue samples. *Lab Invest*, 88(12), 1367–1375, **2008**.
- W. I. Beveridge, L. H. Sobin, International histological classification of tumours of domestic animals. introduction. *Bull World Health Organ*, 50(1-2), 1–6, **1974**.
- K. P. L. Bhat, V. Balasubramaniyan, B. Vaillant, R. Ezhilarasan, K. Hummelink, F. Hollingsworth, K. Wani, L. Heathcock, J. D. James, L. D. Goodman, S. Conroy, L. Long, N. Lelic, S. Wang, J. Gumin, D. Raj, Y. Kodama, A. Raghunathan, A. Olar, K. Joshi, C. E. Pelloski, A. Heimberger, S. H. Kim, D. P. Cahill, G. Rao, W. F. A. Den Dunnen, H. W. G. M. Boddeke, H. S. Phillips, I. Nakano, F. F. Lang, H. Colman, E. P. Sulman, K. Aldape, Mesenchymal differentiation mediated by NF- κ B promotes radiation resistance in glioblastoma. *Cancer Cell*, 24(3), 331–346, **2013**.
- R. Bonavia, M.-d.-M. Inda, W. K. Cavenee, F. B. Furnari, Heterogeneity maintenance in glioblastoma: a social network. *Cancer Res*, 71(12), 4055–60, **2011**.
- B. Campos, F.-S. Centner, J. L. Bermejo, R. Ali, K. Dorsch, F. Wan, J. Felsberg, R. Ahmadi, N. Grabe, G. Reifenberger, A. Unterberg, J. Burhenne, C. C. Herold-Mende, Aberrant expression of retinoic acid signaling molecules influences patient survival in astrocytic gliomas. *Am J Pathol*, 178(5), 1953–64, **2011**.
- B. Campos, F. Wan, M. Farhadi, A. Ernst, F. Zeppernick, K. E. Tagscherer, R. Ahmadi, J. Lohr, C. Dictus, G. Gdynia, S. E. Combs, V. Goidts, B. M. Helmke, V. Eckstein, W. Roth, P. Beckhove, P. Lichter, A. Unterberg, B. Radlwimmer, C. Herold-Mende, Differentiation therapy exerts antitumor effects on stem-like glioma cells. *Clin Cancer Res*, 16(10), 2715–2728, **2010**.
- M. Candolfi, J. F. Curtin, W. S. Nichols, A. G. Muhammad, G. D. King, G. E. Pluhar, E. A. McNiel, J. R. Ohlfest, A. B. Freese, P. F. Moore, J. Lerner, P. R. Lowenstein, M. G. Castro, Intracranial glioblastoma models in preclinical neuro-oncology: neuropathological characterization and tumor progression. *J Neurooncol*, 85(2), 133–148, **2007**.

Bibliography

- S. A. Choi, J. Y. Lee, J. H. Phi, K.-C. Wang, C.-K. Park, S.-H. Park, S.-K. Kim, Identification of brain tumour initiating cells using the stem cell marker aldehyde dehydrogenase. *Eur J Cancer*, 50(1), 137–49, **2014**.
- J. P. Chute, G. G. Muramoto, J. Whitesides, M. Colvin, R. Safi, N. J. Chao, D. P. McDonnell, Inhibition of aldehyde dehydrogenase and retinoid signaling induces the expansion of human hematopoietic stem cells. *Proc Natl Acad Sci U S A*, 103(31), 11707–11712, **2006**.
- C. A. Cornil, G. F. Ball, J. Balthazart, Rapid control of male typical behaviors by brain-derived estrogens. *Front Neuroendocrinol*, 33(4), 425–446, **2012**.
- P. Dalerba, R. W. Cho, M. F. Clarke, Cancer stem cells: models and concepts. *Annu Rev Med*, 58, 267–284, **2007**.
- B. W. Davis, E. A. Ostrander, Domestic dogs and cancer research: a breed-based genomics approach. *ILAR J*, 55(1), 59–68, **2014**.
- G. J. De Vries, E. F. Rissman, R. B. Simerly, L.-Y. Yang, E. M. Scordalakes, C. J. Auger, A. Swain, R. Lovell-Badge, P. S. Burgoyne, A. P. Arnold, A model system for study of sex chromosome effects on sexually dimorphic neural and behavioral traits. *J Neurosci*, 22(20), 9005–9014, **2002**.
- G. L. Defer, H. Adle-Biassette, F. Ricolfi, L. Martin, F. J. Authier, C. Chomienne, L. Degos, J. D. Degos, All-trans retinoic acid in relapsing malignant gliomas: clinical and radiological stabilization associated with the appearance of intratumoral calcifications. *J Neurooncol*, 34(2), 169–177, **1997**.
- K. M. Dhandapani, D. W. Brann, Estrogen-astrocyte interactions: implications for neuroprotection. *BMC Neurosci*, 3, 6, **2002**.
- A. C. Diserens, N. de Tribolet, A. Martin-Achard, A. C. Gaide, J. F. Schnegg, S. Carrel, Characterization of an established human malignant glioma cell line: LN18. *Acta Neuropathol*, 53(1), 21–28, **1981**.
- G. Duester, F. A. Mic, A. Molotkov, Cytosolic retinoid dehydrogenases govern ubiquitous metabolism of retinol to retinaldehyde followed by tissue-specific metabolism to retinoic acid. *Chem Biol Interact*, 143-144, 201–210, **2003**.
- V. Dupé, N. Matt, J.-M. Garnier, P. Chambon, M. Mark, N. B. Ghyselinck, A newborn lethal defect due to inactivation of retinaldehyde dehydrogenase type 3 is prevented by maternal retinoic acid treatment. *Proc Natl Acad Sci U S A*, 100(24), 14036–14041, **2003**.
- D. I. Eneanya, J. R. Bianchine, D. O. Duran, B. D. Andresen, The actions of metabolic fate of disulfiram. *Annu Rev Pharmacol Toxicol*, 21, 575–96, **1981**.

Bibliography

- S. A. Erich, G. R. Rutteman, E. Teske, Causes of death and the impact of histiocytic sarcoma on the life expectancy of the dutch population of bernese mountain dogs and flat-coated retrievers. *Vet J*, 198(3), 678–683, **2013**.
- B. Fazi, A. Felsani, L. Grassi, A. Moles, D. D’Andrea, N. Toschi, D. Sicari, P. De Bonis, C. Anile, M. G. Guerrisi, E. Luca, M. G. Farace, G. Maira, S. A. Ciafré, A. Mangiola, The transcriptome and mirnome profiling of glioblastoma tissues and peritumoral regions highlights molecular pathways shared by tumors and surrounding areas and reveals differences between short-term and long-term survivors. *Oncotarget*, **2015**.
- M. J. Felini, A. F. Olshan, J. C. Schroeder, S. E. Carozza, R. Miike, T. Rice, M. Wrensch, Reproductive factors and hormone use and risk of adult gliomas. *Cancer Causes Control*, 20(1), 87–96, **2009**.
- P. A. Flecknell, M. Mitchell, Midazolam and fentanyl-fluanisone: assessment of anaesthetic effects in laboratory rodents and rabbits. *Lab Anim*, 18(2), 143–146, **1984**.
- C. Ginestier, M. H. Hur, E. Charafe-Jauffret, F. Monville, J. Dutcher, M. Brown, J. Jacquemier, P. Viens, C. G. Kleer, S. Liu, A. Schott, D. Hayes, D. Birnbaum, M. S. Wicha, G. Dontu, ALDH1 is a marker of normal and malignant human mammary stem cells and a predictor of poor clinical outcome. *Cell Stem Cell*, 1(5), 555–67, **2007**.
- C. Ginestier, J. Wicinski, N. Cervera, F. Monville, P. Finetti, F. Bertucci, M. S. Wicha, D. Birnbaum, E. Charafe-Jauffret, Retinoid signaling regulates breast cancer stem cell differentiation. *Cell Cycle*, 8(20), 3297–3302, **2009**.
- C. J. Green, Neuroleptanalgesic drug combinations in the anaesthetic management of small laboratory animals. *Lab Anim*, 9(3), 161–178, **1975**.
- X. Guan, J. Vengoechea, S. Zheng, A. E. Sloan, Y. Chen, D. J. Brat, B. P. O’Neill, J. de Groot, S. Yust-Katz, W.-K. A. Yung, M. L. Cohen, K. D. Aldape, S. Rosenfeld, R. G. W. Verhaak, J. S. Barnholtz-Sloan, Molecular subtypes of glioblastoma are relevant to lower grade glioma. *PLoS One*, 9(3), e91216, **2014**.
- K. Hansen, C. Khanna, Spontaneous and genetically engineered animal models; use in preclinical cancer drug development. *Eur J Cancer*, 40(6), 858–880, **2004**.
- E. E. Hatch, M. S. Linet, J. Zhang, H. A. Fine, W. R. Shapiro, R. G. Selker, P. M. Black, P. D. Inskip, Reproductive and hormonal factors and risk of brain tumors in adult females. *Int J Cancer*, 114(5), 797–805, **2005**.
- P. Hau, R. Stupp, M. E. Hegi, MGMT methylation status: the advent of stratified therapy in glioblastoma? *Dis Markers*, 23(1-2), 97–104, **2007**.

Bibliography

- H. M. Hayes, W. Priester, Jr, T. W. Pendergrass, Occurrence of nervous-tissue tumors in cattle, horses, cats and dogs. *Int J Cancer*, 15(1), 39–47, **1975**.
- M. E. Hegi, A.-C. Diserens, S. Godard, P.-Y. Dietrich, L. Regli, S. Ostermann, P. Otten, G. Van Melle, N. de Tribolet, R. Stupp, Clinical trial substantiates the predictive value of *o6*-methylguanine-dna methyltransferase promoter methylation in glioblastoma patients treated with temozolomide. *Clin Cancer Res*, 10(6), 1871–1874, **2004**.
- M. E. Hegi, L. Liu, J. G. Herman, R. Stupp, W. Wick, M. Weller, M. P. Mehta, M. R. Gilbert, Correlation of *o6*-methylguanine methyltransferase (MGMT) promoter methylation with clinical outcomes in glioblastoma and clinical strategies to modulate MGMT activity. *J Clin Oncol*, 26(25), 4189–99, **2008**.
- J. Hilton, Role of aldehyde dehydrogenase in cyclophosphamide-resistant L1210 leukemia. *Cancer Res*, 44(11), 5156–5160, **1984**.
- E. H. Huang, M. J. Hynes, T. Zhang, C. Ginestier, G. Dontu, H. Appelman, J. Z. Fields, M. S. Wicha, B. M. Boman, Aldehyde dehydrogenase 1 is a marker for normal and malignant human colonic stem cells (SC) and tracks SC overpopulation during colon tumorigenesis. *Cancer Res*, 69(8), 3382–9, **2009**.
- B. L. Isfoss, B. Holmqvist, H. Jernström, P. Alm, H. Olsson, Women with familial risk for breast cancer have an increased frequency of aldehyde dehydrogenase expressing cells in breast ductules. *BMC Clin Pathol*, 13(1), 28, **2013**.
- A. Iwanami, B. Gini, C. Zanca, T. Matsutani, A. Assuncao, A. Nael, J. Dang, H. Yang, S. Zhu, J. Kohyama, I. Kitabayashi, W. K. Cavenee, T. F. Cloughesy, F. B. Furnari, M. Nakamura, Y. Toyama, H. Okano, P. S. Mischel, Pml mediates glioblastoma resistance to mammalian target of rapamycin (mTOR)-targeted therapies. *Proc Natl Acad Sci U S A*, 110(11), 4339–4344, **2013**.
- B. Jackson, C. Brocker, D. C. Thompson, W. Black, K. Vasiliou, D. W. Nebert, V. Vasiliou, Update on the aldehyde dehydrogenase gene (ALDH) superfamily. *Hum Genomics*, 5(4), 283–303, **2011**.
- R. J. Jones, J. P. Barber, M. S. Vala, M. I. Collector, S. H. Kaufmann, S. M. Ludeman, O. M. Colvin, J. Hilton, Assessment of aldehyde dehydrogenase in viable cells. *Blood*, 85(10), 2742–2746, **1995**.
- S. E. Kaba, A. P. Kyritsis, C. Conrad, M. J. Gleason, R. Newman, V. A. Levin, W. K. Yung, The treatment of recurrent cerebral gliomas with all-trans-retinoic acid (tretinoin). *J Neurooncol*, 34(2), 145–151, **1997**.
- E. K. Karlsson, I. Baranowska, C. M. Wade, N. H. C. Salmon Hillbertz, M. C. Zody, N. Anderson, T. M. Biagi, N. Patterson, G. R. Pielberg, E. J. Kulbokas, 3rd, K. E. Comstock, E. T. Keller, J. P. Mesirov, H. von Euler, O. Kämpe, A. Hedhammar,

Bibliography

- E. S. Lander, G. Andersson, L. Andersson, K. Lindblad-Toh, Efficient mapping of mendelian traits in dogs through genome-wide association. *Nat Genet*, 39(11), 1321–1328, **2007**.
- R. E. Kast, G. Karpel-Massler, M.-E. Halatsch, CUSP9* treatment protocol for recurrent glioblastoma: aprepitant, artesunate, auranofin, captopril, celecoxib, disulfiram, itraconazole, ritonavir, sertraline augmenting continuous low dose temozolomide. *Oncotarget*, 5(18), 8052–82, **2014**.
- Y. Kirihara, M. Takechi, K. Kurosaki, Y. Kobayashi, Y. Saito, T. Takeuchi, Anesthetic effects of a three-drugs mixture-comparison of administrative routes and antagonistic effects of atipamezole in mice. *Exp Anim*, **2014**.
- M. A. Lane, S. J. Bailey, Role of retinoid signalling in the adult brain. *Prog Neurobiol*, 75(4), 275–293, **2005**.
- T. Li, Y. Su, Y. Mei, Q. Leng, B. Leng, Z. Liu, S. A. Stass, F. Jiang, ALDH1A1 is a marker for malignant prostate stem cells and predictor of prostate cancer patients' outcome. *Lab Invest*, 90(2), 234–244, **2010**.
- J. Liu, P. Wang, X. Zhang, W. Zhang, G. Gu, Effects of different concentration and duration time of isoflurane on acute and long-term neurocognitive function of young adult c57bl/6 mouse. *Int J Clin Exp Pathol*, 7(9), 5828–5836, **2014a**.
- Y. Liu, D.-L. Lv, J.-J. Duan, S.-L. Xu, J.-F. Zhang, X.-J. Yang, X. Zhang, Y.-H. Cui, X.-W. Bian, S.-C. Yu, ALDH1A1 expression correlates with clinicopathologic features and poor prognosis of breast cancer patients: a systematic review and meta-analysis. *BMC Cancer*, 14, 444, **2014b**.
- T. W. Loo, D. M. Clarke, Blockage of drug resistance in vitro by disulfiram, a drug used to treat alcoholism. *J Natl Cancer Inst*, 92(11), 898–902, **2000**.
- M. López-Lázaro, Stem cell division theory of cancer. *Cell Cycle*, pages 2547–2548, **2015**.
- D. N. Louis, H. Ohgaki, O. D. Wiestler, W. K. Cavenee (Editors), *WHO Classification of Tumours of the Central Nervous System*. International Agency for Research on Cancer (IARC), 69008 Lyon, France, 4th edition, **2007**.
- I. Ma, A. L. Allan, The role of human aldehyde dehydrogenase in normal and cancer stem cells. *Stem Cell Rev*, 7(2), 292–306, **2011**.
- P. Mao, K. Joshi, J. Li, S.-H. Kim, P. Li, L. Santana-Santos, S. Luthra, U. R. Chandran, P. V. Benos, L. Smith, M. Wang, B. Hu, S.-Y. Cheng, R. W. Sobol, I. Nakano, Mesenchymal glioma stem cells are maintained by activated glycolytic metabolism involving aldehyde dehydrogenase 1A3. *Proc Natl Acad Sci U S A*, 110(21), 8644–9, **2013**.

Bibliography

- P. Marcato, C. A. Dean, C. A. Giacomantonio, P. W. Lee, Aldehyde dehydrogenase: its role as a cancer stem cell marker comes down to the specific isoform. *Cell Cycle*, 10(9), 1378–84, **2011a**.
- P. Marcato, C. A. Dean, R.-Z. Liu, K. M. Coyle, M. Bydoun, M. Wallace, D. Clements, C. Turner, E. G. Mathenge, S. A. Gujar, C. A. Giacomantonio, J. R. Mackey, R. Godbout, P. W. K. Lee, Aldehyde dehydrogenase 1a3 influences breast cancer progression via differential retinoic acid signaling. *Mol Oncol*, 9(1), 17–31, **2015**.
- P. Marcato, C. A. Dean, D. Pan, R. Araslanova, M. Gillis, M. Joshi, L. Helyer, L. Pan, A. Leidal, S. Gujar, C. A. Giacomantonio, P. W. K. Lee, Aldehyde dehydrogenase activity of breast cancer stem cells is primarily due to isoform ALDH1A3 and its expression is predictive of metastasis. *Stem Cells*, 29(1), 32–45, **2011b**.
- S. A. Marchitti, C. Brocker, D. Stagos, V. Vasiliou, Non-p450 aldehyde oxidizing enzymes: the aldehyde dehydrogenase superfamily. *Expert Opin Drug Metab Toxicol*, 4(6), 697–720, **2008**.
- L. C. Matsumiya, R. E. Sorge, S. G. Sotocinal, J. M. Tabaka, J. S. Wieskopf, A. Zaloum, O. D. King, J. S. Mogil, Using the mouse grimace scale to reevaluate the efficacy of postoperative analgesics in laboratory mice. *J Am Assoc Lab Anim Sci*, 51(1), 42–49, **2012**.
- L. D. McCullough, K. Blizzard, E. R. Simpson, O. K. Oz, P. D. Hurn, Aromatase cytochrome p450 and extragonadal estrogen play a role in ischemic neuroprotection. *J Neurosci*, 23(25), 8701–8705, **2003**.
- M. M. Mrugala, L. K. Crew, J. R. Fink, A. M. Spence, Carboplatin and bevacizumab for recurrent malignant glioma. *Oncol Lett*, 4(5), 1082–1086, **2012**.
- G. G. Muramoto, J. L. Russell, R. Safi, A. B. Salter, H. A. Himburg, P. Daher, S. K. Meadows, P. Doan, R. W. Storms, N. J. Chao, D. P. McDonnell, J. P. Chute, Inhibition of aldehyde dehydrogenase expands hematopoietic stem cells with radioprotective capacity. *Stem Cells*, 28(3), 523–534, **2010**.
- I. Nakano, Stem cell signature in glioblastoma: therapeutic development for a moving target. *J Neurosurg*, pages 1–7, **2014**.
- W. Ni, L. Luo, Z. Ping, H. P. Yuan, X. D. Zhao, W. Xu, Prognostic value of ALDH1A3 promoter methylation in glioblastoma: a single center experience in western china. *Asian Pac J Cancer Prev*, 16(2), 591–4, **2015**.
- S. Nobusawa, T. Watanabe, P. Kleihues, H. Ohgaki, IDH1 mutations as molecular signature and predictive factor of secondary glioblastomas. *Clin Cancer Res*, 15(19), 6002–6007, **2009**.

Bibliography

- M. R. Olin, G. E. Pluhar, B. M. Andersen, R. Shaver, N. N. Waldron, C. L. Moertel, Victory and defeat in the induction of a therapeutic response through vaccine therapy for human and canine brain tumors: a review of the state of the art. *Crit Rev Immunol*, 34(5), 399–432, **2014**.
- T. Ozawa, C. D. James, Establishing intracranial brain tumor xenografts with subsequent analysis of tumor growth and response to therapy using bioluminescence imaging. *J Vis Exp*, (41), **2010**.
- J. Pallud, E. Audureau, G. Noel, R. Corns, E. Lechapt-Zalcman, J. Duntze, V. Pavlov, J. Guyotat, P. D. Hieu, P.-J. Le Reste, T. Faillot, C.-F. Litre, N. Desse, A. Petit, E. Emery, J. Voirin, J. Peltier, F. Caire, J.-R. Vignes, J.-L. Barat, O. Langlois, E. Dezamis, E. Parraga, M. Zanello, E. Nader, M. Lefranc, L. Bauchet, B. Devaux, P. Menei, P. Metellus, C. , Long-term results of carmustine wafer implantation for newly diagnosed glioblastomas: a controlled propensity-matched analysis of a french multicenter cohort. *Neuro Oncol*, **2015**.
- A. C. Palmer, Comparative aspects of tumours of the central nervous system in the dog. *Proc R Soc Med*, 69(1), 49–51, **1976**.
- C. Y. Park, D. Tseng, I. L. Weissman, Cancer stem cell-directed therapies: recent data from the laboratory and clinic. *Mol Ther*, 17(2), 219–230, **2009**.
- J. M. Petrosino, D. Disilvestro, O. Ziouzenkova, Aldehyde dehydrogenase 1a1: friend or foe to female metabolism? *Nutrients*, 6(3), 950–73, **2014**.
- S. Phuphanich, C. Scott, A. J. Fischbach, C. Langer, W. K. Yung, All-trans-retinoic acid: a phase ii radiation therapy oncology group study (rtog 91-13) in patients with recurrent malignant astrocytoma. *J Neurooncol*, 34(2), 193–200, **1997**.
- R. J. Plunkett, A. Lis, T. A. Barone, M. D. Fronckowiak, S. J. Greenberg, Hormonal effects on glioblastoma multiforme in the nude rat model. *J Neurosurg*, 90(6), 1072–1077, **1999**.
- V. Quillien, A. Lavenu, L. Karayan-Tapon, C. Carpentier, M. Labussière, T. Lesimple, O. Chinot, M. Wager, J. Honnorat, S. Saikali, F. Fina, M. Sanson, D. Figarella-Branger, Comparative assessment of 5 methods (methylation-specific polymerase chain reaction, methylight, pyrosequencing, methylation-sensitive high-resolution melting, and immunohistochemistry) to analyze O6-methylguanine-DNA methyltransferase in a series of 100 glioblastoma patients. *Cancer*, 118(17), 4201–4211, **2012**.
- D. Raha, T. R. Wilson, J. Peng, D. Peterson, P. Yue, M. Evangelista, C. Wilson, M. Merchant, J. Settleman, The cancer stem cell marker aldehyde dehydrogenase is required to maintain a drug-tolerant tumor cell subpopulation. *Cancer Res*, 74(13), 3579–90, **2014**.

Bibliography

- M. Rasper, A. Schäfer, G. Piontek, J. Teufel, G. Brockhoff, F. Ringel, S. Heindl, C. Zimmer, J. Schlegel, Aldehyde dehydrogenase 1 positive glioblastoma cells show brain tumor stem cell capacity. *Neuro Oncol*, 12(10), 1024–33, **2010**.
- D. Sano, J. N. Myers, Xenograft models of head and neck cancers. *Head Neck Oncol*, 1, 32, **2009**.
- A. Schäfer, J. Teufel, F. Ringel, M. Bettstetter, I. Hoepner, M. Rasper, J. Gempt, J. Koeritzer, F. Schmidt-Graf, B. Meyer, C. P. Beier, J. Schlegel, Aldehyde dehydrogenase 1A1—a new mediator of resistance to temozolomide in glioblastoma. *Neuro Oncol*, 14(12), 1452–64, **2012**.
- N. O. Schmidt, M. Ziu, G. Carrabba, C. Giussani, L. Bello, Y. Sun, K. Schmidt, M. Albert, P. M. Black, R. S. Carroll, Antiangiogenic therapy by local intracerebral microinfusion improves treatment efficiency and survival in an orthotopic human glioblastoma model. *Clin Cancer Res*, 10(4), 1255–1262, **2004**.
- S. K. Singh, I. D. Clarke, M. Terasaki, V. E. Bonn, C. Hawkins, J. Squire, P. B. Dirks, Identification of a cancer stem cell in human brain tumors. *Cancer Res*, 63(18), 5821–8, **2003**.
- N. R. Smoll, K. Schaller, O. P. Gautschi, Long-term survival of patients with glioblastoma multiforme (GBM). *J Clin Neurosci*, 20(5), 670–675, **2013**.
- J. M. Snyder, F. S. Shofer, T. J. Van Winkle, C. Massicotte, Canine intracranial primary neoplasia: 173 cases (1986-2003). *J Vet Intern Med*, 20(3), 669–675, **2006**.
- R. B. Song, C. H. Vite, C. W. Bradley, J. R. Cross, Postmortem evaluation of 435 cases of intracranial neoplasia in dogs and relationship of neoplasm with breed, age, and body weight. *J Vet Intern Med*, 27(5), 1143–1152, **2013**.
- B. Stangeland, A. A. Mughal, Z. Grieg, C. J. Sandberg, M. Joel, S. Nygård, T. Meling, W. Murrell, E. O. Vik Mo, I. A. Langmoen, Combined expressional analysis, bioinformatics and targeted proteomics identify new potential therapeutic targets in glioblastoma stem cells. *Oncotarget*, **2015**.
- G. Stoica, G. Lungu, H. Martini-Stoica, S. Waghela, J. Levine, R. Smith, 3rd, Identification of cancer stem cells in dog glioblastoma. *Vet Pathol*, 46(3), 391–406, **2009**.
- T. Strojnik, R. Kavalari, T. A. Barone, R. J. Plunkett, Experimental model and immunohistochemical comparison of u87 human glioblastoma cell xenografts on the chicken chorioallantoic membrane and in rat brains. *Anticancer Res*, 30(12), 4851–4860, **2010**.
- J. B. Stubbs, R. H. Frankel, K. Schultz, I. Crocker, D. Dillehay, J. J. Olson, Pre-clinical evaluation of a novel device for delivering brachytherapy to the margins of resected brain tumor cavities. *J Neurosurg*, 96(2), 335–343, **2002**.

Bibliography

- R. Stupp, M. E. Hegi, W. P. Mason, M. J. van den Bent, M. J. Taphoorn, R. C. Janzer, S. K. Ludwin, A. Allgeier, B. Fisher, K. Belanger, P. Hau, A. A. Brandes, J. Gijtenbeek, C. Marosi, C. J. Vecht, K. Mokhtari, P. Wesseling, S. Villa, E. Eisenhauer, T. Gorlia, M. Weller, D. Lacombe, J. G. Cairncross, R. O. Mirimanoff, Effects of radiotherapy with concomitant and adjuvant temozolomide versus radiotherapy alone on survival in glioblastoma in a randomised phase III study: 5-year analysis of the EORTC-NCIC trial. *Lancet Oncol*, 10(5), 459–66, **2009**.
- R. Stupp, W. P. Mason, M. J. van den Bent, M. Weller, B. Fisher, M. J. B. Taphoorn, K. Belanger, A. A. Brandes, C. Marosi, U. Bogdahn, J. Curschmann, R. C. Janzer, S. K. Ludwin, T. Gorlia, A. Allgeier, D. Lacombe, J. G. Cairncross, E. Eisenhauer, R. O. Mirimanoff, Radiotherapy plus concomitant and adjuvant temozolomide for glioblastoma. *N Engl J Med*, 352(10), 987–96, **2005**.
- M. E. Sughrue, T. Sheean, P. A. Bonney, A. J. Maurer, C. Teo, Aggressive repeat surgery for focally recurrent primary glioblastoma: outcomes and theoretical framework. *Neurosurg Focus*, 38(3), E11, **2015**.
- C. Sun, D. Zhao, X. Dai, J. Chen, X. Rong, H. Wang, A. Wang, M. Li, J. Dong, Q. Huang, Q. Lan, Fusion of cancer stem cells and mesenchymal stem cells contributes to glioma neovascularization. *Oncol Rep*, 34(4), 2022–2030, **2015**.
- T. Sun, N. M. Warrington, J. Luo, M. D. Brooks, S. Dahiya, S. C. Snyder, R. Sengupta, J. B. Rubin, Sexually dimorphic rb inactivation underlies mesenchymal glioblastoma prevalence in males. *J Clin Invest*, 124(9), 4123–4133, **2014**.
- A. Suzuki, P. Leland, H. Kobayashi, P. L. Choyke, E. M. Jagoda, T. Inoue, B. H. Joshi, R. K. Puri, Analysis of biodistribution of intracranially infused radiolabeled interleukin-13 receptor-targeted immunotoxin IL-13PE by SPECT/CT in an orthotopic mouse model of human glioma. *J Nucl Med*, 55(8), 1323–1329, **2014**.
- T. Szatmári, K. Lumniczky, S. Désaknai, S. Trajceviski, E. J. Hídvégi, H. Hamada, G. Sáfrány, Detailed characterization of the mouse glioma 261 tumor model for experimental glioblastoma therapy. *Cancer Sci*, 97(6), 546–553, **2006**.
- M. Uhlén, E. Björling, C. Agaton, C. A.-K. Szigyarto, B. Amini, E. Andersen, A.-C. Andersson, P. Angelidou, A. Asplund, C. Asplund, L. Berglund, K. Bergström, H. Brumer, D. Cerjan, M. Ekström, A. Elobeid, C. Eriksson, L. Fagerberg, R. Falk, J. Fall, M. Forsberg, M. G. Björklund, K. Gumbel, A. Halimi, I. Hallin, C. Hamsten, M. Hansson, M. Hedhammar, G. Hercules, C. Kampf, K. Larsson, M. Lindskog, W. Lodewyckx, J. Lund, J. Lundeberg, K. Magnusson, E. Malm, P. Nilsson, J. Odling, P. Oksvold, I. Olsson, E. Oster, J. Ottosson, L. Paavilainen, A. Persson, R. Rimini, J. Rockberg, M. Runeson, A. Sivertsson, A. Sköllermo, J. Steen, M. Stenvall, F. Sterky, S. Strömberg, M. Sundberg, H. Tegel, S. Tourle, E. Wahlund, A. Waldén, J. Wan, H. Wernérus, J. Westberg, K. Wester, U. Wrethagen, L. L. Xu, S. Hober, F. Pontén, A human protein atlas for normal and cancer

Bibliography

- tissues based on antibody proteomics. *Mol Cell Proteomics*, 4(12), 1920–1932, **2005**.
- V. Vasiliou, D. W. Nebert, Analysis and update of the human aldehyde dehydrogenase (aldh) gene family. *Hum Genomics*, 2(2), 138–43, **2005**.
- R. G. W. Verhaak, K. A. Hoadley, E. Purdom, V. Wang, Y. Qi, M. D. Wilkerson, C. R. Miller, L. Ding, T. Golub, J. P. Mesirov, G. Alexe, M. Lawrence, M. O’Kelly, P. Tamayo, B. A. Weir, S. Gabriel, W. Winckler, S. Gupta, L. Jakkula, H. S. Feiler, J. G. Hodgson, C. D. James, J. N. Sarkaria, C. Brennan, A. Kahn, P. T. Spellman, R. K. Wilson, T. P. Speed, J. W. Gray, M. Meyerson, G. Getz, C. M. Perou, D. N. Hayes, C. G. A. R. N. , Integrated genomic analysis identifies clinically relevant subtypes of glioblastoma characterized by abnormalities in PDGFRA, IDH1, EGFR, and NF1. *Cancer Cell*, 17(1), 98–110, **2010**.
- K. Vigneswaran, S. Neill, C. G. Hadjipanayis, Beyond the world health organization grading of infiltrating gliomas: advances in the molecular genetics of glioma classification. *Ann Transl Med*, 3(7), 95, **2015**.
- G. H. Vince, M. Bendszus, T. Schweitzer, R. H. Goldbrunner, S. Hildebrandt, J. Tilgner, R. Klein, L. Solymosi, J. Christian Tonn, K. Roosen, Spontaneous regression of experimental gliomas—an immunohistochemical and MRI study of the C6 glioma spheroid implantation model. *Exp Neurol*, 190(2), 478–485, **2004**.
- K. Wang, X. Wu, J. Wang, J. Huang, Cancer stem cell theory: therapeutic implications for nanomedicine. *Int J Nanomedicine*, 8, 899–908, **2013**.
- W. A. Weiss, M. Israel, C. Cobbs, E. Holland, C. D. James, D. N. Louis, C. Marks, A. I. McClatchey, T. Roberts, T. Van Dyke, C. Wetmore, I.-M. Chiu, M. Giovannini, A. Guha, R. J. Higgins, S. Marino, I. Radovanovic, K. Reilly, K. Aldape, Neuropathology of genetically engineered mice: consensus report and recommendations from an international forum. *Oncogene*, 21(49), 7453–7463, **2002**.
- C. Wismeth, P. Hau, K. Fabel, U. Baumgart, B. Hirschmann, H. Koch, T. Jauch, O. Grauer, L. Drechsel, A. Brawanski, U. Bogdahn, A. Steinbrecher, Maintenance therapy with 13-cis retinoid acid in high-grade glioma at complete response after first-line multimodal therapy—a phase-ii study. *J Neurooncol*, 68(1), 79–86, **2004**.
- T.-W. Wu, J. M. Wang, S. Chen, R. D. Brinton, 17beta-estradiol induced ca²⁺ influx via l-type calcium channels activates the src/erk/cyclic-amp response element binding protein signal pathway and bcl-2 expression in rat hippocampal neurons: a potential initiation mechanism for estrogen-induced neuroprotection. *Neuroscience*, 135(1), 59–72, **2005**.
- W. Xiong, M. Candolfi, C. Liu, A. K. M. G. Muhammad, K. Yagiz, M. Puntel, P. F. Moore, J. Avalos, J. D. Young, D. Khan, R. Donelson, G. E. Pluhar, J. R. Ohlfest, K. Wawrowsky, P. R. Lowenstein, M. G. Castro, Human flt3l generates

Bibliography

- dendritic cells from canine peripheral blood precursors: implications for a dog glioma clinical trial. *PLoS One*, 5(6), e11074, **2010**.
- N. Xu, M. M. Shao, H. T. Zhang, M. S. Jin, Y. Dong, R. J. Ou, H. M. Wang, A. P. Shi, Aldehyde dehydrogenase 1 (ALDH1) expression is associated with a poor prognosis of bladder cancer. *Cancer Epidemiol*, 39(3), 375–81, **2015a**.
- S.-L. Xu, S. Liu, W. Cui, Y. Shi, Q. Liu, J.-J. Duan, S.-C. Yu, X. Zhang, Y.-H. Cui, H.-F. Kung, X.-W. Bian, Aldehyde dehydrogenase 1A1 circumscribes high invasive glioma cells and predicts poor prognosis. *Am J Cancer Res*, 5(4), 1471–1483, **2015b**.
- J. S. Yakisich, A. Sidén, P. Eneroth, M. Cruz, Disulfiram is a potent in vitro inhibitor of dna topoisomerases. *Biochem Biophys Res Commun*, 289(2), 586–590, **2001**.
- S. Yamada, V. Khankaldyyan, X. Bu, A. Suzuki, I. Gonzalez-Gomez, K. Takahashi, J. G. McComb, W. E. Laug, A method to accurately inject tumor cells into the caudate/putamen nuclei of the mouse brain. *Tokai J Exp Clin Med*, 29(4), 167–73, **2004**.
- Y. Yanagawa, J. C. Chen, L. C. Hsu, A. Yoshida, The transcriptional regulation of human aldehyde dehydrogenase i gene. the structural and functional analysis of the promoter. *J Biol Chem*, 270(29), 17521–17527, **1995**.
- L.-c. Yang, Q.-G. Zhang, C.-f. Zhou, F. Yang, Y.-d. Zhang, R.-m. Wang, D. W. Brann, Extranuclear estrogen receptors mediate the neuroprotective effects of estrogen in the rat hippocampus. *PLoS One*, 5(5), e9851, **2010**.
- J. Ye, G. Coulouris, I. Zaretskaya, I. Cutcutache, S. Rozen, T. L. Madden, Primerblast: a tool to design target-specific primers for polymerase chain reaction. *BMC Bioinformatics*, 13, 134, **2012**.
- D. York, R. J. Higgins, R. A. LeCouteur, A. N. Wolfe, R. Grahn, N. Olby, M. Campbell, P. J. Dickinson, TP53 mutations in canine brain tumors. *Vet Pathol*, 49(5), 796–801, **2012**.
- W. Zhang, W. Yan, G. You, Z. Bao, Y. Wang, Y. Liu, Y. You, T. Jiang, Genome-wide DNA methylation profiling identifies ALDH1A3 promoter methylation as a prognostic predictor in G-CIMP- primary glioblastoma. *Cancer Lett*, 328(1), 120–5, **2013**.
- D. Zhao, Y. Mo, M.-T. Li, S.-W. Zou, Z.-L. Cheng, Y.-P. Sun, Y. Xiong, K.-L. Guan, Q.-Y. Lei, Notch-induced aldehyde dehydrogenase 1a1 deacetylation promotes breast cancer stem cells. *J Clin Invest*, **2014**.
- L. Zhao, R. D. Brinton, Estrogen receptor alpha and beta differentially regulate intracellular ca(2+) dynamics leading to erk phosphorylation and estrogen neuroprotection in hippocampal neurons. *Brain Res*, 1172, 48–59, **2007**.

Bibliography

- C. J. Zuurbier, A. Koeman, S. M. Houten, M. W. Hollmann, W. J. Florijn, Optimizing anesthetic regimen for surgery in mice through minimization of hemodynamic, metabolic, and inflammatory perturbations. *Exp Biol Med (Maywood)*, 239(6), 737–746, **2014**.

10 Danksagung

Mein besonderer Dank geht an Herrn Prof. Dr. Kaspar Matiasek, der mir die Möglichkeit gegeben hat in die spannende Welt der Neuropathologie hineinzutauchen. Bei Herrn Prof. Dr. Jürgen Schlegel bedanke ich mich herzlich dafür, dass er mir nicht nur sein Labor zu Verfügung gestellt hat, mir Geduld und Vertrauen während der Zeit geschenkt hat, sondern auch immer dafür gesorgt hat, dass ich nicht unter einer Brücke schlafen musste.

Ich danke Herrn Prof. Dr. Höfler, an dessen Institut ich diese Arbeit anfertigen durfte.

Ich bedanke mich auch herzlich bei meinen Kolleginnen und Kollegen, für anregende wissenschaftliche Diskussionen und unterhaltsame Stunden auch außerhalb des Labors. Dabei sind Christine Grubmüller und Sandra Baur namentlich zu nennen, die mich bei der Durchführung der RT-PCR und IHC tatkräftig unterstützt haben.

An Claire Delbridge geht mein Dank für Tee, Eis und Kuchen, sowie kritisches Korrekturlesen, IHC-scores,...

Ein Dank geht auch an Ebba Beller und Tobias Boeckh-Behrens für die humanen und Anne Kluge für die murinen MRT Bilder. Katja Steiger hat mich tatkräftig während der Anfertigung dieser Arbeit unterstützt, ihr sind Farbe und Qualität der Bilder zu verdanken.

Ich danke auch dem StaBLab Team der LMU München und besonders Felix Günther für den R-Kurs und die Beratung bei der statistischen Auswertung.

Danke Eckhart, für die persönliche Unterstützung und für den L^AT_EX-Support.

Zuletzt möchte ich mich bei meinen Eltern bedanken, die mich während des Studiums durchgefüttert haben. Es ist auch ein Teil eures Verdienstes, dass diese Arbeit fertig gestellt werden konnte.